University of Washington
Department of Civil and Environmental Engineering

EVALUATION OF EXTENDED STREAMFLOW PREDICTION RUNOFF FORECASTS USING A SIMPLE WATER BALANCE MODEL

Chia-Ling Chenlai
Dennis P. Lettenmaier

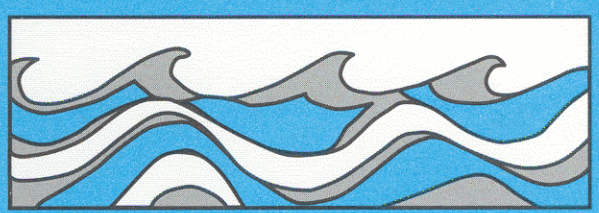

Water Resources Series
Technical Report No.126
December 1990

Seattle, Washington
98195

Department of Civil Engineering
University of Washington
Seattle, Washington 98195

EVALUATION OF EXTENDED STREAMFLOW PREDICTION RUNOFF FORECASTS USING A SIMPLE WATER BALANCE MODEL

Chia-Ling Chenlai
Dennis P. Lettenmaier

Water Resources Series
Technical Report No. 126

December 1990

TABLE OF CONTENTS

LIST OF FIGURES

LIST OF TABLES

ACKNOWLEDGMENTS

This study was supervised by Dr. Dennis P. Lettenmaier, Research Professor of Civil Engineering. The author would like to thank both Dr. Lettenmaier and Dr. Wen-Sen Chu for the opportunity to pursue graduate studies at the University of Washington, and for their assistance and support throughout. The author also wishes to acknowledge Kristin Mingus for her assistance in editing and revising the text.

CHAPTER 1 INTRODUCTION

1.1 Background

An adequate water supply has always been an essential factor for human life. In modern civilizations, the planning and management of water supply systems has become increasingly important because of resource limitations and the growth in demand for municipal, industrial, and agricultural water supply.

As the demand for water increases along with competition for alternative interests, there is rising pressure for more efficient water management. Improved streamflow forecasting is one way that the efficiency of water resource systems operations can be improved. In the Western United States, runoff originates primarily from snowmelt. During the spring and summer, much of this snowmelt occurs in primitive and wilderness mountain areas. Therefore, streamflow forecasting is primarily based on methods that estimate the accumulation of snow during the previous winter season, as well as the ablation, watershed routing, and channel routing processes which govern the transformation of moisture stored in the snowpack to streamflow.

1.2 Application of Streamflow Forecasting

Federal agencies, such as the U.S. Bureau of Reclamation and the U.S. Army Corps of engineers, rely on meteorological data and runoff forecasting for the operation of reservoirs in the Western U.S. These reservoirs are managed for municipal, industrial and agricultureal water supply, flood control, and hydropower generation, among other purposes. The conflicting demands of reservoir regulation require careful planning to maximize the benefits. Among the areas that can benefit most from improved streamflow forecasting are water supply management for hydroelectric power generation, irrigation, and municipal and industrial water supply. Hydropower

systems can benefit from more efficient allocation of reservoir storage and the reduced risk of water shortages. Irrigation systems can benefit from advance information regarding water availability for crop selection, and for planning the allocation of water to various crops. For reservoirs with both flood control and water supply purposes, improved forecasts can reduce flood damage, and can avoid the necessity of maintaining flood freeboard to the detriment of water supply storage in low flow years.

1.2.1 Hydroeletric Power Generation

Because of the large amount of water needed for power generation and the economic value of energy production, hydropower generation is among the most valuable water uses. In addition, it is potentially the largest beneficiary of improved streamflow forecasts in terms of the amount of energy produced due to improved streamflow forecasts. In addition to the value of streamflow forecasts in negotiating contracts for excess power production in high flow periods and or years, accurate short-term runoff forecasts can result in improved hydropower scheduling.

1.2.2 Irrigation

Although irrigation is second to hydropower as the largest beneficial use of water in the western U.S., it is by far the largest consumptive use. Improved streamflow forecasts can lead both to crop selection and water allocation, thereby reducing the production costs and improving crop yield. Secondary benefits in terms of reduced erosion and use of herbicides and pesticides that accompany better crop management are also likely.

1.2.3 Municipal and Industrial Water Supply

With the growth of population and the development of industry, water demands have grown substantially in the last 40 years. Municipal and industrial water supply is a highly valued water use compared to irrigation water; the provision of minimum water supply

for human use is considered essential by most water purveyors, and most industrial uses are highly valued as well. Streamflow forecasts improve water supply operation, especially in drought periods where they can reduce the risk of incorrect decissions regarding implementation of drought response measures. (see, for example, Lettenmaier, et al., 1990)

1.2.4 Other Uses

Other uses of streamflow forecasting include planning reservoir releases to enhance fish migration: streamflow forecasts are used in the Columbia River Basin of the Pacific Northwest to mitigate poor migration conditions for salmon and steelhead fingerling (Buettner, 1988). In low runoff years, hatchery smolts may be released early in order to take advantage of higher streamflow which reduces downstream travel time and hence susceptibility to predation. In addition, fish traps are set to catch smolts and transport them around some dams on the Snake River, expediting their migration to the ocean.

1.3 The Value of Streamflow Forecasts

Some publications have shown that runoff forecasts are critical to the economy of the western U.S. and that runoff forecasts are vital for efficient management of water supply, especially for agriculture and hydropower production (Shafer and Huddleson, 1984). It has been estimated by Elliott (1977) that the value of streamflow forecasts to irrigated agriculture alone is $43.3 million annually (1975 dollars). Castruccio, et al. (1981), pointed out that approximately 23 million acres of irrigated land in the West can benefit from streamflow forecasts. They estimate the annual value (1979 dollars) of snowmelt runoff to hydropower generation at $4.86 billion and irrigated agriculture at $1.74 billion in the western 11 states.

Because of the value of water for hydroelectric power generation and agricultural uses, even small improvements in forecast accuracy can produce large profits. A one percent improvement in average

forecast accuracy for the Columbia River at the Dalles, Oregon, represents a combined benefit of $6.2 million annually to hydropower and agriculture (Ramon, 1972). A six percent relative accuracy improvement in seasonal snowmelt forecasts in the Western U.S. would be worth $28.1 million per year for irrigated agriculture, and $10.1 million per year (both in 1979 dollars) for hydropower (Castruccio, et al., 1981).

These estimates demonstrate that accurate forecasts are extremely valuable. Because of the economic impact of erroneous forecasts, it is essential to understand as much as possible about streamflow forecasting methods, error sources, the relative magnitude of errors, and the prospects for better forecasts.

CHAPTER 2 LITERATURE REVIEW

2.1 Rainfall-runoff Processs

The hydrologic cycle can be divided into three subsystems: the atmospheric system which includes precipitation, evaporation, interception, and transpiration; the land surface system which includes overland flow, surface runoff, subsurface and groundwater outflow, and runoff to streams and the ocean; and the subsurface system which includes infiltration, groundwater, recharge, subsurface flow and groundwater flow. The cycle is continuous, however, the time scales vary greatly; cycling times in the atmosphere range from hours to days, in the surface system from hours to weeks, and in the subsurface system from days to years or longer.

The rainfall-runoff process is part of the hydrologic cycle. In the long-term, and in the absence of net groundwater inflow or outflow, precipitation falling on a catchment will either evaporate or transpire or will leave the catchment as runoff.

Rainfall-runoff models can be used to characterize the hydrologic cycle in such a way that runoff can be predicted, given knowledge of the temporal and spatial distribution of rainfall inputs. The models generally require knowledge of some of the physical properties of the watershed. These physical properties may include catchment area, channel configuration, surface slopes, soil types, and other surface characteristics. Initial conditions including runoff, soil moisture and groundwater level, and storage in natural and artificial impoundments must also be known for hydrologic prediction. Even though the rainfall-runoff process is well understood conceptually, the measurement of many of its components (especially the spatial distribution of precipitation and soil moisture) are difficult.

Deterministic rainfall runoff models predict runoff, given precipitation and initial conditions, by characterizing the physical

processes governing the rainfall-runoff process. Among the physical processes that must be characterized are:

(a) the relationship of infiltration to initial soil moisture and rainfall;

(b) the hydrologic routing of overland flow to the channel system;

(c) the conveyance mechanism by which water passes through the unsaturated zone to the water table and the response of the water table to precipitation;

(d) the interaction of groundwater storage with channel runoff, including the role of bank storage; and

(e) evaporation from the soil surface and the vegetation cover (Lettenmaier, 1988b).

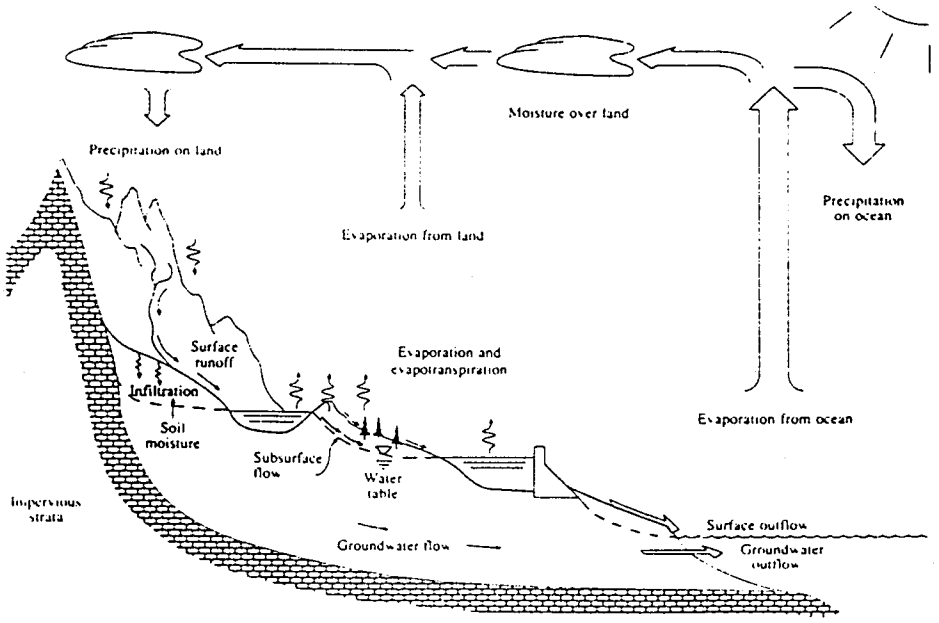

Figure 2.1 Elements of Hydrologic Cycle for A Hillslope (taken from Chow, 1976)

Fig.2-1 is an idealized conceptualization of the physical transformation of rainfall to runoff taken from Chow (1976, Chapter 1). Precipitation may be intercepted by a vegetation canopy. That

portion not intercepted may either infiltrate into the ground or, if the rainfall rate exceeds the infiltration capacity or the water table is at the land surface, it may contribute to channel runoff or may be ponded. Ponded water may either reinfiltrate or it may discharge to the stream as surface runoff, and eventually contribute to runoff. Subsurface water may also contribute to streamflow, although the stream response is usually delayed.

During flood periods, the soil moisture near the channel system may become saturated, and precipitation will contribute to direct runoff as soon as it falls on the ground. Hydrograph separation methods (see Fig. 2.2) can be used to interpret the proportion of direct runoff and baseflow in flood periods. These methods only estimate direct runoff roughly because the criteria for separation are empirical, rather than physically based.

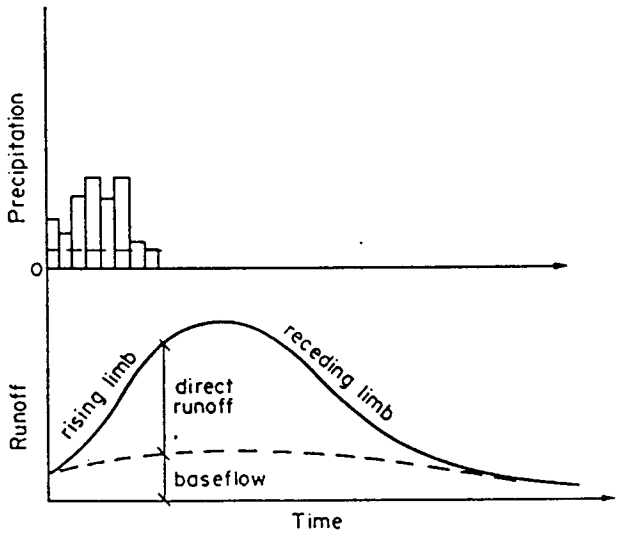

Figure 2.2 Typical Storm Hydrograph
(taken from Lettenmaier, 1988)

Prediction of the hydrologic processes is complicated because the rainfall-runoff transformation is nonlinear in the input-output

sense, and because the spatial variability of precipitation, soil properties, surface slopes and vegetation cover, as well as the channel configuration, are difficult to characterize. For these reasons, a number of approaches ranging from stochastic transfer function models to detailed physically based deterministic models have been developed for hydrologic prediction.

2.2 Hydrologic Model Classification

Hydrologic models may be divided into two categories: physical and mathematical. Physical models include scale models, such as hydraulic models which represent the system on a reduced scale; and analogue models, which exploit the behavior of another physical system which has properties similar to those of the prototype. Mathematical models attempt to characterize the system through equations that describe the interaction of the major fluxes and storages, which in turn link the input and the output variables. The input and output variables may be functions of space and time, and they may also be probabilistic or random variables which are replaced by probability distribution. In the latter case the model is termed stochastic.

Although physical models have been widely used for hydraulic prediction, and some experiments have been conducted in the laboratory to identify subsurface transport mechanisms, physical models of catchment runoff are not practical because of the multiple, conflicting mechanisms that would govern scaling from the model to the prototype. Therefore, hydrologic prediction is, for practical purposes, exclusively the province of mathematical models.

A mathematical model can be

(a) either deterministic or stochastic, depending on whether or not the variability in inputs, subsurface structure, model parameters, and model structure is explicitly considered;

(b) linear or nonlinear, depending on whether or not the model is linear in the inputs;

(c) empirical or conceptual, depending on whether or not the input-output transformation parameters are determined by theoretical consideration or are data-based; and

(d) lumped or distributed in time and space, depending on whether the principal driving variables and catchment descriptors are aggregated or distributed (Clarke, 1973).

According to Loague and Freeze (1985), and Chow (1976), five techniques are used in practice: the rational method (RM), the instantaneous unit hydrograph (IUH), input-output methods, continuous conceptual simulation models (CSM), and event conceptual simulation models (event model). Three of these techniques (input-output models, and continuous and event conceptual simulation models) are of particular interest for runoff forecasting in mountainous regions, and are described in more detail.

2.2.1 Input-Output Methods

Input-output methods are based on time series analysis transfer function theories (e.g., Box and Jenkins, 1976) which are sometimes also broadly termed the system analysis approach. The distinguishing feature of input-output methods is that relationships inferred from the data, rather than physical knowledge of the system, are used to infer the input-output relationship. The best known of these models is the autoregressive moving average (ARMA), or more generally, autoregressive moving average with external input (ARMAX) models. In such models, the input is precipitation and the output is runoff.

A general formulation of an input-output model for prediction of runoff at multiple stream gauges is:

$$R_{0t} = \sum_{i=1}^{m} \sum_{k=0}^{q_i} \alpha_{ik} \cdot P_{i,t-k} + \sum_{j=1}^{n} \sum_{k=0}^{p_j} \beta_{jk} \cdot R_{j,t-k} + \sum_{k=1}^{q_0} \alpha_{0k} \cdot R_{0,t-k} + \sum_{k=0}^{r} \gamma_{0k} \cdot \epsilon_{t-k} \quad \cdots\cdots\cdots (2.1)$$

where the input P_{it} is precipitation at gauge i at time t, and R_{jt} is upstream tributary flow at gauge j at time t. R_{0t} is predicted runoff at time t. The order (number of) of the autoregressive terms (p_j), moving average terms (q_i), and external input (r) as well as α_{ik} and β_{jk} are estimated from the data. In practice, the rainfall-runoff process is highly nonlinear and this type of linear model should not be expected to forecast adequately over a wide range of conditions. However, input- output models can be quite useful over limited ranges of conditions, e.g, forecasting of flood when runoff is governed primarily by channel routing and direct runoff from largely saturated areas, or for lengthy time steps such as monthly where nonlinearities are less important. In addition, sophisticated adaptive estimation methods exist that allow the model parameters to change depending on previous prediction error, which can compensate to some extent for nonlinearities in the input-output relationships.

Input-output methods are stochastic, partially lumped in space and distributed in time, linear, and empirical.

2.2.2 Conceptual Simulation Models — Continuous

CSM's use long records of precipitation and/or snowmelt as input, and predict runoff continuously by accounting for the movement of water accumulation and depletion of soil moisture storage. Some of the best known models in this family are the National Weather Service River Forecast System (Burnash, et al., 1973; Anderson, 1973) and HSPF (Hydrologic Simulation Program -- Fortran, Johanson et al., 1980), which is an outgrowth of the Stanford Watershed Model (Crawford and Linsley, 1966).

Implementation of a CSM requires estimation of a number of site-specific model parameters, as well as the initial model states, which are usually soil moisture storages and different conceptual zones. This is commonly done by a trial-and-error procedure, although automated procedures have also been used (e.g., Sorooshian et al., 1983). In practice, it is necessary to specify a feasible range of parameters to constrain the parameter search. In addition, CSM's

must be run for an initial period long enough to allow the effects of the initial conditions to abate. For example, when applied in regions with strongly seasonal climates, one year is usually enough to eliminate the effects of the initial conditions. Accepted practice is to ignore the first year of simulation for parameter estimation purposes. During model implementation, the historic record is usually split into independent calibration and verification periods. Because CSM's may contain a large number of parameters to be estimated, it is important to assure that the model is not overfit (that is, artificially good agreement obtained between observed and predicted runoff in calibration which can not be maintained in an independent verification period). CSM's are classified as deterministic, lumped in space and distributed in time, nonlinear and conceptual.

2.2.3 Conceptual Simulation Models – Event

Event models are usually used for prediction of storm runoff, and do not account explicitly for runoff between storms. Compared with CSM's, event models are distinguished by the following:

1) Event models use shorter time steps than CSM's, sometimes as short as minutes for very small catchments;

2) Event models are often distributed in space, usually by dividing a catchment into subcatchments, and specifying a different parameter set for each subcatchment;

3) Event models usually use surface and subsurface hydraulic properties for prediction of overland flow; and

4) Event models are often used on smaller catchments and may be considered to be more physically realistic than CSM's are.

Event models are classified as deterministic (generally), distributed in space and time, nonlinear, and conceptual.

2.3 Hydrologic Forecasting

Rainfall-runoff forecasting problems can be divided into two

categories: short-term and long-term. Short-term forecasts can be defined to have lead times of hours to days; the most common application is flood forecasting. Long-term forecasts, which are mostly applicable to water management, have lead times of weeks to months; the most common applications are to water supply or hydropower operations of reservoir systems.

According to Lettenmaier et al.,(1990), rainfall-runoff forecasting methods can be divided into three general classes: index variable, storage accounting, and conceptual simulation. Index variable methods are the simplest and the oldest methods of forecasting long-term runoff. They treat runoff as the dependent variable in a relationship, usually linear, with a set of explanatory index variables, such as previous precipitation or snowpack, which are likely to affect future runoff. Storage accounting models attempt to estimate the amount of water stored in a catchment (either as surface, subsurface, or snowpack storage) that is available to contribute to future runoff; the forecast is some (linear) function of the storage estimate. The conceptual simulation approach makes use of a CSM run up the time of forecast using observed precipitation and temperature, and throughout the forecast period using an estimate of future precipitation. Each of these forecast model types is discussed below.

2.3.1 Index Variable Methods

Early index methods generally used graphical techniques (for example, Linsley et al., 1958). Later, statistical techniques such as multiple regression, principle components, and pattern search were introduced (Marsden and Davis, 1968; Zuzel et al., 1975). Statistical and stochastic models are now the most commonly used approaches in this class. Stochastic or time-series methods have been used to forecast streamflow, usually using only streamflow in previous time period(s) as the dependent variable(s). These methods fall into the class of stationary autoregressive moving average models, and can be expressed as

$$R_t = \sum_{i=1}^{p} \alpha_i R_{t-i} + \sum_{j=0}^{q} \beta_j \epsilon_{t-j} + C \quad \text{.....(2.2)}$$

where the ϵ_i are uncorrelated (white) noise terms, and α_i and β_j are estimated from data directly, as are the p and q. Eq.2.2 is a special case of the input-output method (Eq 2.1) for which there is only one gauge used and no external input. In the case where there is an external input,

$$R_t = \sum_{k=0}^{q_i} \alpha_k \cdot P_{t-k} + \sum_{k=0}^{p_j} \beta_k \cdot R_{t-k} + \sum_{k=1}^{q_0} \alpha_k \cdot R_{t-k} + \sum_{k=0}^{r} \gamma_k \cdot \epsilon_{t-k} + C$$

$$= \sum_{k=1}^{p} a_k \cdot R_{t-k} + \sum_{j=0}^{q} b_j \cdot P_{t-j} + \sum_{l=0}^{r} c_l \cdot \epsilon_{t-l} + C \quad \text{.....(2.3)}$$

It is assumed that the present state depends on the previous states (R_{t-j}) and external input (P_{t-j}) as well as having some noise terms (ϵ_{t-j}). Time series models usually perform best when little or no rainfall occurs and the basin acts like a linear reservoir.

Index methods have the major advantage of being simple and easily implemented. Virtually all statistical packages available for small computers have multiple regression and other applicable routines for implementing index variable forecasts. Moreover, index methods are well adapted to risk analysis, since most stochastic and statistical methods predict the forecast error distribution as well as the "best" forecast. In practice, the forecast error distribution is often more important than the " best " forecast (Hirsch, 1981).

The primary drawback to index methods is that the relationship between the dependent and explanatory variable must be linear; therefore, while acceptable forecasts may result in average years, the method can break down in extreme years, in which the forecasts are most important. For example, one problem encountered in snowmelt runoff forecasting is that regression methods can yield negative runoff forecasts in very dry years.

2.3.2 Storage Accounting

Storage accounting models are based on the concept that runoff in a future forecast period is determined by the amount of water presently in storage in a catchment and forecast period precipitation. This idea was introduced by Tangborn and Rasmussen (1976) for forecasting of snowmelt runoff. They suggested that basin storage (S_t) should be estimated as a linear function of precipitation less runoff (R_t) : $S_t = a + bP_t - R_t$, where P_t is the total precipitation (up to the forecast date) at one or more precipitation gage, and R_t is the total runoff in the same period. Later, Tangborn (1977) suggested that the coefficients a and b be estimated by regression.

The model can be thought of as a special case of the index variable methods with regression estimates. Tangborn (1977) also suggested that improved forecast accuracy could be obtained by using an observed runoff period, prior to the forecast date, to correct forecast errors. The basin moisture storage (S_1) is estimated from the observed streamflow on the forecast date, and the simulated water storage (S_2) is obtained from the soil moisture accounting model; the observed cumulative runoff (Q_1) is the total runoff from a beginning date (T_0) to the forecast date (T_1), and the predicted cumulative runoff (Q_2) is the accumulation of the predicted runoff in the same period. To adjust the soil moisture storage to update the runoff prediction, the regression equation $\Delta S = S_1 - S_2 = a*(Q_1 - Q_2) + b$ can be used to determine how much adjustment of the water storage is needed. A more efficient approach was developed by Stedinger (1989). He showed that a modified storage accounting model which used snowpack and precipitation for basin water storage estimation performed better than a storage accounting model using precipitation only.

2.3.3 Conceptual Models

Extended Streamflow Prediction (ESP), as termed by National Weather Service, is an application of CSM's to long-term forecasting. In

ESP, a CSM is run with recorded meteorological data up to the time of forecast. During the forecast period, the model input is one of the following: (1) all sequences of the historical data during the forecasting period; (2) a range of high, medium and low historic precipitation; or (3) synthetically generated realizations of possible future meteorology, which can be weighted according to their prior probabilities.

The inputs usually have a time scale of one day or less, and the model is run with observed inputs to the forecast date. Because soil moisture storage is estimated by CSM's given precipitation, ESP should give an accurate forecast of runoff if the forecast period precipitation actually occurring is similar to that used in making the forecasts. Because forecast period runoff is dominated by antecedent soil moisture storage during years or seasons when little precipitation occurs in the forecast period, ESP forecasts can be quite accurate in these conditions. In particular, ESP forecasts should perform well under drought conditions. This hypothesis is evaluated in Chapter 5.

The advantage of ESP is that it incorporates a physical understanding of the processes contributing to runoff so that forecasters can evaluate not only the "best" forecast, but can evaluate alternative scenarios as well. This can be especially useful during droughts, when evaluation of "worst case" scenarios may be needed. The disadvantage of ESP is that data requirements are much greater than for the simple models, since the time scale of the model is much shorter. Further, the quality of forecasts depends on the calibration procedure (Lettenmaier, 1984). In addition, the performance of ESP method is dependent on the particular CSM used. Model selection can be time consuming; most commonly it is accomplished based on evaluation criteria other than direct comparison, which is often unproductive due to differences in model data requirements and other model restrictions (WMO, 1975; 1986).

2.4 Forecasting Errors

There are three sources of long-term forecasting errors: climate variability, model error, and data error (Schaake and Peck, 1985). Climatic variability is usually the largest source of forecast error. It results from the inability to obtain meteorological forecasts much better than climatic averages for forecast lead times exceeding several days. Therefore, for practical purposes, accurate long-term runoff forecasts are possible only in situations where the variables affecting future runoff (through variations in soil or snow water storage) can be measured at the time of forecast. Model error results from lack of perfect knowledge of the physical processes governing snowmelt and the rainfall to runoff transformation, as well as spatial variability in catchment properties which must be idealized to some extent, especially in spatially lumped models. Even with perfect knowledge of the present states of the hydrologic process and future inputs, most models still cannot fully describe the evolution of the underlying processes. Data error is the result of errors in representation of spatially distributed inputs by a small number of point (station) measurements, in addition to measurement error due to sensor inaccuracies, data transmission problems, and human factors.

2.5 Summary

Streamflow forecasts are based on the present or previous states of the hydrologic processes, in particular snow and soil moisture storage, as well as future meteorological inputs. Hydrologic forecasts can be classified as short-term and long-term. Short-term forecasts are applicable to real time operation of water management systems, and for flood warning. Long-term forecasts are more applicable to operation and management of water supply systems. Of major concern in the use of long-term forecasts is the issue of forecast uncertainty. Forecast accuracy is an important determinant of the accuracy with which a water resource system can be operated, therefore there are important potential economic benefits associated

with improvements in forecast accuracy.

Among possible approaches that could reduce forecasting errors are the use of optimization schemes for updating future forecasts. The lack of updating has been identified by several authors (e.g., Dawdy, 1984) as a major shortcoming in many current forecasting procedures. As a result of model and input error, forecast models may not properly track the true system state up to the forecast time. This is especially of concern when CSM's are used. Updating amounts to adjustment of the model state, (usually using predicted soil moisture and snow water storage) to best reflect knowledge of the current system state. In chapter 5, a simple updating scheme is evaluated for ESP forecasting.

CHAPTER 3 EXPERIMENTAL DESIGN I - HYDROLOGIC MODELS

3.1 Model Selection

Model selection is the first step in designing a streamflow forecasting system. Many models have been used for streamflow forecasting in mountainous regions; Howard and Associates (1989) reviewed three models (CHARMS, HSPF, and NWSRFS) that might be suitable for forecasting inflows to Chester Morse Reservoir in the Cedar River Watershed, of which the Rex River (studied in detail in this project) is a tributary. In this section, the criteria used for the selection of the two models evaluated in this thesis are reviewed.

The criteria for hydrologic model selection have been described by James and Burges, 1978. They recommend four watershed simulation model selection criteria: 1) the model must provide the kind of information needed; 2) the watershed characteristics represented by the model parameters must in fact govern watershed response in the intended application; 3) the equations used must be in agreement with the state of the art, available data, and available computer facilities; and 4) the model must provide results within the required time frame which are suitable for the interested usages, and are of acceptable quality at a reasonable cost.

Howard and Associates (1989) further discuss model selection criteria. They suggest the following: 1) the models must be compatible with watershed hydrology, and with existing temporal and spatial data; 2) the models must be able to provide output at the desired time steps such as seasonal and short-term forecasts; 3) the models must be able to provide estimates of forecast uncertainty, and be accurate at low flows; and 4) the model source codes must be available and the cost of model implementation must be considered.

From the above studies, the criteria for model selection used in this study are: 1) the models must have the ability to provide not only daily simulation but also seasonal forecasts; in this thesis

forecast accuracy for time periods from one week to seasonal (months) are evaluated; 2) the model's source code must be available and the models must be consistent with the ESP structure, which is a major focus of this work; 3) the models must be suitable for existing temporal and spatial data for the Rex River watershed; these data include daily maximum and minimum temperature, precipitation and runoff; and 4) the models must have been proven in previous applications that they can perform well under extreme conditions.

The two models selected for this study are the NWSRFS snow accumulation and ablation model, coupled with the so-called Nanjing model and a time-series model. The NWSRFS has previously been used in a number of studies in the Northwest including water supply forecasting in the Cedar River basin (Lettenmaier et al., 1980) and assessment of the effects of Mt. St. Helens' eruption on downstream flooding (Lettenmaier and Burges, 1980).

3.2 Studied Watershed–Rex River Basin

The Rex River basin lies southeast of Cedar Falls, Washington, in the Snoqualmie National Forest. Its drainage area is 13.4 square miles; the average discharge for the 40 year period 1945-1985 was 104.4 inches per year; with a range from 0.85 inches (August) to 19.17 inches (April). The monthly coefficient of variation range from 0.014 (July) to 0.27 (April). The maximum elevation of the catchment is about 4450 ft.; the elevation at the USGS gauge is 1600 ft. Figure 3.1 gives the location of Rex River Basin and Figure 3.2 shows the relationship between elevation and drainage area which is computed from the USGS 90 meter digital elevation map of the catchment.

3.3 Experimental Design

Figure 3.3 shows the experimental design schematically. The implementation of the two hydrologic models is described in this chapter; forecasting methods are described Chapter 4.

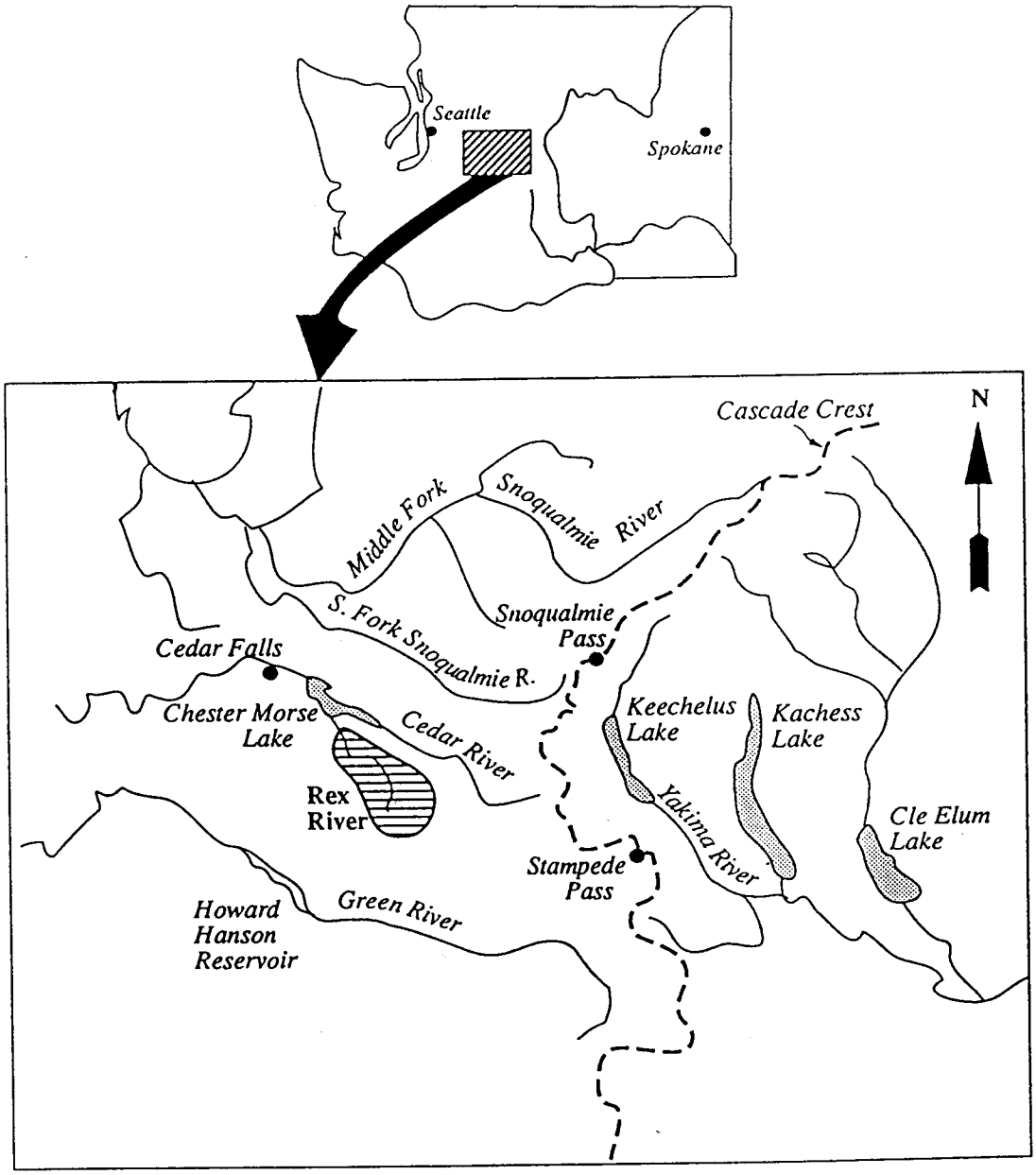

Figure 3.1 Rex River Basin Location map

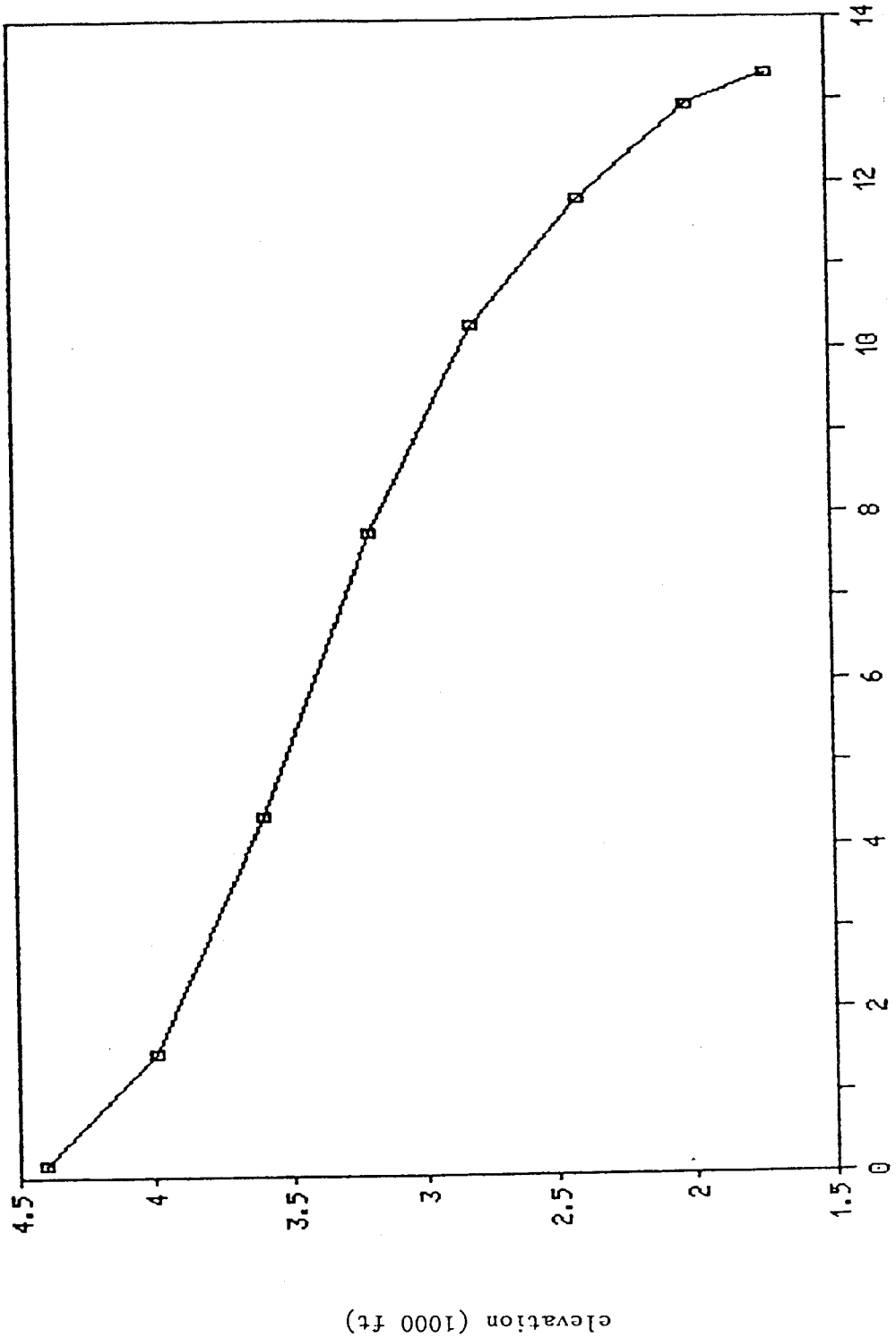

Figure 3.2 Hypsometric Curve – Rex River Basin
(After Howard & Associates, 1989)

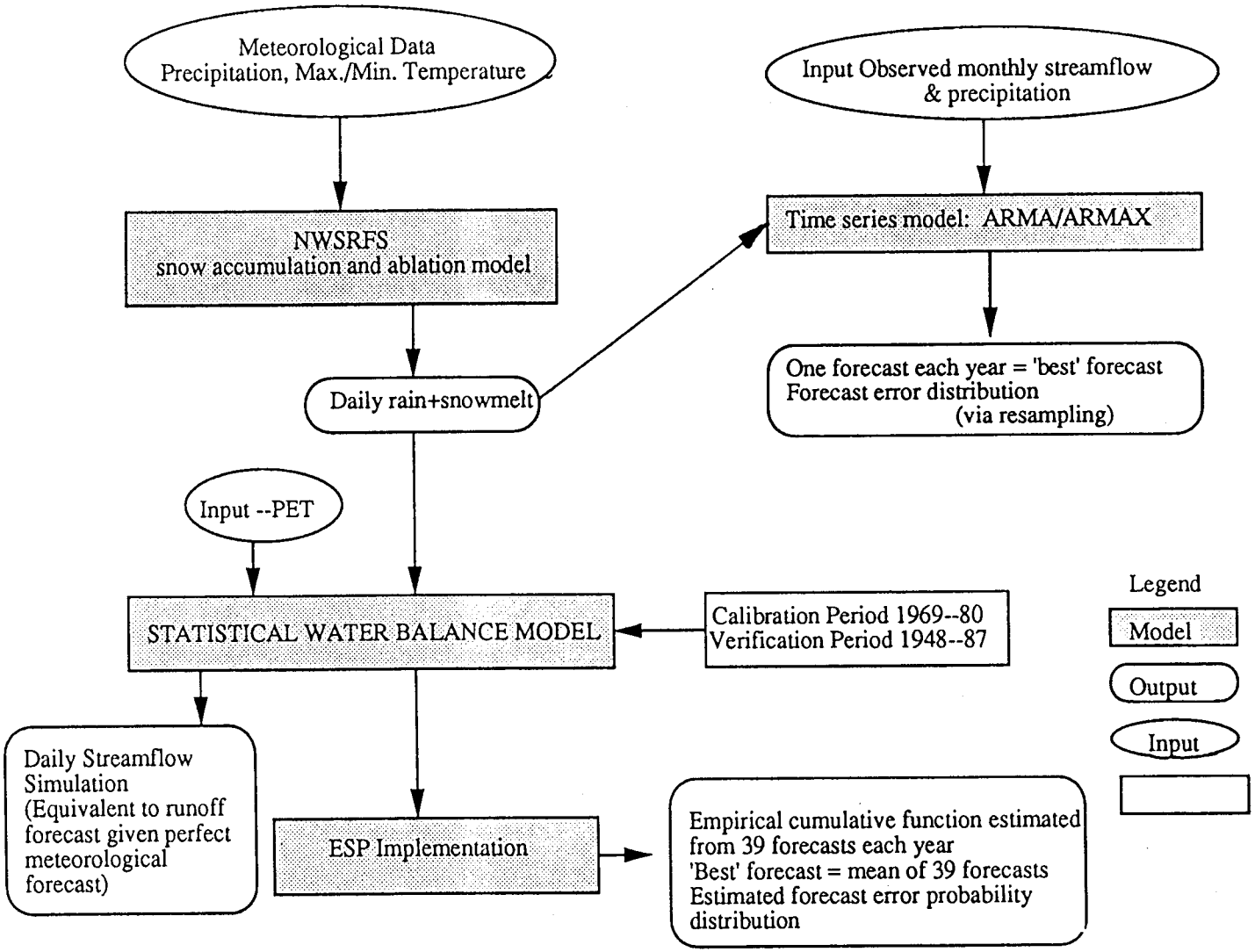

Figure 3.3 Forecast Model Implementation

3.4 Snowmelt Model

3.4.1 Model Introduction

The snowmelt model used was developed by Eric Anderson of the U.S. National Weather Service Hydrologic Research Laboratory (Anderson, 1973). The model performs a balance of energy and mass of the snowpack, using a simplified formulation of the energy budget where the dominant terms are indexed to air temperature, based on heat exchange in the snowpack.

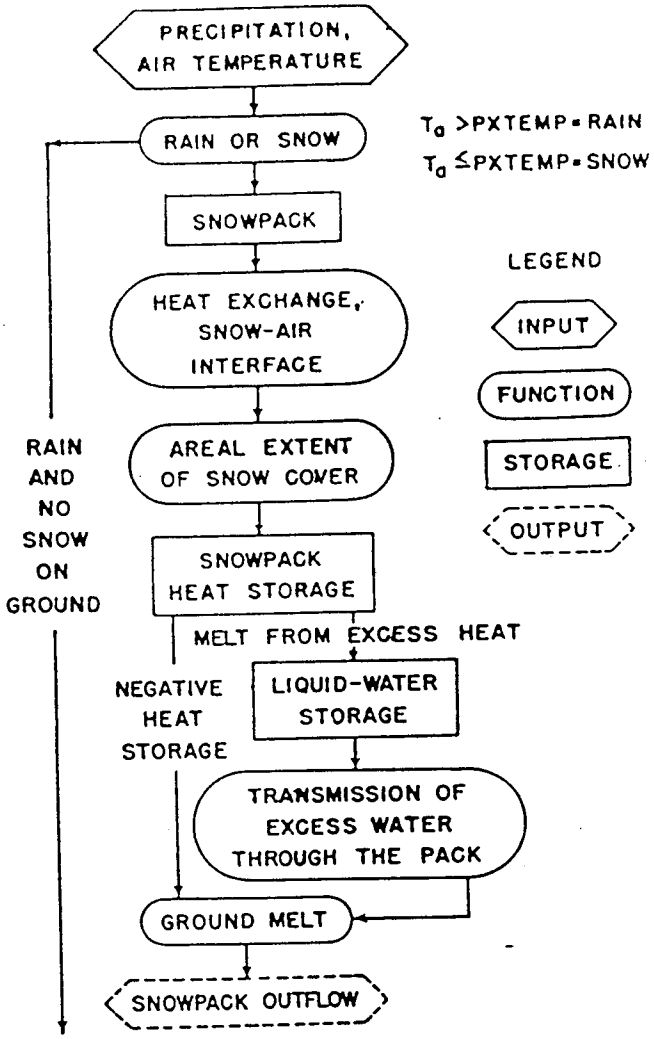

Figure 3.4 Flowchart of Snow Accumulation and Ablation Model (After Anderson (1973))

Figure 3.4 is a flowchart of the snow accumulation and ablation model. This flowchart shows each of the physical components which are represented in the model. They include water accumulation in the snowpack, heat exchange at the air-snow interface, areal extent of snow cover, heat storage within the snowpack, liquid-water retention and transmission, and heat exchange at the soil-snow interface (Anderson, 1973). A brief discussion of each of these components follows.

Air temperature is used as an index to determine whether the form of precipitation is rain or snow. In this application the critical temperature was set to 32°F. Heat exchange at the air-snow interface is the most critical factor controlling the ablation of a snowpack. The model uses air temperature as the index for the heat exchange mechanisms which control heat flow into or out of the snowpack. Two basic conditions for heat exchange are determined by the model, depending on whether or not the air is warm enough for snowmelt to take place at the snow surface. The percent of the area covered by snow must be estimated to determine the area over which heat exchange can take place, and to determine how much rain falls on bare ground.

Snowpack heat storage is continuously accumulated in the model. The heat storage of snowpack is assumed to be zero when the snowpack is isothermal at 32°F, and becomes negative when heat is transferred from snow to air.

The snowpack is assumed to retain and transmit liquid-water in the same manner as a soil column. Liquid-water retention is a constant (the percent of liquid-water holding capacity) multiplied by the water equivalent of the solid portion of the snowpack. Liquid-water transmission is computed from the amount of excess liquid-water stored in the snowpack at the beginning of the period and the amount of lagged inflow for the current period. Heat exchange at the soil-snow interface is assumed to be small compared to the heat exchange at the snow-air interface. The model assumes that the rate of snowmelt at the soil-snow interface is constant.

3.4.2 The Model Input-output

The input data to the model are limited to daily precipitation and maximum/minimum temperature, because other information on which the snowpack energy budget must be based is not usually obtainable in mountainous areas. Daily precipitation is interpolated to six-hour increments. Six-hour temperatures are estimated from daily maximum/minimum temperatures, using equations given by Anderson (1973).

The model output is simulated effective precipitation (rain plus snowmelt) which is determined by a set of equations that describe the energy exchange in the storage of snowpack and by using a critical temperature T_0 (32°F) to decide whether or not snowmelt occurs. The conditions influencing whether or not the snowmelt occurs are summarized in Table 3.1.

Table 3.1 National Weather Service River Forecast System Snowmelt Model Summary

	No Precipitation	Precipitation
$T > T_0$	Type I	Type I & Type II
$T < T_0$	Type III	Type III

Type I: Air temperature is greater than T_0; snowmelt will occur if the ground is not bare.

Type II: Bare ground, no snowmelt computation.

Type III: Temperature is not high enough to have snow melt.

In short, snowmelt computation is only performed under Type I conditions.

3.4.3 Model Calibration and Verification Introduction

Calibration of the snow accumulation and ablation model is accomplished by a combination of trial-and-error and automatic parameter optimization. Usually, both the snowmelt model and the

soil moisture model are run together and the objective function is some measure of the difference between observed and simulated streamflow while simulated snow water equivalent from the snowpack can be compared with observations, the observations often represent areal average conditions poorly so the calibration usually relies primarily on runoff errors. The procedure is implemented as follows: 1) select the initial parameter values for both the snowmelt model and the runoff model, 2) simulate the entire calibration data period by running the two models, 3) check the performance of simulated streamflows , and 4) repeat from step 2 on until the simulations are reasonable.

3.5 Rainfall-runoff Model

3.5.1 Model Theory

The so-called Nanjing model was developed at the Water Resources Institute in Nanjing, China. D.P. Lettenmaier and E.F. Wood (unpublished) have experimented with this model for simulation of summer flows for the Cedar River above USGS gage 12-1150; the results suggest that the model is adaptable to Northwest conditions and lead to the research reported herein. The model is described in more detailed by Wood et al., (1990); the presentation here is intended to give only a general overview of the model dynamics.

The input data are precipitation, measured streamflow, and estimated evaporation. For application to mountainous watersheds, pseudo-precipitation (rain plus melt) obtained from a snowmelt model is used instead of raw precipitation.

The Nanjing model is a simplified conceptual model, which links the spatial distribution of soil moisture to storm runoff response. The model is described by the following equations.

Infiltration capacity (i_0):

$$i_0 = i_m[1-(1- W_0/W_m)^{1/B}] \qquad (3.1)$$

where W_0 is soil moisture storage, W_m is total soil moisture capacity, and i_m is maximum infiltration capacity.

Evaporation (e):

$$\frac{e}{e_p} = 1-[1-(W_0/W_m)]^{1/B_e} \tag{3.2}$$

where e_p is the potential evaporation, and B_e is evaporation coefficient.

Baseflow (R_b):

$$R_b = K_b W_0 \tag{3.3}$$

where K_b is recession ratio of soil moisture.

Direct runoff (R_d):

$$R_d = p-(W_m-W_0) \qquad \text{if } i_0+p > i_m \tag{3.4a}$$

$$R_d = p-(W_m-W_0)+W_m*[1-\frac{i_0+p}{i_m}]^{1+B} \qquad \text{if } i_0+p \le i_m \tag{3.4b}$$

where p is precipitation, and B is a function of time step.

Total runoff (R):

$$R = R_b + R_d \tag{3.5}$$

If there is no rainfall, runoff is equal to baseflow; if there is rainfall, streamflow is the sum of baseflow and direct runoff where the latter is a function of antecedent soil moisture distribution (see section 3.5.2) and precipitation.

3.5.2 Model Approach

The motivation for the Nanjing model is that infiltration can be related to precipitation and the spatial distribution of antecedent soil moisture, as shown in Figure 3.5, which represents soil moisture as a function of fractional basin area of the form as in eq. 3.6

$$A = 1-(1-\frac{i}{i_m})^B \tag{3.6}$$

where i is infiltration capacity (in practice calculated from antecedent soil moisture), and i_m is the maximum infiltration capacity (see Figure 3.5).

The maximum moisture storage capacity in the basin is W_m which is integrated from eq. 3.6 as follows:

$$W_m = i_m - \int_0^{i_m} A \, di = i_m - \int_0^{i_m} [\, 1 - (1 - \frac{i}{i_m})^B \,] \, di$$

$$= i_m - i_m + \int_0^{i_m} (1 - \frac{i}{i_m})^B di$$

$$= -\frac{i_m}{B+1} (1 - \frac{i}{i_m})^{B+1} \Big|_{i=0}^{i=i_m} = \frac{i_m}{B+1} \qquad (3.7)$$

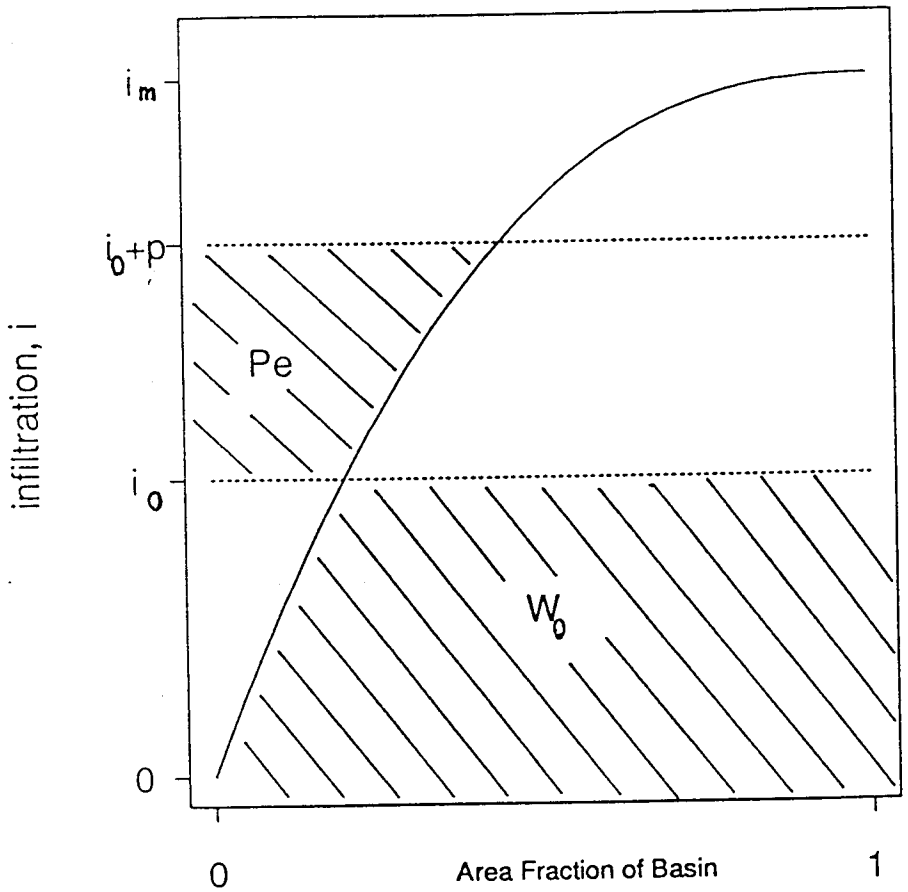

Figure 3.5 Saturated Fraction of Basin

The moisture storage at time t is W_0 integrated from eq.3.6 as follows:

$$W_0 = i_0 - \int_0^{i_0} A\, di = i_0 - \int_0^{i_0} [\, 1 - (1 - \frac{i}{i_m})^B \,]\, di$$

$$= -\frac{i_m}{B+1}\,(1-\frac{i}{i_m})^{B+1}\Big|_{i=0}^{i=i_0}$$

$$= \frac{i_m}{B+1}\,[1-(1-\frac{i_0}{i_m})^{B+1}]$$

$$= W_m[1-(1-\frac{i_0}{i_m})^{B+1}] \qquad (3.8)$$

from eq. 3.8

$$i_0 = i_m * [1-(1-\frac{W_0}{W_m})^{1/(B+1)}] \qquad (3.9)$$

$$1-\frac{W_0}{W_m} = (1-\frac{i_0}{i_m})^{B+1} \qquad (3.10)$$

If we now define the effective precipitation P_e to be equal to the direct runoff, then at time t, the effective precipitation is integrated from eq. 3.6 as

$$R_d = P_e = \int_{i_0}^{i_0+P} A\, di = \int_{i_0}^{i_0+P} [\, 1 - (1 - \frac{i_0}{i_m})^B \,]\, di$$

$$= P + \frac{i_m}{B+1}(1-\frac{i_0+P}{i_m})^{B+1} - \frac{i_m}{B+1}(1-\frac{i_0}{i_m})^{B+1}$$

substituting eq.(3.10),

$$R_d = P + W_m(1-\frac{i_0+P}{i_m})^{B+1} - \frac{i_m}{B+1}(1-\frac{W_0}{W_m})$$

$$= P + W_m(1-\frac{i_0+P}{i_m})^{B+1} - (W_m - W_0)$$

$$= P - (W_m - W_0) + W_m(1-W)^{B+1} \qquad (3.11)$$

where $W = \frac{i_0+P}{i_m}$, $0 \le W \le 1$; if $W > 1$ then $R_d = p - (W_m - W_0)$.

In practice, observed precipitation must be scaled to obtain basin precipitation as

$$P = P_{obs} * F_p \tag{3.12}$$

Likewise, estimated potential evaporation usually must be adjusted by a calibration parameter as

$$e = e_p * F_e * [1 - (1 - \frac{W_0}{W_m})^{1/B_e}] \tag{3.13}$$

Baseflow is calculated using a linear recession:

$$R_b = K_b * W_0 \tag{3.14}$$

Total runoff is then the sum of base flow and direct runoff:

$$Q = R_d + R_b \tag{3.15}$$

The water balance equation is computed by updating the soil moisture from the previous time step by adding infiltration and subtracting baseflow and evaporation:

$$W_0^{+} = W_0^{-} + i_0 - R_b - e \tag{3.16}$$

W_0^{-}, which represents the soil moisture storage at the end of the previous time step, is used for W_0 in the above eqs.; and W_0^{+} is the updated soil moisture storage.

In the above equations, the following notation is used:

e_p = potential evaporation
B_e = evaporation equation parameter
F_e = adjusted factor of evaporation
p = precipitation
F_p = precipitation adjustment factor.
W_m = Maximum capacity for infiltration and evaporation
B = point infiltration/area ratio

In this study, the model was applied at the daily time scale so the output was predicted daily streamflow, soil moisture storage, and infiltration.

Table 3.2 summarizes the model equations and parameters:

Table 3.2 Nanjing Model Summary

Flux	Parameters
Infiltration	
$i(t)=i_m*[1-(1-\frac{W_0(t)}{W_m})^{1/(1+B)}]$	B, W_m
Runoff	
$R_d(t)=p(t)-i(t)$	
$R_b(t)=K_b*W_0(t)$	
$Q(t)=R_d(t)+R_b(t)$	K_b
Evaporation	
$e(t)=e_p*F_e*[1-(1-\frac{W_0(t)}{W_m})^{1/B_e}]$	F_e, B_e
Precipitation	
$p(t)=p_{obs}(t)*F_p$	F_p
Soil Moisture	
$W_0(t+1)=W_0(t)+i_0(t)-R_b(t)-e(t)$	

3.6 Snowmelt Model Implementation

As with the soil moisture model, the snowmelt model is implemented in two steps. The first is calibration, for which an initial set of parameters is used, and through a manual trial-and-error search procedure the final model parameters are estimated. The second step is model verification, which is used to confirm that the model performs adequately during a period of record which is separate from the period used to estimate the parameters. There are thirteen parameters calibrated in the snowmwlt model, but most of them are either fixed physical constants, or can only vary in a relatively small range. The definitions of the snowmwlt model parameters and

their values are given in Appendix A.

The snowmelt model input data are daily precipitation and maximum/minimum temperatures from two meteorological stations, Cedar Lake and Stampede pass. The snowmelt model was implemented for three elevation bands; temperatures for each elevation band were interpolated, using data from the Stampede Pass and Cedar Lake stations. Table 3.3 gives the directions and locations of the streamflow gage, and the two hydrometeorological stations. The elevation of the three elevation bands, and the fraction of the basin represented, are given in Table 3.4.

Table 3.3 Hydrometeorological Stations Used in Snowmelt Model

Station	Elevation(ft)	Latitude	Longitude	Variables
Rex River	1600	47 21	121 39	streamflow
Stampede Pass	3958	47 17	121 20	P,T[a]
Cedar Lake	1560	47 25	121 94	P,T[a]

[a] P:precipitation, T:temperature

Table 3.4 Characteristics of Elevation Bands

	Median	Reference Meteorological Stations		
Zone	Elevation(m)	Precipitation	Temperature[a]	Fraction of Basin
1	670	Cedar Lake	Stampede Pass, Cedar Lake	0.228
2	975	Stampede Pass	Stampede Pass, Cedar Lake	0.445
3	1219	Stampede Pass	Stampede Pass, Cedar Lake	0.327

[a] interpolated

Two approaches to estimating elevation band temperatures were considered. The most commonly used approach is to use a single station with a fixed lapse rate. The other, which was used in this study, interpolates the temperature from high and low elevation stations to compute an "actual" lapse rate. Consideration was given

to partitioning the elevation bands by aspect. However, the temperature based energy and mass balance computations in the model do not make use of aspect information directly, so this was not pursued.

In this study, the primary purpose of running the snowmelt model was to simulate effective precipitation (rain plus melt) which is the input to the soil moisture (runoff) model. The snowmelt model runs on six-hour time steps, with the results were aggregated to daily and summed over the three elevation bands. Snowmelt model parameters previously estimated for the Rex River basin were used (CDD Howard and Associates, 1989).

3.7 Rainfall-runoff Model Implementation

3.7.1 Input Data

The Nanjing model requires time series of three variables for model calibration: streamflow, effective precipitation, and potential evaporation. For this study, the model was run at a daily time step. The origin of the daily streamflow, effective precipitation, and evaporation are described briefly as follows:

Daily observed streamflow data were taken from U.S. Geological Survey records. The 1983 U.S. Geological Water Resource Data for Washington rates the Rex River record as excellent, which means that more than 95 percent of the reported daily values are expected to be within 5 percent of the true streamflow. The period of record for the Rex River station (USGS gage 12-1155) is 1945 to the present; our analysis was based on water years 1948 to 1987.

Daily effective precipitation data is rainfall plus snowmelt, which is the output from the NWSRFS snow accumulation and ablation model as described above. These data were taken from National Climatic Data Center magnetic tapes.

Daily evaporation data were not available directly. Instead, long-term climatological estimates were used, based on the same method employed by the NWSRFS soil moisture accounting model. It computes daily evaporation by interpolating linearly between the sixteenth day of each month. For example, if the daily mean evaporation of June is 0.15 inch and for July it is 0.19 inch; the evaporation of Jun.16 is then set to equal to 0.15 inch and that of July 16 is set to equal to 0.19 inch. The amount of evaporation for each day between June 16 and July 16 is

$0.15 + i*(0.19-0.15)/30,\ i=1,2,\ldots,30,$

where i means the number of days past June 16. Climatological average daily evaporation (interpolated from monthly to daily values) adjusted from the Puyallup Experiment Station by CDD Howard and Associates (1989) was used.

3.7.2 Model Calibration and Verification

Calibration:

The Nanjing model has six calibration parameters:

W_m: the maximum capacity of moisture storage
B: point infiltration/area ratio
B_e : evaporation equation parameter
K_b: baseflow parameter (recession ratio)
F_e: evaporation scaling factor
F_p: precipitation scaling factor

Calibration was based on the 12-year (1969-1980) period of record. Calibration was performed using the same optimization algorithm (Nelder-Mead method) employed by the National Weather Service River Forecast Model (Gan, 1988), but the initial values and upper and lower bounds in the parameter searches were determined manually. The optimization algorithm allows three types of objective functions:

1. $\sum(Q_{obs}-Q_{pred})^2$;
2. $\sum(\text{Log}(Q_{obs}) - \text{Log}(Q_{pred}))^2$
3. $\sum((Q_{obs} - Q_{pred})/Q_{obs})^2$, where

Q_{obs} is observed streamflow; and Q_{pred} is predicted streamflow.

Using the same initial values and constraints for the parameter set in different objective functions leads to different parameter estimates. The final decision as to objective function was based on the magnitude of the mean monthly and annual errors, and on consideration of the physical realism of the parameter values identified (for instance, the parameter estimate values generally not at the bounds). Other considerations include how close the inferred annual evaporation is to the climatological average, and a review of the simulated and observed hydrographics. Table 3.5 shows the optimized values of the parameters.

Table 3.5 Optimized Parameter Values and Ranges

Parameter Name	Value	Lower Limit	Upper Limit	Unit
W_m	150.010	1.00	200.01	mm
B	0.432	0.01	3.50	--
B_e	0.857	0.01	1.00	--
K_b	0.050	0.01	1.00	1/day
F_e	1.162	0.50	2.00	--
F_p	1.238	0.90	2.00	--

Verification

The general approach to model verification is to use an independent period of data to confirm that the model still performs properly under conditions which are different from those which were present during the period used for calibration.

Two verification approaches were used in this study. The first was to compare the simulated runoff from the Nanjing model with that of three other rainfall-runoff models applied to the Rex River in a

previous study (Howard & Associates, 1989): CHARMS (Charles Howard and Associates Runoff Modeling System) model, the HSPF (Hydrologic Simulation Program --Fortran) model, and the NWSRFS (National Weather Service River Forecast System) soil moisture model. Table 3.6 summarizes the comparison of these three rainfall-runoff models for the Rex River Basin. The results show that the simulated runoff from the Nanjing model was quite close to that of the NWSRFS soil moisture accounting model. The other method of verification was to simulate runoff for the entire 40-year data sequence to determine how the model performs. Table 3.7 gives the average monthly and annual error statistics.

In Table 3.6, the poor performance years for the Nanjing model are the same as for the NWSRFS model. This might be due to snowmelt or data errors, because these two models both used the psuedo-precipitation data generated from the NWSRFS snow accumulation and ablation model with the same input data (CHARMS and HSPF use different snowmelt models). The model replication of the observed streamflow ranges from good to poor, with the widest variation most commonly noted during the extreme years and/or when there are some problems in the model itself. For example, Figure 3.6 shows how the simulated runoff fits the observed runoff in water year 1963. Figure 3.7 shows the worst result from the Nanjing model, 1954. Simular results for all other years in the 1969-80 verification period are given in Appendix B.

3.7.3 Forecast Analysis

Although model verification was carried out as described above, an accuracy analysis can be made also. C_p, the coefficient of prediction, is used as the measure of forecast accuracy (Tangborn, 1977). It is defined as:

$$C_p = 1 - \frac{\mathrm{Var}(Q_{pre} - Q_{obs})}{\mathrm{Var}(Q_{obs})}$$

where Var(.) is the statistical variance, Q_{pre} is the predicted

streamflow, and Q_{obs} is the observed streamflow. If simulated streamflows are used for Q_{pre}, C_p is an indication of the limiting forecast accuracy, that is, the forecast accuracy that would be achieved if future meteorological conditions were known perfectly. C_p normally ranges between 0.0 and 1.0, where a value of 0.0 corresponds to forecasts that are always exactly the historical mean flow, and 1.0 corresponds to perfect forecasts. Ideally, if there were no data or model error, a C_p of 1.0 would be achievable if simulated flows were used for Q_{pre}. Figure 3.8 shows that this is not the case. The predictions in May, especially, have poor C_p's because the mean daily temperature and precipitation in May have greater variance than in any other month. May also has large, and highly variable, streamflows.

3.7.4 Model Application

Once the model has been calibrated, it can be implemented with real-time hydrometeorologic data to forecast streamflow. The model can also be used to simulate long-term sequences of runoff for record extension. In this project, the purpose of the model was to be incorporated into an extended streamflow prediction algorithm. Implementation of the model for this purpose is described in the next chapter.

Table 3.6 Comparison of Simulation Results for The Rex River Basin for Four Snowmelt-rainfll-runoff Models: Average Annual Flows (in inches) for Water Year 1969-80

CHARMS model (from Howard & Associates, 1989)

Year	Observed	Modeled	Abs. Error
1969	100	94	6
1970	85	87	2
1971	124	122	2
1972	145	126	19
1973	73	82	9
1974	145	133	12
1975	104	112	8
1976	131	125	6
1977	64	77	13
1978	98	102	4
1979	82	81	1
1980	81	91	10
Average	102.7	102.8	7.7

HSPF model (from Howard & Associates, 1989)

Observed	Modeled	Abs. Error
100	93	7
85	88	3
124	125	1
145	130	15
73	83	10
145	137	8
104	109	5
131	131	0
64	73	9
98	106	8
82	82	0
81	89	8
102.7	103.8	6.2

NWSRFS model (from Howard & Associates, 1989)

Year	Observed	Modeled	Abs. Error
1969	100	111	11
1970	85	80	5
1971	124	113	11
1972	145	141	4
1973	73	70	3
1974	145	129	16
1975	104	110	6
1976	131	138	7
1977	64	72	8
1978	98	104	6
1979	82	76	6
1980	81	79	2
Average	102.8	101.9	7.1

Nanjing model

Observed	Modeled	Abs. Error
100	91	9
85	92	6
124	143	15
145	156	7
73	79	8
145	169	16
104	102	2
131	129	2
64	54	16
98	95	3
82	88	7
81	82	1
102.8	101.7	7.7

Table 3.7 Mean Absolute Monthly and Annual Errors (in percent) for Nanjing Model Simulation

YEAR	OBSERVED (inches)	MODELED (inches)	ANNUAL ERROR (percent)	MEAN MONTHLY ERROR (percent)
1948	119.16	133.54	12.07	16.08
1949	100.87	113.00	12.03	42.13
1950	124.27	128.25	3.20	24.54
1951	109.32	116.62	6.68	37.12
1952	79.55	73.93	7.06	25.79
1953	88.86	85.73	3.53	43.34
1954	119.10	109.44	8.11	23.95
1955	101.06	99.31	1.73	24.73
1956	121.38	132.85	9.45	36.92
1957	103.01	109.91	6.70	18.42
1958	75.54	69.58	7.89	40.25
1959	143.95	154.98	7.66	14.63
1960	112.51	109.80	2.41	19.94
1961	113.81	117.18	2.96	40.68
1962	91.99	88.83	3.44	21.06
1963	85.69	87.79	2.45	16.66
1964	126.27	139.35	10.36	16.90
1965	101.96	112.07	9.92	36.47
1966	93.26	111.82	19.90	21.58
1967	108.98	117.69	8.00	34.52
1968	116.13	108.63	6.46	18.93
1969[a]	101.60	91.23	10.20	22.27
1970[a]	86.40	91.57	5.98	21.97
1971[a]	126.06	142.76	13.25	26.93
1972[a]	146.72	156.29	6.52	30.98
1973[a]	74.42	79.17	6.38	34.58
1974[a]	147.67	169.40	14.72	31.70
1975[a]	105.67	102.31	3.18	20.59
1976[a]	133.82	128.99	3.61	20.64
1977[a]	64.45	53.98	16.25	33.07
1978[a]	99.48	95.01	4.49	31.19
1979[a]	83.25	88.94	6.83	35.28
1980[a]	82.40	82.91	0.62	34.05
1981	91.75	87.56	4.57	32.12
1982	106.92	122.12	14.22	18.93
1983	90.31	101.84	12.77	16.47
1984	105.73	119.98	13.48	24.69
1985	88.37	103.44	17.05	30.33
1986	94.85	102.37	7.93	19.94
1987	83.36	87.77	5.29	22.99
Average	103.98	108.28	7.68	28.20

[a] calibration year

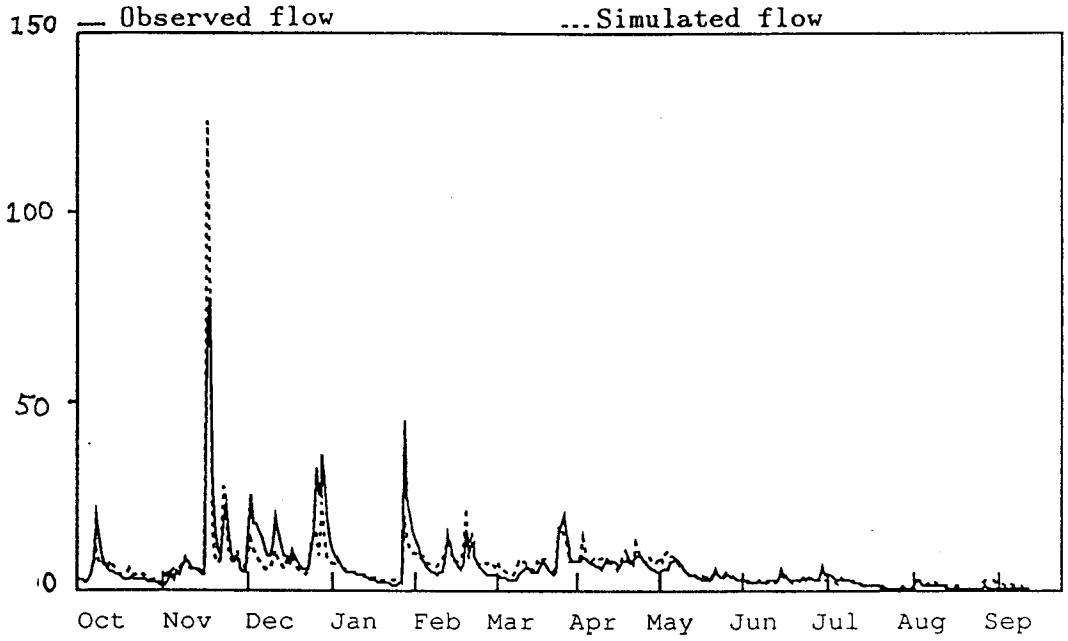

Figure 3.6 Best Annual Simulation, Water Year 1963

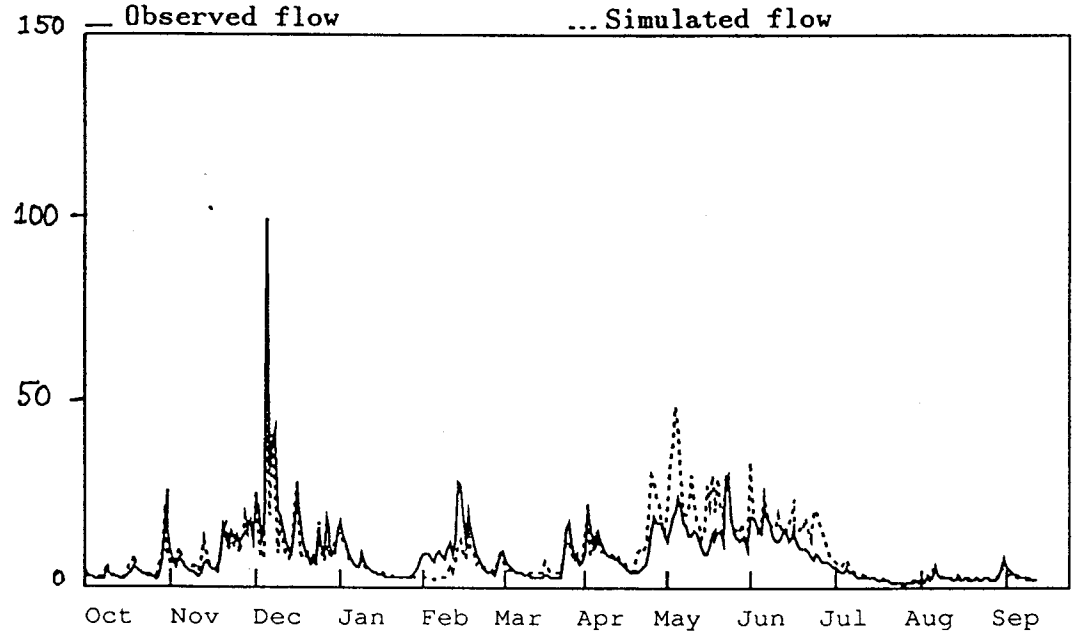

Figure 3.7 Worst Annual Simulation, Water Year 1954

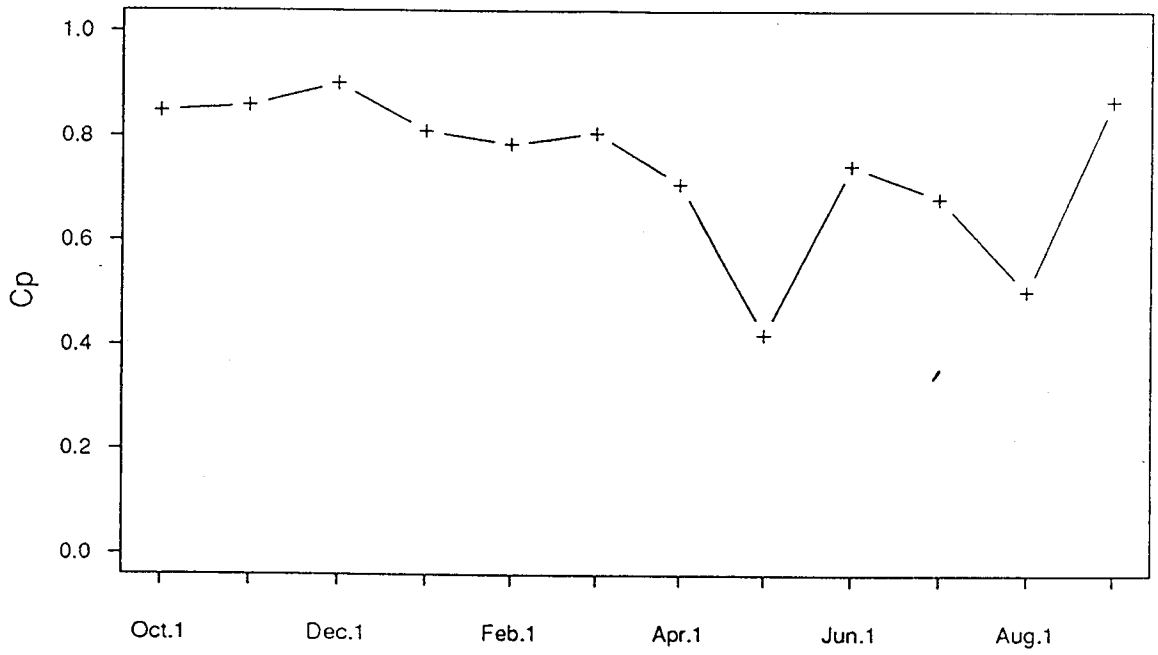

Figure 3.8 Estimated Coefficient of Prediction for Rex River ESP Forecasts with Perfect Precipitation Forecast

CHAPTER 4 EXPERIMENTAL DESIGN II - FORECASTING METHODS

4.1 Overview Of Forecasting Methods

The most widely used method of streamflow forecasting in the western U.S. remains regression of seasonal runoff on previous hydrometeorological variables (e.g., runoff, precipitation, soil moisture and snow course observations). This approach has been used by both the National Weather Service (NWS) and the Soil Conservation Service (SCS) in the western U.S. for many years (Twedt, et al., 1977; 1978). Regression methods use a combination of previous precipitation, snow water equivalent, and past streamflow measurements to predict streamflow volumes. Other statistical and stochastic methods also have been adopted. Time series methods exploit the persistence structure of historical time series of runoff to predict streamflow conditional on previous streamflow observations. Time series models work best during periods when streamflow are highly correlated, e.g., during summer and fall when baseflow dominates.

The U.S. National Weather Service (NWS) has developed the Extended Streamflow Prediction (ESP) method, which can provide probabilistic streamflow predictions for any user-designated time period. The ESP procedure was apparently first used in California in the early 1970's by the NWS California-Nevada River Forecast Center (RFC) and the State of California (Twedt, et al., 1978). The motivation for the development of ESP was the need for an accurate and efficient procedure for forecasting runoff from headwater basins that would be capable of providing the full probability distribution of the forecasted streamflows, from which occurrence probabilities could be estimated.

For purposes of comparison, a more limited investigation of an autoregressive moving average forecast model is made. The main emphasis of this study is evaluation of an ESP implementation of the Nanjing model to determine the validity of the ESP estimate of the

forecast error distribution to determine the accuracy of the method, and to determine the potential for improved forecast accuracy using updating methods. In the next two sections, the models used are described, along with the model implementation approach.

4.2 Extended Streamflow Prediction (ESP) Method

4.2.1 Introduction To The ESP Method

ESP is a framework within which alternative scenarios from a hydrologic model (generally a continuous, conceptual model) are combined to form forecasts. Future streamflows are simulated starting with the current snow and soil moisture as initial conditions. Each year of historic meteorological data beginning with the forecast date is assumed to be a possible representation of the future and is used to simulate a streamflow sequence from the forecast date through the end of the forecast period. From the simulated streamflow sequences, the total runoff during the forecast period can be estimated. Given n years of historical hydrometeorological information, the probability distribution of the forecast period can then be estimated. The mean of the n scenarios is usually considered the "best" forecast. In addition, from the empirical probability distribution formed from the n scenarios, the p-percentile flow for arbitrary p can be estimated. If the streamflows represent inflows to a reservoir system, a risk analysis can be performed using derived distribution methods. Although the ESP procedure was developed for water supply forecasting in snowmelt areas, it can also be used to evaluate spring snowmelt flood probabilities; for navigation forecasting, and for drought management.

4.2.2 Model Implementation

ESP is effected by running the hydrologic model up to the forecast date using observed meteorological data, and then sequentially using

as input n years of historic observations. For each year of historic data, one forecasting run is made. In this study, the evaluation of ESP required n*(n-1) runs, that is, for each year i and given forecast beginning and ending times T_1 and T_2, n-1 simulations (for each year of the historic record except the year being tested) were made. Therefore, the total number of runs for any forecast period was n*(n-1). These runs were made by building an internal loop in the Nanjing model.

Three kinds of data need to be set up before a hydrologic model can be structured in ESP mode. They are hydrologic model parameters, initial conditions, and meteorological time series data. Hydrologic model parameters are obtained by off-line model calibration procedures, as explained in Chapter 3. The initial basin conditions represent the current state of the catchment, and include soil moisture storage and snow-water equivalent. A minimum of ten to twenty years of climatological time series are required. In this study, the 40-year period 1948-87 was used. While conceptual simulation models can usually be calibrated using only a few years of observations (especially if the calibration period contains a diversity of high and low flow years), a longer period is required to estimate the probability distribution of the forecast period runoff accurately.

After the ESP structure has been created, the prediction period must be selected. Under ESP, the prediction period is flexible; daily, weekly, monthly, or any other seasonal period can be accommodated. The performance of ESP forecasts made using the Nanjing model was evaluated for a number of forecast begin and end days. In this study, beginning days T_1 = Oct.1, Nov.1, Dec.1, Jan.1, Feb.1, Mar.1, Apr.1, May 1, and Jun.1 were used, and $T_2 = T_1 + \Delta t_i$, where Δt_i = 1 week, 2 weeks, 3 weeks, 4 weeks, 1 month, 2 months, 3 months, and 4 months were used.

4.3 Autoregressive Moving Average Forecasts

4.3.1 Model Theory

Stochastic or time series methods have been used to forecast streamflow, usually using only streamflow in a previous time period as the dependent variable. These methods treat runoff as the dependent variable in a linear relationship. The form and parameters of the functions are estimated directly from the data (for example, Box and Jenkison, 1970; Loucks et al., 1980; and Salas et al., 1980). These methods can be thought of as seasonally stationary. The parameters of such models can be estimated using least squares methods.

A general autoregressive moving average stochastic model (ARMA(p,q)) is of the form

$$\tilde{Z}_t = \sum_{i=1}^{p} \alpha_i \, Z_{t-i} + \sum_{j=0}^{q} \beta_j \, a_{t-j} \qquad \text{.....(4.1)}$$

where α_i , β_j are estimated from the data directly, and the a_j's are uncorrelated normally distributed white noise. $\tilde{Z}_t$ represents the residual of the observation from its mean, $\tilde{Z}_t = Z_t - \mu_t$.

A simpler form for the case $q=0$ is the autoregressive process of order p, AR(p), which is defined as

$$\tilde{Z}_t = a_t + \phi_1 \tilde{Z}_{t-1} + \phi_2 \tilde{Z}_{t-2} + \cdots + \phi_p \tilde{Z}_{t-p} \qquad \text{.....(4.2)}$$

where the current state $\tilde{Z}_t$ is "regressed" on past values $\tilde{Z}_{t-1}$, $\tilde{Z}_{t-2}$, $\cdots$, of the process, and ϕ_i are the autoregressive parameters.

A moving average model (MA(q)) is given by the case $p=0$:

$$\begin{aligned} \tilde{Z}_t &= a_t - \theta_1 a_{t-1} - \theta_2 a_{t-2} - \cdots - \theta_q a_{t-q} \\ &= (1 - \theta_1 B - \theta_2 B^2 - \cdots - \theta_q B^q) \, a_t \\ &= \theta(B) a_t \end{aligned} \qquad \text{.....(4.3)}$$

An alternative case is the autoregressive moving average model with external input (ARMAX(p,q,r)) model, which is expressed in the form

$$\phi(B)\tilde{Z}_t = a_t - \theta_1 a_{t-1} - \theta_2 a_{t-2} - \cdots - \theta_q a_{t-q} + w_t + \xi_1 w_{t-1} + \xi_2 w_{t-2} + \cdots + \xi_r w_{t-r}$$
$$= (1 - \theta_1 B - \theta_2 B^2 - \cdots - \theta_q B^q) a_t + (1 + \xi_1 B + \xi_2 B^2 + \cdots + \xi_r B^r) w_t$$
$$= \theta(B) a_t + \xi(B) w_t \qquad \text{.....(4.4)}$$

where w_t is an external variable. When ARMAX models are used to model runoff, w_t can be precipitation; when they are used for snowmelt forecasting, the external variables in the model may include snow-water-equivalent measurements at selected snow courses, seasonal precipitation, soil moisture measurement and cumulative runoff measurements up to the time of the forecast.

The drawback of this approach is that the relationship between the dependent and external variables must be linear. Therefore, while the forecast results may be acceptable in average years, the method can break down in extreme years, for which the forecasts are most important.

4.3.2 Model Approach

The model used in this study was a special case of the general seasonal autoregressive moving average forecasting method described by Hirsch (1981), with a few changes (Lettenmaier, et al., 1990). The specific model form was seasonal autoregressive, which means that the forecast runoff in a future time period is assumed to be a linear combination of the observed residuals (difference between observed and recorded runoff) in several previous time periods. Since negative forecasts can not occur, streamflow logarithms were used instead of forecasting future streamflow directly.

The form of the model used to forecast runoff in period k as described by Lettenmaier (1990) was:

$$\ln(Q_k^*) - \mu_k = \sum_{t=1}^{p} \beta_{kt} [\ \ln\ (Q_{k-t}) - \mu_{k-t}] \qquad \text{.....(4.5)}$$

where Q_k^* = the forecasted runoff in period k

Q_{k-t} , $t = 1 \ldots p$ are the observed runoff in period k-t if available, and otherwise is the forecasted runoff for period k-t.

β_{kt} , $t = 1 \ldots p$ is coefficients to be estimated, and μ_k is the mean of the streamflow logarithms in period k.

Box and Jenkins (1976) outline an approach for estimating the coefficients β_{kt}, and for determining the order of the model, that is the number of lags, p. The recommended parameter estimation method is maximum likelihood, which means that the estimated parameters have the property that their posterior likelihood, or probability of occurrence given the data, is maximum. Maximum likelihood parameter estimates require that the form of the probability distribution describing the data be assumed; the usual assumption is that the data (or, in this case, the logarithms of the data) are normal. For normally distributed data, Box and Jenkins show that the maximum likelihood parameter estimates are obtained by minimizing the sum of squares of residuals of conditional forecasts from the observations. However, for an autoregressive model, the maximum likelihood parameter estimates are also nearly equivalent to the ordinary least squares parameter estimates used in classical regression. The least squares parameters are given by:

$$\underline{\beta}_k = (\underline{X}^T \underline{X})^{-1} (\underline{X}^T \underline{Y})$$

where:

$\underline{\beta}_k$: p×1 column vector of the coefficients; and

$\underline{X}$: n×p matrix made up of the n×1 column vectors of the logarithmic residuals of the streamflows $(x_{t-\tau,1}, \ldots x_{t-\tau,j}, \ldots x_{t-\tau,n})^T$, where the second subscript indicates the year of observation, and the p column vectors correspond to $\tau = 1, \ldots p$, respectively, and $x_{t-\tau,0} = \ln(Q_{t-\tau}) - \mu_\tau$. $\underline{Y}$ is the n×1 column vector corresponding to τ=0. This representation of the β_k's is equivalent to a linear regression of the (logarithms) of the streamflows in period t on the τ preceding streamflows. Note that a separate regression is performed for each period.

The covariance matrix of the parameter estimates is: $\underline{\Sigma} = (\underline{X}^T \underline{X})^{-1} \sigma^2_\epsilon$, where σ^2_ϵ is the estimated mean square of the residuals, that is, prediction errors obtained by applying the forecast model to the historic flow logarithms. The diagonal elements of $\underline{\Sigma}$ are the variances of the estimated parameters, which are asymptotically normally distributed.

Once the parameters $\underline{\beta}_k$ are estimated for each season (k), streamflow forecasts can be made. The forecasted streamflow logarithms were transformed to forecasted streamflows by:

$$Q^*_k = \exp(\mu_k + \beta_{kt} (\ln(Q_{k-t}) - \mu_{k-t}) + \sigma^2_\epsilon/2) \quad \ldots\ldots\ldots\ldots\ldots\ldots (4.6)$$

The probability distribution of Q^*_k could be estimated directly, based on an assumption of normality of the streamflow logarithms. However, it is known that the assumption that the logarithms of the flows are normal is most questionable for the tails of the probability distribution, which are of interest for risk estimation. Therefore, following Lettenmaier et al. (1990), the forecast error probability distribution was estimated empirically using a variation of the procedure known in the statistical literature as bootstrapping (Efron, 1982). The bootstrap procedure applied the forecast model to all n years of historic data sequences, with parameter estimates based on the (n-1) years of record not including the forecasted year. Then a variable $R_{kj} = Q_{kj}/Q^*_{kj}$ was formed, which is the ratio of the observed flow to the forecasted flow for season k in year j. The quantiles of the forecast ratios were estimated from the n values of R_{kj}, using the Weibull plotting position formula; that is, if R'_{kj} represents the ordered values of R_{kj} from smallest to largest, the jth value is assumed to have probability $\frac{j}{n+1}$.

4.4 Implementation of ESP Procedure

The Nanjing model was calibrated off-line as described in Chapter

3. The snowmelt model which produced the rain plus melt input to the Nanjing model was implemented using parameters described in CDD Howard and Associates, (1989).

All analyses were performed for the 40 water years 1948-87 (n=40). Meteorological data files were constructed for each of the 3 elevation bands used by the snowmelt model, which produces three rain-plus-melt files (one for each elevation band). As described in Section 4.2.2, for each T_1 (forecast date) and year i, the model was run up to the forecast date using observed meteorological data for year i; n runs of the model were then made from the forecast date through the end of the water year using the meteorological data for year j, j=1,...n. For i=j, the run is simply a simulation using observed data. Therefore, the results for i=j were retained for comparison purposes, but were not used in generation of the ESP forecasts. Eight different forecasting periods ($\Delta t_i = T_2 - T_1 = 1$ week, 2 weeks, 3 weeks, 4 weeks, 1 month, 2 months, 3 months, and 4 months) are included in each of these forecasts. For each of the 40 years for which ESP forecasts were made, therefore, there were 39 (n-1) sequences of forecasts for each (T_1,T_2), and one simulation sequence. Each of these sequences were retained for implementation of the updating procedures and for the forecast error analysis (see Sections 5.3 and 5.4.2-3).

From the ESP scenarios, forecasted and observed streamflows and simulated soil moisture storage were computed and stored. Several summary statistics, described briefly below, were derived from these results.

For each forecast date and each year i, the total runoff from the beginning of the forecast period (T_1) through T_2 was taken from the model. Figure 4.1 shows an example year (1977) for the ESP simulated runoff in the forecast period (T_1 = March 1, T_2 = June 1). This figure also illustrates implementation of the ESP procedure. From the figure, the effect of the alternative scenarios on forecast period runoff can be seen. This figure also clearly shows the need for

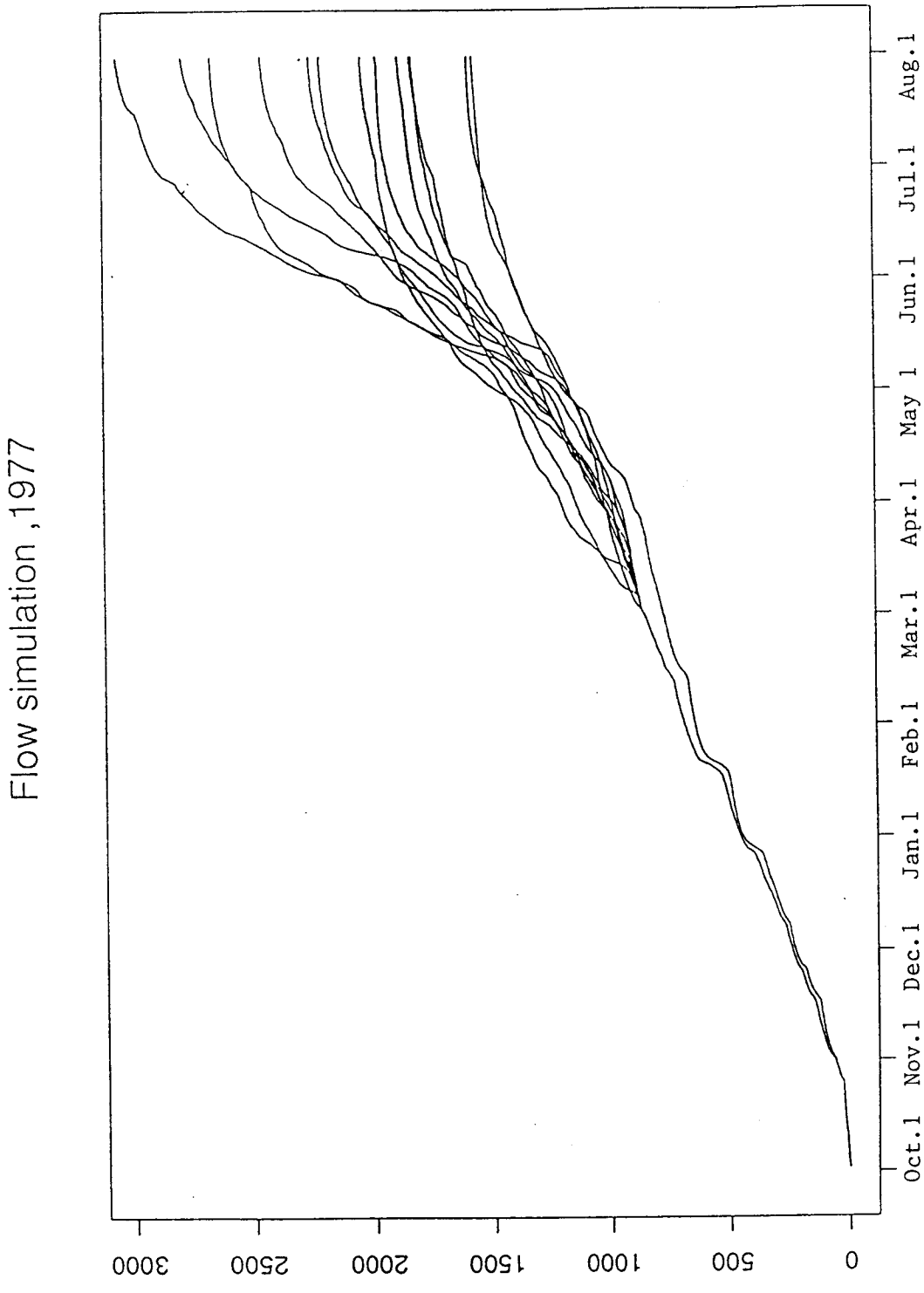

Figure 4.1 ESP Simulation Example

model updating; specifically, the simulated runoff up to the forecast date deviates significantly from the observed runoff, which is quite likely due in part to the fact that the modeled snow storage is incorrect. This error may well persist into the forecast period; in section 5.3 an updating procedure is suggested to reduce this source of forecast error.

For each forecast T_1 and T_2, the "best" (average) forecast and forecast errors, as well as the forecasting error distributions, were compared. Two kinds of forecasting errors are estimated; one is based on the "best" forecast for each year, the other is based on the average of these "best" forecasts. In addition, probability distributions of forecasting errors can be made. The Weibull plotting position formula was used to estimate the empirical probability distribution of the forecast errors.

The performance of the simulated ESP forecasts was evaluated in several ways. First, C_p values for the simulated streamflows were computed using the method of Section 3.7.3 to evaluate rainfall-runoff model performance. C_p values were also computed for each forecast period, with and without updating (see Section 5.1 and 5.3). to determine the potential for the updating procedure.

To determine the accuracy of the estimated forecast error distributions, graphical methods were performed for each of the above probability distributions and the observed streamflow. The statistics allow evaluation of the adequacy of estimates of the forecast error distributions.

4.5 Time Series Model Implementation

The bootstrap procedures described in section 4.3 were performed for each forecast period by running 40 years of historic data, and performing the analysis for each forecast period separately. Following Lettenmaier et al. (1990), $p = 2$ was used for each forecast period. This decision was made in lieu of using a different model

order for each forecast period. Apparent changes in the model order with season are to some extent an artifact of the natural variability of the streamflow time series, and in this respect are undesirable.

The model described by Lettenmaier et al. (1990) was modified to run at a monthly time step and to allow p (lags) and T_1 to be any combination of months within the water year. The reason for using monthly simulations instead of daily, which are used in the ESP model, is that the ARMA model produces forecasts that approach the mean in only few time steps. The other reason for running the model monthly is to compare the results from both the ESP model and the ARMA model.

The AR(2) and ARMAX(2,0,1) model were used in this study. The AR(2) model uses monthly streamflow data only. For year i, the streamflow of month j is forecasted by multiplying the matrix of the previous $p=2$ months' streamflow by a $p \times 1$ column vector of coefficients, β_k, which is defined in section 4.3.2. The ARMAX(2,0,1) model uses the previous month's rain plus melt as the external variable, along with the streamflow from the two previous months, which are the autoregressive terms. The coefficient of prediction, C_p, were computed for comparison purposes and given in Section 5.2.

4.6 Comparison Of ESP and ARMA Model Implementation

Table 4.1 compares the implementation of the ESP and ARMAX models.

Table 4.1 The Procedures For Running The ESP Model And The ARMA Model

ESP MODEL	ARMA MODEL
Forecast Period	
Δt_i: the length of forecast period	
T_1: the forecast date	T: forecast period
T_2: the end of forecast period	
Δt_i = 1 week, 2 weeks, 3 weeks, 4 weeks, 1 month, 2 months, 3 months, and 4 months.	Δt_i = 1 month, 2 months, 3 months and 4 months.
T_1=Oct. 1, Jan. 1, Feb. 1, Mar. 1, Apr. 1, May 1, and Jun. 1,	T_1 = Dec.-Mar., Jan.-Apr., Feb.-May, Mar.-Jun., Apr.-Jul., and May-Aug.
$T_2 = T1 + \Delta t_i$	
Data Availability	
water years 1948-87.	water years 1948-87.
Method of Streamflow Probability Distribution Simulation	
Model simulates 39 streamflow forecasts for each forecast period and each year to form the probability distribution.	A bootstrap procedure produces 39 predictions for each forecast period to form the probability distribution

CHAPTER 5 STATISTICAL ANALYSIS AND DISCUSSION

The performance of the ESP procedure using the Nanjing model was evaluated in two ways. First, an analysis of the coefficients of prediction (C_p) was used to evaluate forecast accuracy. Second, a comparison of predicted and observed ESP forecast error distributions was made using graphical methods. Third, a comparison between ESP and ARMA/ARMAX model performances was made using C_p's for different forecast periods for the two models. In conjunction with these evaluations, the value of updating the model soil moisture estimate as a means of correcting persistent errors was also evaluated. Finally, the performance of the ESP forecasts was evaluated in detail for three extreme low flow years (1951, 1958, and 1977).

5.1 Evaluation of ESP forecasts

5.1.1 Coefficient of Prediction

The coefficient of prediction (C_p) is a measure of forecast accuracy, as described in section 3.7.3:

$$C_p = 1 - \frac{Var(Q_{obs} - Q_{pre})}{Var(Q_{obs})}$$

where $Var(\cdot)$ is the statistical variance, and Q_{obs} and Q_{pre} are observed and forecasted runoff volume, respectively.

High values of C_p indicate highly accurate forecasts, a C_p of 1.0 corresponds to a perfect forecast; a value of 0.0 is achieved when the forecast is always equal to the long-term mean. Table 5.1 gives the C_p's for the ESP 'best' forecasts for the Rex River for different lengths of forecast periods and various forecast dates.

Negative C_p's indicate poor forecast performance, to the extent that a better forecast could be achieved by using the long-term mean. Negative C_p's occurred mostly in the early part of the water year, when precipitation and streamflow is highly variable and there is little moisture accumulation in either the soil or snowpack that

could influence future runoff. Table 5.1 shows that low C_p values occur for long forecast periods for forecast dates prior to the time of maximum snow accumulation (usually between March 1 and April 1). Shorter forecasts tend to be more accurate than long-term forecasts in the fall and winter. The reverse is generally true in the spring.

Table 5.1 Estimated Coefficient of Prediction of ESP Forecasts

	Forecast Period Length							
Forecast Date	1 wk	2 wks.	3 wks.	4 wks.	1 mo.	2mos.	3mos.	4mos.
Oct. 1	0.0576	-0.0068	-0.0262	-0.0413	-0.0458	-0.0550	-0.0507	-0.0431
Nov.1	0.1971	0.1109	0.0544	0.0344	0.0364	0.0273	-0.0043	-0.0053
Dec.1	0.0538	0.0556	0.0168	0.0268	0.0396	-0.0216	-0.0316	-0.0305
Jan. 1	-0.0447	-0.0915	-0.0782	-0.0695	-0.0817	-0.0761	-0.0928	-0.0749
Feb. 1	0.1914	0.1162	0.1074	0.0650	0.0606	0.0220	0.0236	0.2129
Mar. 1	0.2006	0.1992	0.1770	0.1720	0.1437	-0.0021	0.3207	0.4999
Apr. 1	0.2906	0.2207	0.2040	0.0597	-0.0166	0.0348	0.5282	0.6587
May 1	0.0567	0.2217	0.2017	0.1195	0.1564	0.5734	0.6961	0.7019
Jun. 1	0.3294	0.4108	0.4960	0.5988	0.6489	0.7435	0.7488	0.7488
Jul. 1	0.6800	0.6195	0.5531	0.5397	0.5389	0.5300	*a*	*a*

a Forecast end date is past end of water year; no forecast made.

5.1.2 Evaluation of ESP Forecast Error Distribution

A comparison of predicted and observed ESP forecast error distributions was made to determine whether the (retrospectively estimated) probability distribution of the actual forecast errors is consistent with the ESP forecast error distribution estimated when the forecasts are made.

This issue was addressed by comparing the actual number of occurrences of streamflows more severe than the upper or lower p-percent exceedance level with np, the expected number of exceedances in the $n = 40$ year evaluation period. The comparisons were performed

as follows. For each forecast period in each year, the 39 alternative runoff volumes during the forecast period were ranked and an empirical probability distribution was estimated using the Weibull formula. The observed runoff was then compared to the p and 1-p percentile of that distribution. The p-values of 2%, 5%, 10%, 20%, 30%, and 40% as well as 1-p values of 98%, 95%, 90%, 80%, 70%, and 60% were used, so that both lower tail and upper tail exceedances were computed. This process was repeated for each of the 40 years. The results are given in Figures 5.1 and 5.2. Tables of the complete results for each forecast period are included in Appendix C.

Four figures for different forecast periods were chosen to evaluate the forecast error distributions. Figure 5.1 summarizes results for forecasts from one week, two week, one month, and three month periods for the upper tail of the runoff forecast distributions. Figure 5.2 shows similar results for the lower tail of the distribution. The results show that, especially for the upper tail of the distribution and short forecast periods, the actual number of exceedances of the p-percentile flows greatly exceeds the expected number. This suggests that the actual forecast error distribution has considerably heavier tails than the error distribution estimated by ESP. Figure 5.2 shows that the expected and actual exceedances are much more consistent for the lower tail of the distribution. There is, however, an indication that the extreme lower tail of the distribution is not properly represented, especially for the longest forecasts.

5.2 Comparing ESP and ARMA/ARMAX Model Performances

5.2.1 Comparison by Coefficient of Prediction (C_p)

The ARMA and ARMAX model described in Section 4.3 was applied to the Rex River for comparative purposes. Generally, it is not expected that the ARMA model, which incorporates no direct information about snow accumulation, should perform as well as the ESP approach.

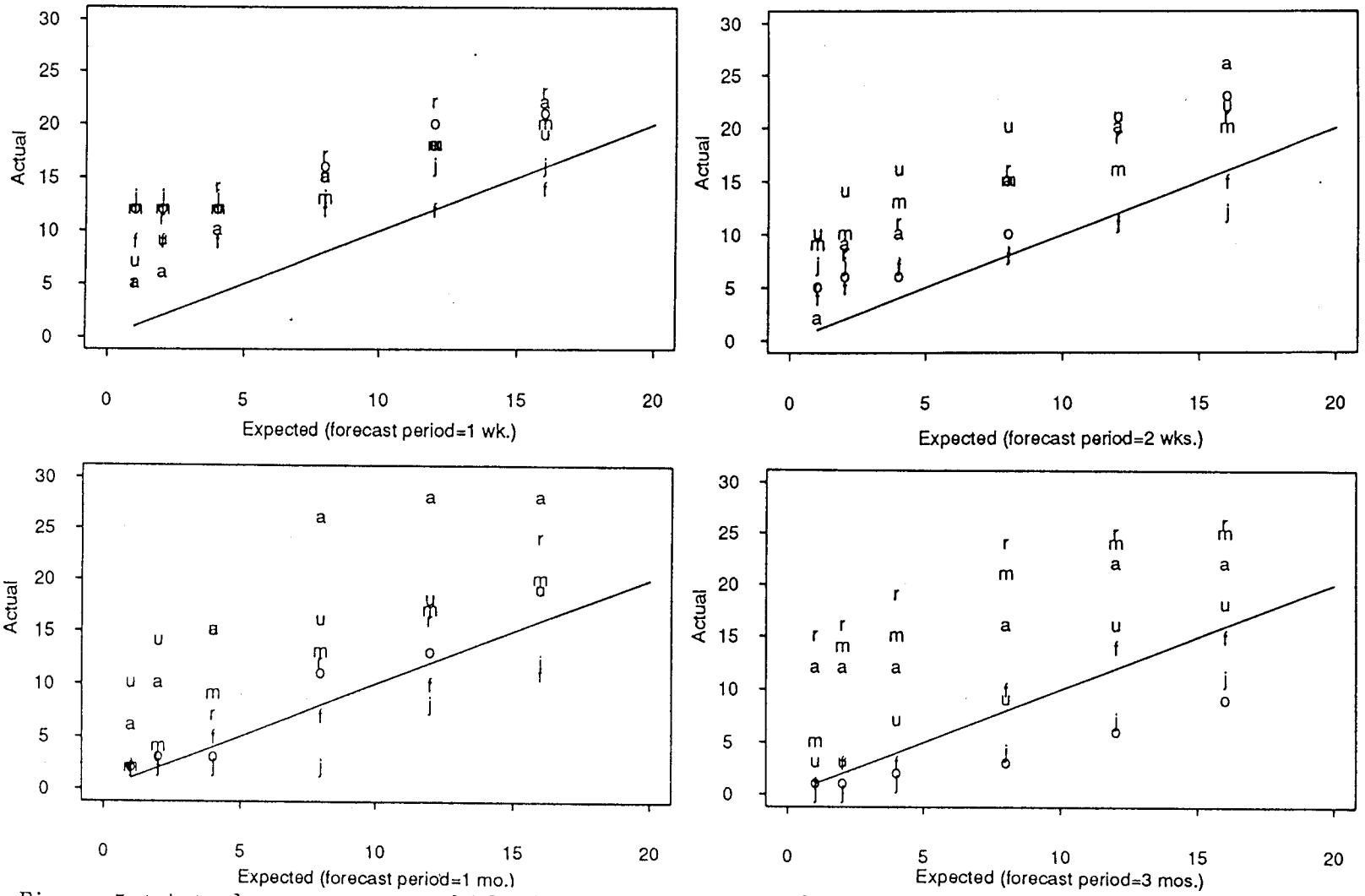

Figure 5.1 Actual versus expected ESP forecast error exceedance, upper tail of predicted forecast error distribution o=Oct.1, j=Jan.1, f=Feb.1, r=Mar.1, a=Apr.1, m=May 1, u=Jun.1

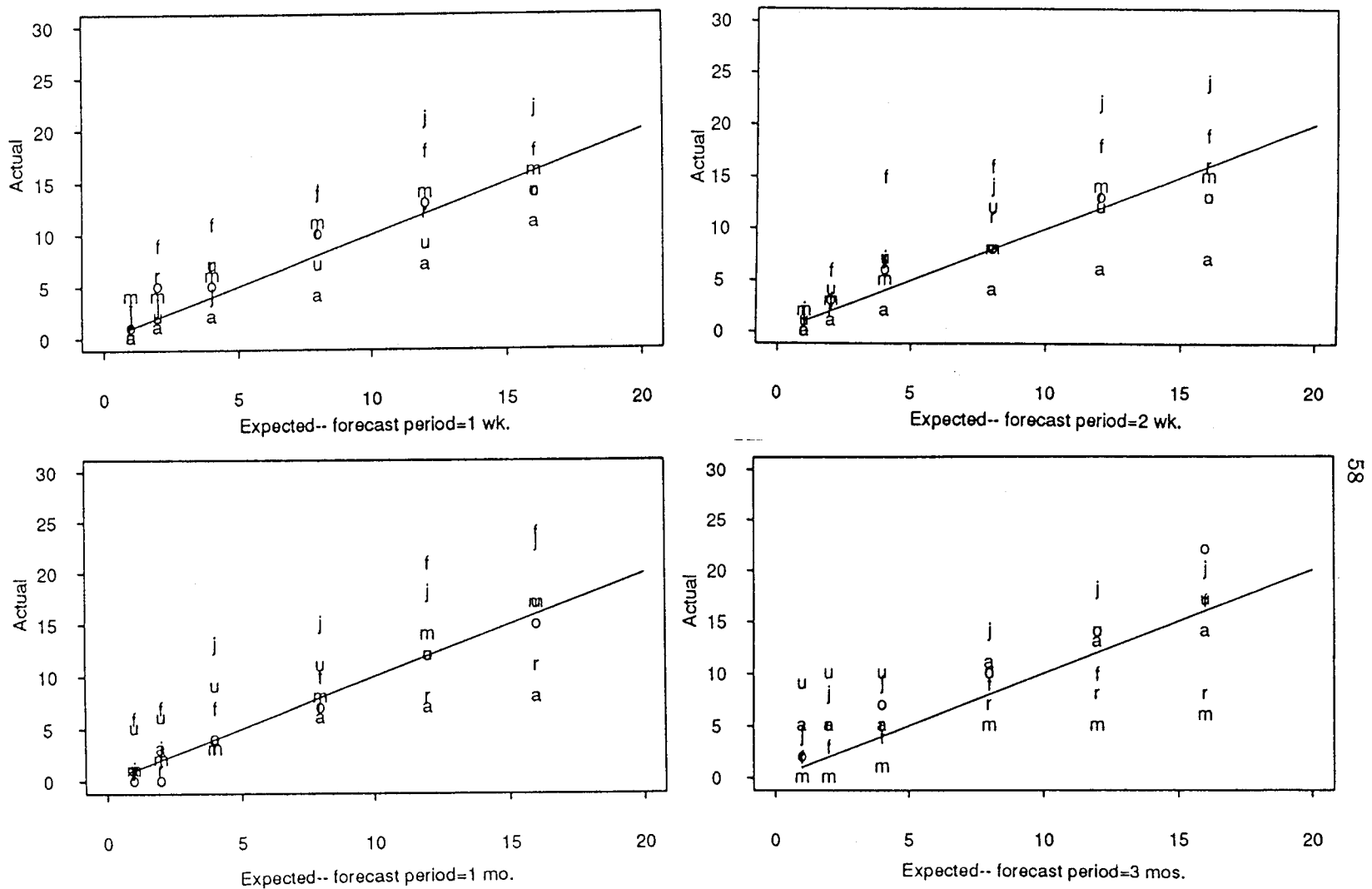

Figure 5.2 Actual versus expected ESP forecast error exceedance, lower tail of predicted forecast error distribution o=Oct.1, j=Jan.1, f=Feb.1, r=Mar.1, a=Apr.1, m=May 1, u=Jun.1

The coefficients of prediction (C_p), similar to those used in the previous section, were used to compare the performance of the ESP and ARMA forecasts. The ARMA model was implemented for a monthly time increment, and the results of forecast periods from one month to four months were compared with ESP results. Table 5.2 gives the coefficients of prediction for ARMA(2,0) and ARMAX(2,0,1) models. Comparison of Tables 5.1 and 5.2 shows that ESP has better performance than the autoregressive and ARMAX models not only in one month forecasts but also in seasonal forecasts.

Table 5.2 C_p of Time Series (ARMA(2,0) and ARMAX(2,0,1)) Models

First Month of Forecast T_1	Model	Forecast Periods 1 month	2 months	3 months	4 months
January	ARMA(2,0)	-0.1263	-0.0647	-0.0570	-0.2613
	ARMAX(2,0,1)	-0.4494	-0.3497	-0.3414	-1.3970
February	ARMA(2,0)	-0.0042	-0.0608	-0.0339	-0.1423
	ARMAX(2,0,1)	-0.1185	-0.1122	-0.2138	-1.8173
March	ARMA(2,0)	-0.0055	-0.0818	-0.0435	-0.0017
	ARMAX(2,0,1)	-0.0873	-0.2019	-0.3183	-1.7583
April	ARMA(2,0)	-0.0110	-0.0202	-0.0191	-0.1239
	ARMAX(2,0,1)	-0.0958	-0.2228	-0.2641	-2.0514
May	ARMA(2,0)	0.3854	0.3109	0.2807	0.1999
	ARMAX(2,0,1)	-0.4766	-0.3673	-0.3261	-0.9670
June	ARMA(2,0)	0.4067	0.3478	0.3214	0.2390
	ARMAX(2,0,1)	0.3089	0.2518	0.2285	0.1826

Almost all of the C_p's from the ARMA model are smaller than those from ESP in every forecast period. However, in T_1=June, the C_p's are considerably larger than in the other months. Generally, however, forecasts made using the time series models would not be practically useful. Investigation of the lag one, two and three correlation coefficients of the observed streamflow time series shows why these models are not able to make accurate predictions. The ARMA model

uses observed monthly streamflows in the previous month to forecast the streamflows, and the ARMAX model uses both observed streamflows and precipitation (rain-plus-melt) as an external variable. The lagged autocorrelation coefficients of streamflow for lags 1-3 as well as the correlation coefficients between streamflow and rain-plus-melt are listed in Table 5.3.

Table 5.3 Correlation Coefficients of Rex River Historical Streamflow

lag	Oct.	Nov.	Dec.	Jan.	Feb.	Mar.	Api.	May	Jun.	Jul.	Aug.	Sep.
1	*0.238*	*0.413*	*0.179*	*-0.050*	*0.169*	*0.342*	*-0.041*	*0.046*	*0.666*	*0.805*	*0.607*	*0.298*
2	*0.128*	*0.294*	*0.098*	*-0.162*	*-0.136*	*0.069*	*-0.263*	*0.159*	*0.028*	*0.453*	*0.590*	*0.018*
3	*0.116*	*0.030*	*-0.038*	*-0.200*	*-0.109*	*-0.212*	*-0.331*	*-0.063*	*-0.018*	*-0.133*	*0.185*	*-0.005*
0[a]	*0.872*	*0.903*	*0.938*	*0.943*	*0.920*	*0.879*	*0.817*	*0.879*	*0.890*	*0.790*	*0.593*	*0.846*
1[b]	*0.277*	*0.324*	*0.186*	*-0.035*	*0.086*	*0.238*	*0.031*	*0.027*	*0.626*	*0.801*	*0.612*	*0.416*

[a] correlation coefficient of rain-plus-melt and streamflow

[b] correlation coefficient of streamflow and rain-plus-melt of previous time step

5.3 Updating Procedure

5.3.1 Storage Accounting And Regression

A simple scheme for updating streamflow forecasts to account for persistent model errors is described in this section. It uses a storage accounting method to correct the model-estimated soil moisture storage on the forecast date. The general approach used is to optimize the model water storage retrospectively on the forecast date so that the error between "forecasted" (actually simulated, since the analysis is retrospective) and observed runoff during the forecast period is minimized. Then, the resulting 40 values of soil moisture adjustments are regressed on the difference in the observed and simulated runoff from the start of the season (usually October 1)

through the forecast date. From the regression, the resulting two coefficients are used for water storage updating, since the cumulative difference of simulated and observed flows is known on the forecast date. Exploratory analyses showed that the relationships are not strongly dependent on the length of the forecast period, but that they do depend on the forecast date and the beginning of the forecast season. Three different season starting dates were used: October 1, November 1, and December 1 respectively.

The regression equation is of the form $\Delta S = (S_{sim} - S_{opt}) = \Delta Q * a + b$ where ΔS is the difference between simulated moisture storage (S_{sim}) and the optimized soil moisture storage (S_{opt}), and ΔQ is the difference between observed and simulated cumulative streamflow, and a and b are regression coefficients. The R^2 of the regression can be used to determine whether the relationship between ΔS and ΔQ is significant, and hence, whether or not the updating procedure should be used.

Table 5.4 Regression Coefficients for Updating Relationship (for forecast season begin date, October 1, November 1, December 1, respectively).

Forecast date	a	b
January 1	0.0479/0.0455/0.0738	-16.341/-16.525/-16.282
February 1	-0.0345/-0.067/-0.071	-33.680/-41.386/-38.583
March 1	0.0074/0.0013/-0.022	-0.2946/-2.0586/-7.7941
April 1	0.0824/0.0916/0.0870	32.4916/35.5579/29.7248
May 1	-0.0207/-0.011/-0.013	18.7807/21.5761/21.6714
June 1	-0.0150/-0.027/-0.030	8.6825/ 5.8083/ 6.5455
July 1	0.0246/0.0247/0.0258	-7.9366/-7.8096/-8.8504

For a sample size 40 and significance level 0.10, R^2 is 0.05; therefore if the R^2 value was larger than 0.05, then the updating procedure was used. Table 5.4 gives the regression coefficients for

each forecast date with different forecast season start dates (T_0). Table 5.5 gives the corresponding R^2 values.

Generally, the relationship between cumulative streamflow and the model water storage is not strong, and the R^2 values are small. This is, in part, because other factors (especially forecast period rain plus melt) than the initial soil moisture affect forecast period runoff. However, the results do show that the updating relationship is quite strong on April 1, which is approximately the time of maximum snow accumulation.

Table 5.5 R^2 Values, for Updating Equation

T_0,	T_1, Jan.1	Feb.1	Mar.1	Apr.1	May 1	Jun.1	Jul.1
Oct.1	0.1375	0.1082	0.0374	0.4113	0.0980	0.0794	0.1908
Nov.1	0.1030	0.1836	0.0000	0.4192	0.0480	0.1319	0.1822
Dec.1	0.1145	0.1612	0.0922	0.3581	0.0510	0.1371	0.1780

5.3.2 Adjustment

Because the forecast accuracy varies depending upon the season, the updating procedures were implemented on T_1 = Jan.1, Feb.1, Mar.1, Apr.1, May 1, and Jun.1. For T_1 = Oct.1, the water storage was not updated because the beginning of the forecast season is the same date, and so there is no prior streamflow accumulation. Table 5.6 gives the magnitude of the adjustment for every forecast period. The detailed soil moisture storage before and after updating for each year is listed in Appendix D.

5.4 Evaluation of ESP Forecasts after Updating

Table 5.6 Updating Adjustments to Water Storage in ESP Model (in mm)

Year	Forecast Date					
	Jan.1	Feb.1	Mar.1	Apr.1	May 1	Jun.1
1948	-27.37	-44.32	0.00	16.21	-2.03	23.94
1949	-12.40	84.50	0.00	-22.20	-119.06	15.95
1950	18.10	51.36	0.00	0.83	-15.59	-42.70
1951	-10.31	-15.29	0.00	76.15	7.60	7.41
1952	-31.68	27.47	0.00	-9.86	-107.62	10.94
1953	-33.56	-37.27	0.00	3.61	-9.18	-6.30
1954	-13.79	53.46	0.00	-24.55	-64.70	-23.08
1955	21.71	38.55	0.00	7.98	-13.15	14.75
1956	-53.84	-12.02	0.00	-78.95	4.11	15.02
1957	-51.41	-2.54	0.00	10.71	-4.78	15.15
1958	34.96	-35.42	0.00	-35.25	-17.11	-22.44
1959	-17.98	-61.24	0.00	19.00	29.46	-33.30
1960	-53.53	14.27	0.00	0.63	8.50	-15.90
1961	71.75	-39.84	0.00	18.52	-7.11	-30.77
1962	-7.67	-131.40	0.00	-0.55	14.19	-12.23
1963	-23.94	55.35	0.00	2.79	7.88	-10.30
1964	4.53	-26.91	0.00	55.54	54.95	-139.14
1965	54.00	-65.99	0.00	61.86	-18.85	-20.12
1966	86.20	-37.37	0.00	-111.94	-16.08	71.68
1967	8.31	-49.85	0.00	-24.88	-10.85	-22.00
1968	-37.66	-82.07	0.00	-11.69	31.56	-35.00
1969	-0.95	-11.46	0.00	8.50	-112.11	22.79
1970	62.95	-76.56	0.00	-28.75	29.96	-21.61
1971	69.86	-50.21	0.00	27.18	-9.00	-7.24
1972	73.69	3.84	0.00	0.36	-92.75	-137.85
1973	6.37	-69.54	0.00	-2.26	16.74	13.55
1974	32.33	-41.85	0.00	2.27	37.43	-37.79
1975	-27.26	-66.14	0.00	-7.05	-14.65	2.19
1976	-2.14	-73.15	0.00	11.83	14.68	-9.23
1977	-35.39	-65.98	0.00	31.12	38.08	6.38
1978	-50.88	-52.81	0.00	-5.65	-11.45	-24.70
1979	-34.19	67.26	0.00	-30.84	22.38	-6.98
1980	-48.67	-35.12	0.00	-37.25	37.50	-8.05
1981	0.86	57.25	0.00	-7.25	26.24	-31.22
1982	64.95	-29.65	0.00	-43.80	-17.57	7.81
1983	-38.80	-72.39	0.00	22.91	6.59	3.94
1984	10.21	-62.52	0.00	1.83	6.89	-0.08
1985	-9.51	6.70	0.00	50.83	11.27	23.47
1986	-7.66	20.59	0.00	36.58	17.42	-19.62
1987	9.65	44.99	0.00	-41.24	-2.76	11.81

5.4.1 Coefficients of Prediction

C_p values were computed after updating (Table 5.7). Figure 5.3 shows the maximum values of C_p for different forecast dates. Figure 5.4 compares the same values of C_p, all for the same forecast period T_2 = July 1, for the ESP model before and after updating as well as the C_p for the National Weather Service Model as applied to the Cedar River (to which the Rex is tributary) by Lettenmaier (1984).

Table 5.7 Estimated ESP Coefficient of Prediction for Rex River Forecasts with Updating

	Forecast Period							
Forecast Date	1 wk	2 wks.	3 wks.	4 wks.	1 mo.	2mos.	3mos.	4mos.
Oct. 1	-0.0251	-0.0335	-0.0420	-0.0486	-0.0505	-0.0438	-0.0453	-0.0434
Jan. 1	-0.1556	-0.1550	-0.0209	0.0302	0.0252	0.0602	0.0343	0.0632
Feb. 1	0.2173	0.2044	0.1654	0.1657	0.1557	0.1215	0.0895	0.2790
Mar. 1	0.2006	0.1992	0.1770	0.1720	0.1437	-0.0021	0.3207	0.4999
Apr. 1	0.4807	0.3827	0.2251	0.0610	0.0174	0.1752	0.5897	0.7028
May 1	0.0506	0.2414	0.2468	0.2366	0.2831	0.6212	0.7113	0.7165
Jun. 1	0.6500	0.6782	0.7263	0.7607	0.7828	0.7907	0.7881	0.7881

Comparisons between the C_p's in Table 5.1 and Table 5.7 demonstrate that the forecasts after updating do not improve until T_1 = April 1. From Tables 5.5, 5.6, and Appendix D, the R^2 values for all three regressions (forecast season start dates) are highest on T_1 = April 1. In most cases, the water storages on April 1 after updating are close to the maximum soil moisture storage capacity of 150 mm. In addition to indicating the importance of the initial soil moisture for forecasts beginning at the time of maximum snow accumulation, the high R^2 values for T_1 = April 1 also suggest that better results might be achieved by adjusting the snowmelt model snow accumulation, rather than the soil moisture storage.

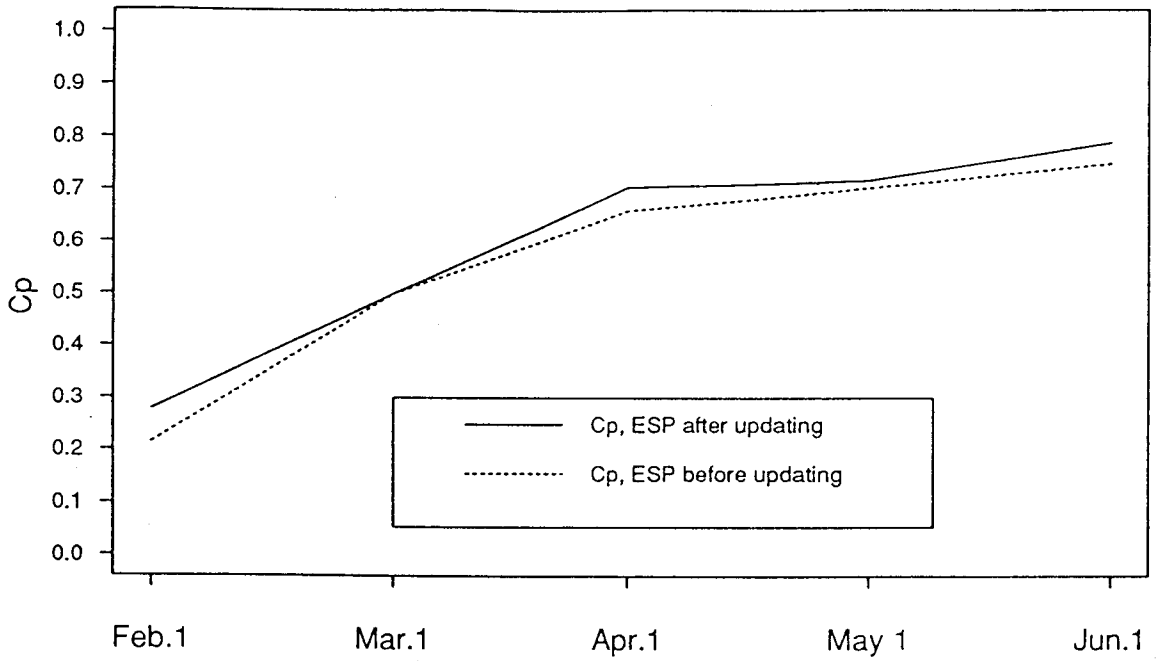

Figure 5.3 Maximum C_p of ESP Model Before and After Updating

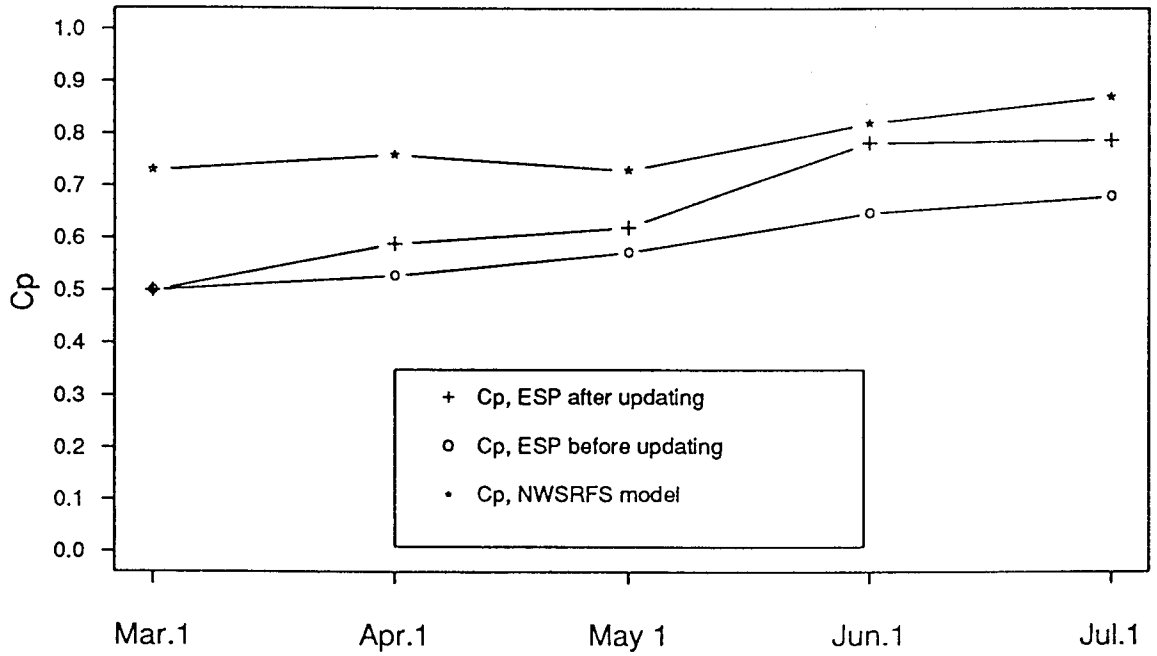

Figure 5.4 C_p for Forecasting July 1 Streamflow by Nanjing Model before and after Updating, and maximum C_p for National Weather Service Model ESP Forecasts for Cedar River (after Lettenmaier, 1984)

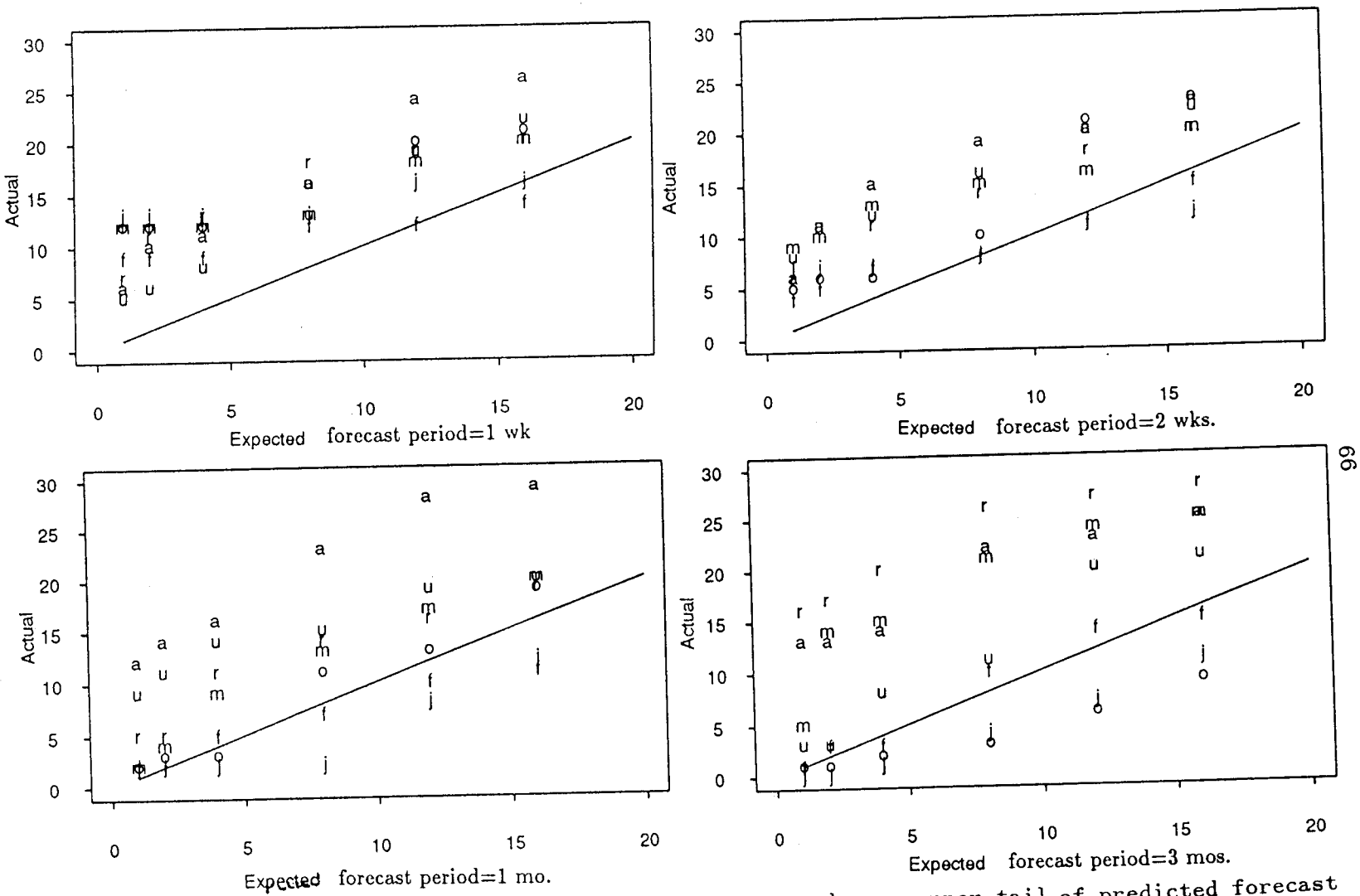

Figure 5.5 Actual versus expected ESP forecast error exceedance, upper tail of predicted forecast error distribution (with updating) o=Oct.1, j=Jan.1, f=Feb.1, r=Mar.1, a=Apr.1, m=May 1, u=Jun.1

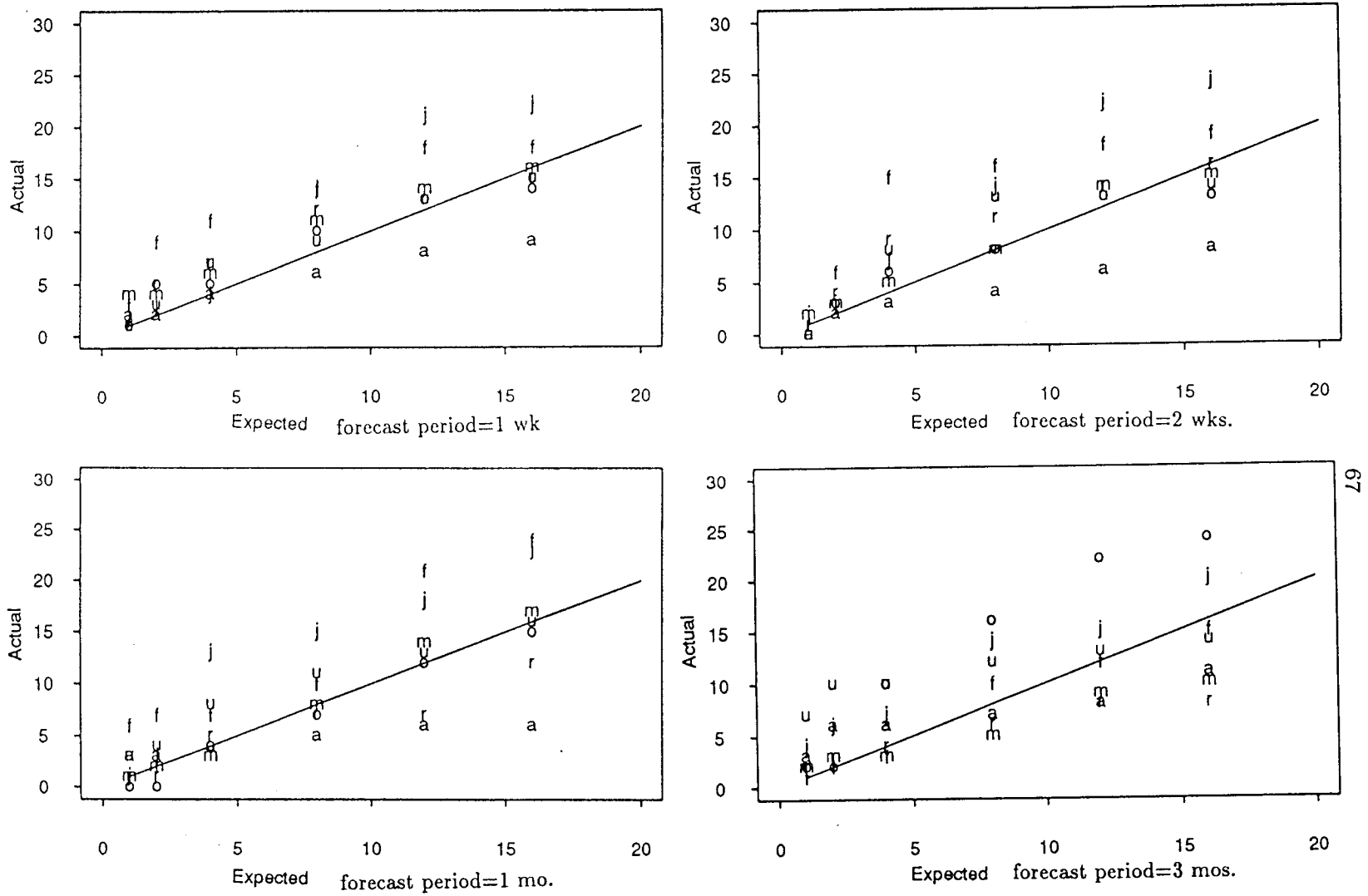

Figure 5.6 Actual versus expected ESP forecast error exceedance, lower tail of predicted forecast error distribution (with updating) o=Oct.1, j=Jan.1, f=Feb.1, r=Mar.1, a=Apr.1, m=May 1, u=Jun.1

5.4.2 ESP Forecast Error Distribution Evaluation

The same comparison of expected and observed exceedances used in Section 5.1.2 was used to determine whether the updating procedure affected the forecast error distribution estimates. Figures 5.5 and 5.6 show that the results are quite similar to those shown in Figures 5.1 and 5.2 for the unupdated forecasts, specifically, the actual number of exceedance for the upper tail of the distribution are much greater than their expectances, especially for the short forecast periods (e.g., 1 week and 2 weeks are better than 3 months). This is not surprising since a major source of the error in the distribution estimates is the failure to include model and parameter uncertainty in the analysis, and this is unrelated to the use of updating.

5.5 Drought Period Forecasts Assessment

One of the claimed advantages of ESP is that it should perform better than simpler methods, such as regression, in extremely dry years. To examine this possibility, ESP forecasts for three extreme low flow years were evaluated, which were selected based on both their seasonal and annual flows, were water years 1951, 1958, and 1977.

All of the analyses were based on forecast periods beginning on April 1. For each year, ESP produced 39 alternative forecasts, from which the lowest and highest were selected to study their daily water storage and daily streamflow. For each of the three years, the lowest streamflow predictions corresponded to the 1967 water year precipitation-temperature scenario and the highest streamflow corresponded to the 1981 water year. Figures 5.7-5.9 c and d give the daily observed streamflow, the daily ESP 'best' forecast streamflow and the highest/lowest predicted streamflow with and without updating for years 1951, 1958, and 1977. Figures 5.7-5.9 a and b show the water storage for comparison purposes. The water storage adjustments are also given in Table 5.6. These figures show that the adjustments only influence the first one to two weeks; for

longer lead times the effects of updating are minimal.

Table 5.8 summarizes the forecast errors for the three low flow years which include the average forecast error in 40 years and the forecast errors made in drought years. Even though the forecast error percentages do not have a significant trend, ESP generally appears to make better weekly forecasts than long-term forecasts in drought periods, and is slightly better than average for forecast periods of around one to two months. For example, the 1977 water year is the extreme dry year of records, in this year the ESP forecast error percentage was much smaller than the average error percentage of 40 years for each forecast period. The 1951 water year ESP forecast error percentages were also much smaller than the average.

Table 5.8 ESP Forecast Error in Drought years 1951, 1958, and 1977

	Forecast Period							
Year	1wk.	2 wks.	3 wks.	4 wks.	1 mo.	2 mos.	3 mos.	4 mos.
1951								
error(cfsd)	-8.05	-11.46	12.24	29.52	51.91	184.26	297.91	347.83
error percent[a]	12.87	8.47	5.58	10.61	16.82	25.58	33.61	37.92
1958								
error(cfsd)	10.63	9.27	-114.75	-119.37	-108.40	21.68	169.56	214.84
error percent[a]	37.88	11.77	44.36	36.45	31.20	3.83	27.00	32.79
1977								
error(cfsd)	2.70	-6.57	10.96	-31.59	-32.14	17.11	49.06	80.78
error percent[a]	4.44	5.01	6.20	11.14	10.24	3.24	7.68	12.03
absolute error percent	40.55	38.81	32.99	31.21	31.80	21.38	21.45	18.79

[a] absolute error percentages

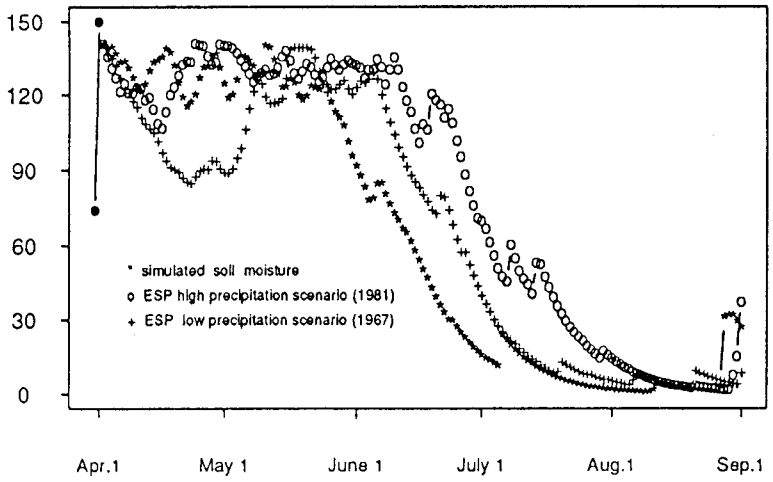

Figure 5.7a 1951 water year soil moisture

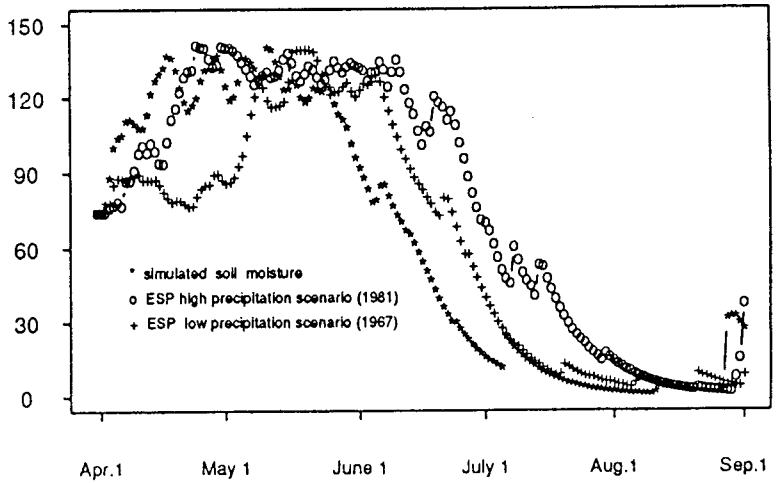

Figure 5.7b 1951 water year soil moisture (no updating)

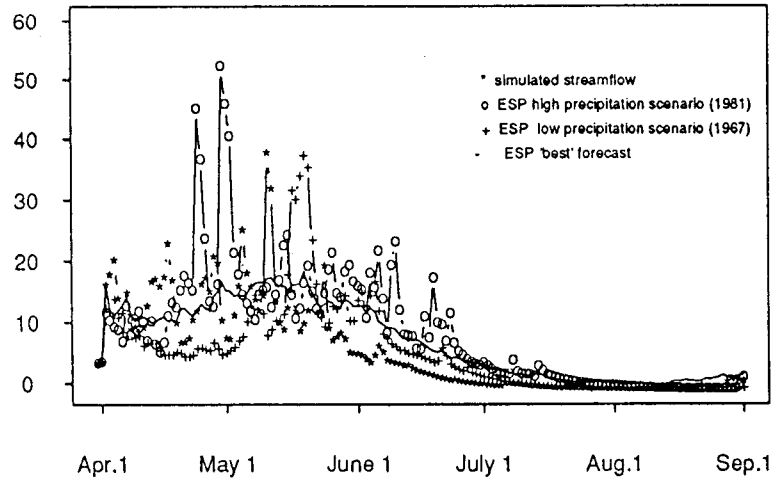

Figure 5.7c 1951 water year streamflow

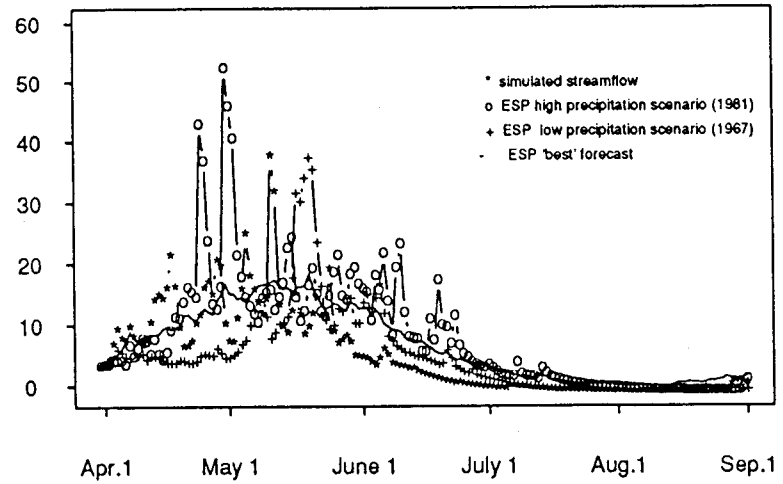

Figure 5.7d 1951 water year streamflow (no updating)

Figure 5.7 ESP performance in drought year, 1951 unit: mm

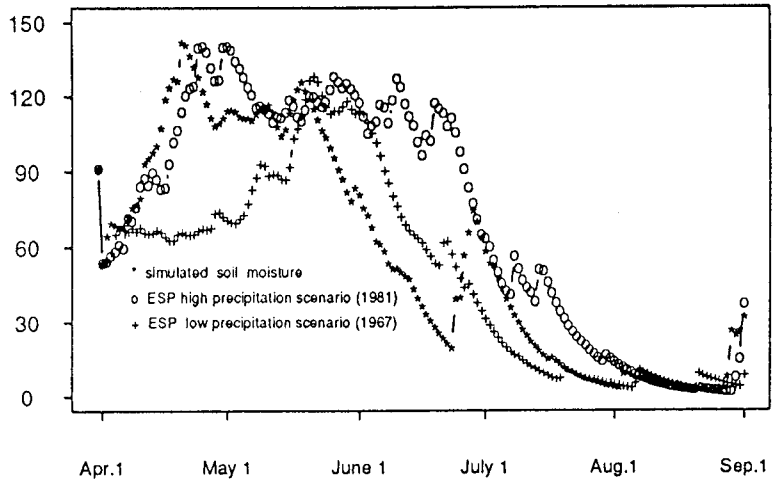

Figure 5.8a 1958 water year soil moisture

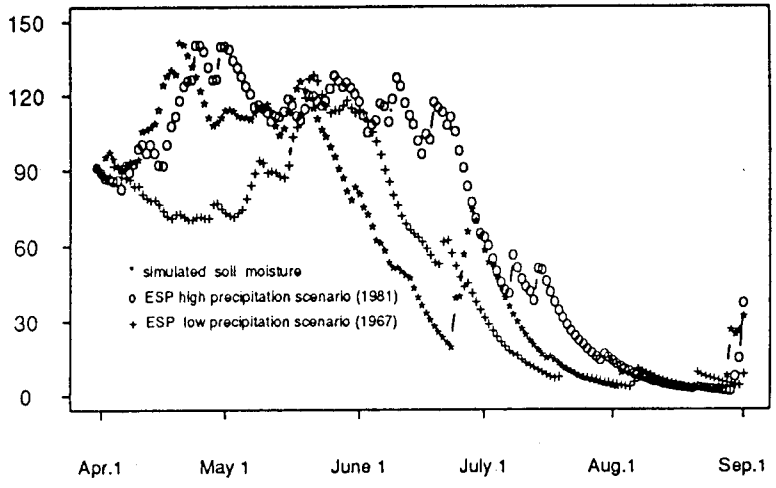

Figure 5.8b 1958 water year soil moisture (no updating)

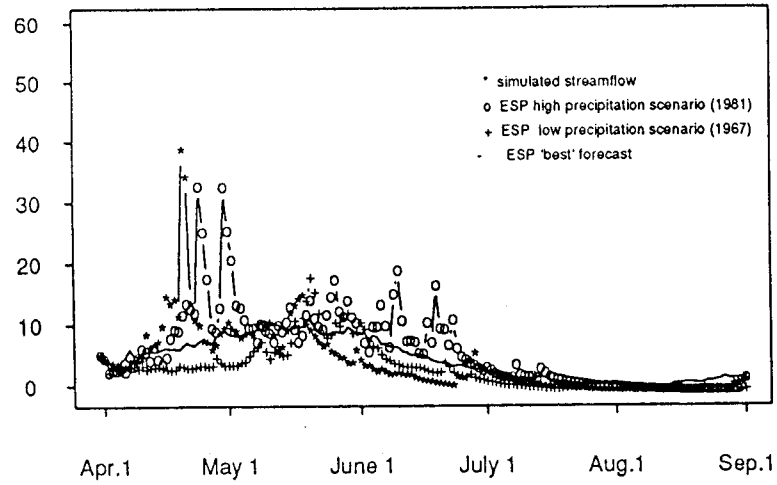

Figure 5.8c 1958 water year streamflow

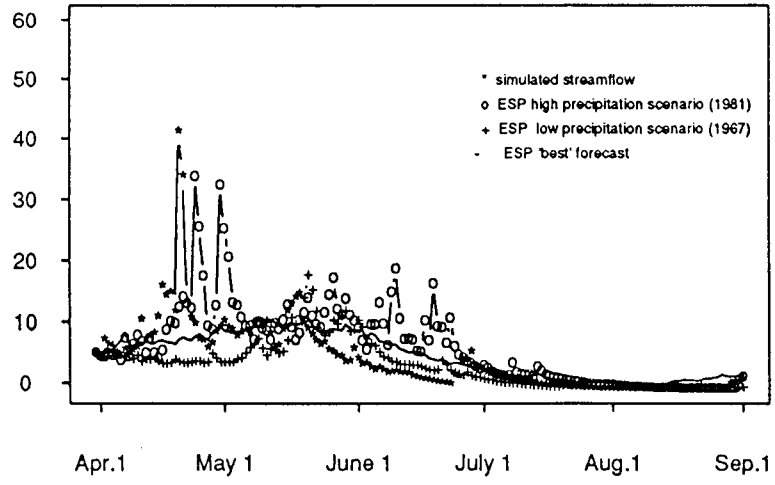

Figure 5.8d 1958 water year streamflow (no updating)

Figure 5.8 ESP performance in drought year, 1958 unit: mm

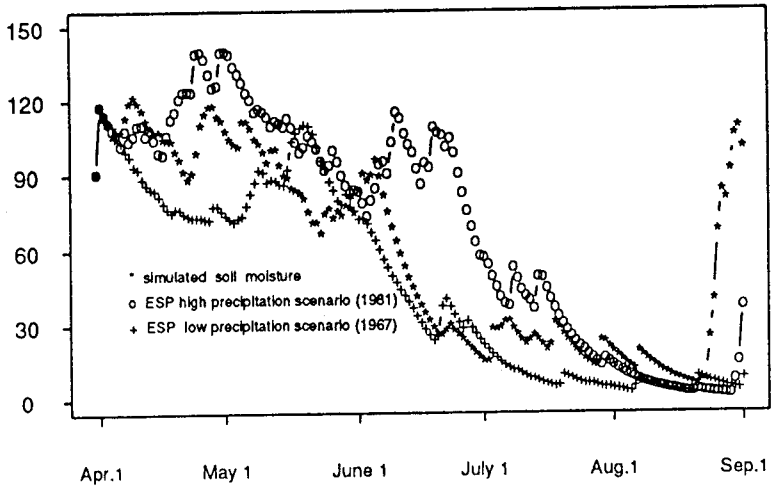

Figure 5.9a 1977 water year soil moisture

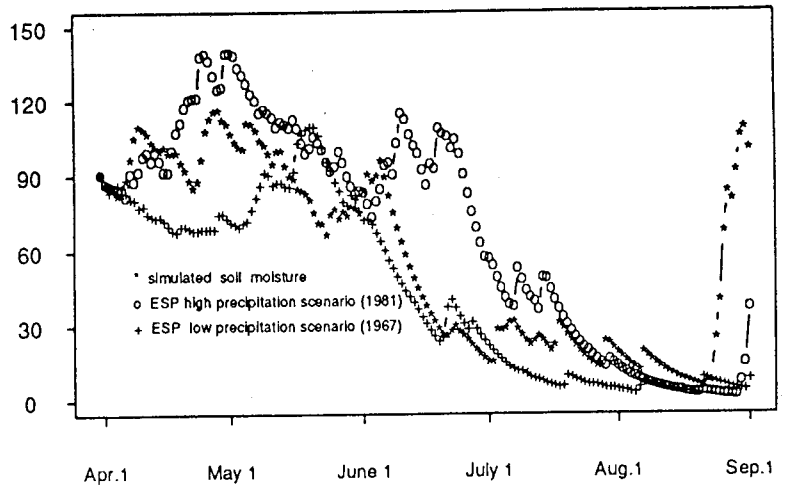

Figure 5.9b 1977 water year soil moisture (no updating)

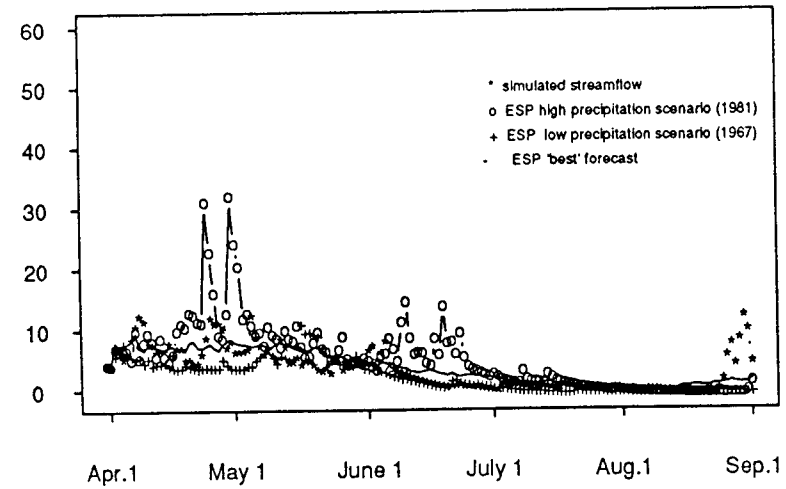

Figure 5.9c 1977 water year streamflow

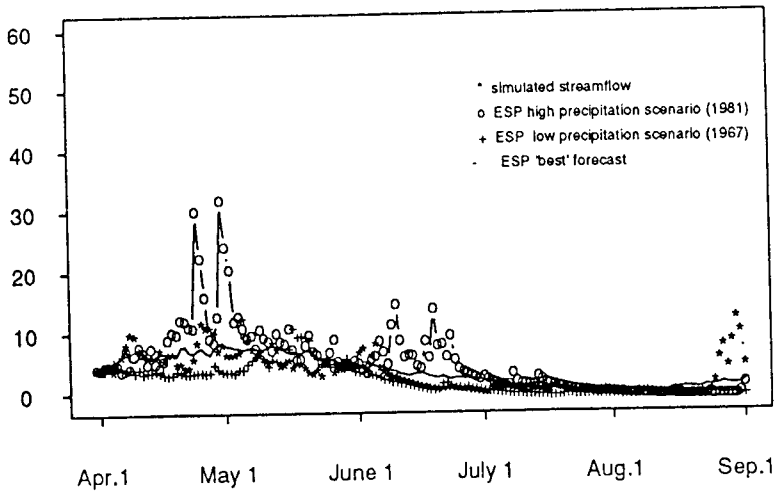

Figure 5.9d 1977 water year streamflow (no updating)

Figure 5.9 ESP performance in drought year, 1977 unit: mm

CHAPTER 6 SUMMARY AND CONCLUSIONS

6.1 Summary

This study evaluates the performance of Extended Streamflow Prediction, a streamflow forecasting method that estimates the probability distribution of future streamflow using deterministic-conceptual precipitation-runoff models. The conceptual simulation models used in this study are the National Weather Service snow accumulation and ablation model and the so-called Nanjing model which is a simple water balance model.

The simple water balance model used as the rainfall-runoff portion of the hydrologic forecast model was initially evaluated by comparing its performance with three other rainfall-runoff models that have been previously applied to the Rex River, Washington, which lies within the Seattle Water Department's Cedar River watershed. The results showed that the performance of the simple water balance model was comparable to that of the National Weather Service Soil Moisture Accounting model, which has been widely used elsewhere in the western U.S. The simple water balance models' performance was also comparable to that of HSPF (Hydrologic Simulation Program --Fortran) and CHARMS (Charles Howard and Associates Runoff Modeling System).

The Rex River study area has a drainage area of 13.4 mile square and 40 year average annual runoff (1945-1985) of 104.4 inches. Because it accounts for about 25 percent of the inflow to Chester Morse Reservoir, accurate forecasts of the runoff from this tributary of the Cedar River are important for water management.

For implementation of hydrologic models, precipitation and temperature data are required as well as the observed streamflow records. Since there are no meteorological data stations in Rex River basin, temperature and precipitation data from Cedar Lake and Stampede Pass were used as the high and the low elevation stations for snowmelt model calibration and verification.

ESP forecasts were made for each of the 40 years in the period

1948-87, the probability distribution of forecast period runoff was estimated using meteorological sequences for each of the remaining 39 years in the study period. For comparison purposes, forecasts were also made using autoregressive moving average ARMA(2,0) and autoregressive moving average - external input ARMAX(2,0,1) models.

6.2 Conclusions

The major conclusions of the study are:

1). The major advantage of ESP is that it estimates the forecast error distribution in addition to a 'best' forecast. The forecast error distribution is an essential element in risk-based water management. ESP is more realistic than the (presently) commonly used regression methods to the extent that it uses historical meteorological data sequences to represent a range of future conditions. As evaluation of the coefficients of prediction (C_p) of ESP and two time series methods showed that ESP was considerably more accurate than the time series methods, and that its accuracy was comparable to a storage accounting method previously applied to the Cedar River.

2). The ESP estimation of the forecast probability distribution tended to underestimate the upper tails, especially for short-term forecast periods. The effect of this is that the actual runoff exceeds the estimated p-percentile forecast with probability considerably larger than 1-p. The discrepancy was reduced as the forecast period increased. This is in part related to the fact that the mean absolute short-term forecast errors were mostly larger than those for longer periods (one to three months). The lower tail of the forecast distribution, which is of particular importance for risk-based decision making, especially during droughts, was better represented.

3). In the simple water balance model, the accuracy of the estimated water storage affects the accuracy of forecasts. The results of this study showed that the most accurate forecasts were

obtained during the period of highest water storage which approximately coincides with the time of maximum snow accumulation. In an attempt to improve forecast accuracy, a water storage updating procedure was developed. The calibrated value of maximum water storage for the Rex River basin is quite small (150 mm), so the updating procedure only affected soil moisture storage and streamflow the first few days after the forecast date; generally the water storage approached its unupdated state in a few time steps. Nonetheless, some improvements in forecast accuracy, especially for short-term forecasts, and long-term forecasts made after the time of maximum snow accumulation, were demonstrated. Further improvements may well be attainable by updating snow storage in addition to soil moisture storage, since the maximum snow water storage considerably exceeds the maximum soil water storage.

4). Detailed evaluation of the ESP forecast performance in three drought years (1951,1958, and 1977) showed that the forecast errors in dry years tended to be lower than the average forecast error of all years analyzed, especially for short-term forecasts. Although this was not demonstrated statistically, it is of potential importance because accurate forecasts under drought conditions may have greater worth than those in average years.

Although the value of the ESP method was demonstrated, there are some problems which are not attributed to the forecast model. The major one is that the input data to the simple water balance model were the output of a snow accumulation and ablation model; therefore, any biases in the snowmelt model were transfered to the ESP results. Improved methods of calibrating the paired snow and water balance models, and improvement of updating methods, appear to be two areas of further research that would permit a more complete examination of the utility of ESP forecast.

References

Anderson, E.A., "National Weather Service River Forecast System - Snow Accumulation and Ablation Model", NOAA Technical Memorandum NWS HYDRO-17, November 1973.

Benjamin, J.R., and Cornell, C.A., *Probability, Statistics, and Decision For Civil Engineers,* McGraw-Hill, New York, 1970.

Box, G.E.P., and Jenkins, G.M., *Time Series Analysis Forecasting and Control,* Holden-Day, Oakland, CA., 1976.

Buettner, E., "Anadromous Fish Trapping Project Memorandum", Idaho Department of Fish and Game, Lewiston, Idaho, 1988.

Burnash, R.J.C., Ferral, R.L., and Mcquire, R.A., "A Generalized Streamflow Simulation System, Conceptual Modeling for Digital Computer", U.S. National Weather Service, Ca., 1973.

Chow, V.T., Maidment, D.R., and Mays, L.W., *Applied Hydrology,* McGraw-Hill, New York, 1976.

Castruccio, P.A., Loats, H.L. Jr., Lloyd, D., and Newman, P.A.B., " Cost/Benefit Analysis for the Operational Applications of Satellite Snowcover Observation (OASSO)", *Operational Applications of Satellite Snowcover Observations,* NASA Conference Publication 2116, April 1981, pp. 239-254.

Clarke, R.T., "A Review of Some Mathematical Models Used in Hydrology, with Observations on their Calibration and Use", *Journal of Hydrology,* Vol. 19, 1973, pp. 1-20.

Crawford, N.C., and Linsley, R.K., "Digital Simulation in Hydrology", *Stanford Watershed Model 4. Tech. Report 39,* Stanford University Department of Civil Engineering, 1966.

Dawdy, D.R., "State of the Art in Hydrologic Forecasting: What next?", *Symposium Proceedings, A Critical Assessment of Forecasting In Western Water Resources Management,* American Water Resources Association, Seattle, Washington, 1984, pp. 11-14.

Day, G.N., "Extended Streamflow Forecasting using NWSRFS", *Journal of Water Resources Planning and Management,* Vol. 111, No. 2, April 1985, pp. 157-170.

Day, N.G., Schaake, J.C., and Ellis, J.H., "A Direction toward Improved Streamflow Forecasting in the Western Mountains", *Proceedings, 57th Western Snow Conference,* Fort Collins, Colorado, 1989, pp. 79-89.

Efron, B., "The Jacknife, the Bootstrap, and Other Resampling Plans", *Monograph No.38, Society for Industrial and Applied Mathematics,* 1982.

Elliot, S.J., "An Evaluation of the Snow Survey and Water Supply Forecasting Program", USDA Soil Conservation Service, Program Evaluation Division, 1977, p. 55.

Gan, T.Y., "Application of Scientific Modeling of Hydrologic Responses from Hypothetical Small Catchments to Validate a Complex Conceptual Rainfall-runoff Model", *Technical Report No. 111,* C. W. Harris Hydraulics Laboratory, Dept. of Civil Engineering, Univ. of Washington, June 1988.

Hirsch, R.M., "Stochastic Hydrologic Model for Drought Management", *Journal of Water Resources Planning and Management Division,* ASCE, Vol. 107, No. WR2, Oct. 1981, pp. 303-314.

Howard & Associates (Charles Howard & Associates Ltd.), "Seattle Water Department, Technical Memorandum 1: Evaluation of Available Data for Water Supply Forecast Model, Tolt and Cedar River Reservoirs", Aug. 1989.

Howard & Associates (Charles Howard & Associates Ltd.), "Seattle Water Department, Technical Memorandum 2: Candidate Runoff Forecast Models and Forecast Updating Procedures, Tolt and Cedar Rivers", Nov. 1989.

James, L.D., and Burges, S.J., "Selection Calibration and Testing of Hydrologic Models of Small Watersheds", *American Society Of Agricultural Engineers,* St. Joseph, Mich., 1982.

Johanson, R.C., Imhof, J.C., and Davis, H.H., "Users Manual for Hydrological Simulation Program - FORTRAN (HSPH)", EPA-600/9-80-015, Environmental Protection Agency, Athens, Georgia, 1980.

Lettenmaier, D.P. and Waddle, T.J., "Forecasting Seasonal Snowmelt Runoff: A Summary of Experience with Two Models Applied to Three Cascade Mountain, Washington Drainages", *Technical Report No. 59,* C. W. Harris Hydraulics Laboratory, Dept. of Civil Engineering, Univ. of Washington, Nov. 1978.

Lettenmaier, D.P. and Garen, D.C., "Evaluation of Streamflow Forecasting Methods", *Proceedings, 47th Western Snow Conference,* Sparks, Nevada, April 1979, pp. 48-55.

Lettenmaier, D.P., and Burges, S.J., "Estimation of Flood Frequency Changes in the Toutle and Cowlitz River Basins Following the Eruption of Mt. St. Helens", *Technical Report No. 69,* C. W. Harris Hydraulics Laboratory, Dept. of Civil Engineering, Univ. of Washington, Jun. 1981.

Lettenmaier, D.P., "Limitations on Seasonal Snowmelt Forecast Accuracy", *Journal of Water Resources Planning and Management,* Vol. 110, No. 3, Jul. 1984, pp. 255-269.

Lettenmaier, D.P., "Some Issues in Assessing the Accuracy of Hydrologic Forecasts", *Symposium Proceedings, A Critical Assessment of Forecasting In Western Water Resources Management,* American Water Resources Association, Seattle, Washington, 1984, pp. 109-116.

Lettenmaier, D.P., Gan, T.Y., and Dawdy, D.R., "Interpretation of Hydrologic Effects of Climate Change in the Sacramento-San Joaquin River Basin, California", *Technical Report No. 110,* C. W. Harris Hydraulics Laboratory, Dept. of Civil Engineering, Univ. of Washington, Jun. 1988.

Lettenmaier, D.P., "Hydrologic Forecasting", *Systems & Control Encyclopedia,* Pergamon Press, 1988a, pp. 2228-2234.

Lettenmaier, D.P., "Rainfall-runoff Model", *Systems & Control Encyclopedia,* Pergamon Press, 1988b, pp. 3940-3944.

Lettenmaier, D.P., Wood, E.F., and Parkinson, D.B., "Operating the Seattle Water System during the 1987 Drought", *American Water Works Association Journal,* May, 1990, pp. 55-60.

Linsley, R.K., Kohler, M.A., and Paulhus, J.L.H., *Hydrology For Engineers, 3rd Edition,* McGraw-Hill, New York, 1958.

Loague, K.M., and Freeze, R.A. "A Comparison of Rainfall-runoff Modeling Techniques on Small Upland Catchments", *Water Resources Research,* Vol. 21, No. 2, Feb. 1985, pp. 229-248.

Loucks, D.P., Stedinger, J.R., and Haith, D.A., *Water Resource Systems Planning and Analysis,* Prentice-Hall, NJ, 1980.

Marsden, M.A., and Davis, R.T., "Regression on Principal Components as a Tool in Water Supply Forecasting", *Proceedings, 36th Western Snow Conference,* Apr. 1968, pp. 33-40.

Pandolfi, C., Gabos, A., and Todini, E., "Real-time Flood Forecasting and Management for the Han River in China", *Proceedings, IUGG General Assembly,* Hamburg, Germany, 1983.

Salas, J.D., Delleur, J.W., Yevjevich, V., and Lane, W.L., *Applied Modelng of Hydrologic Time Series,* Water Resources Publications, 1980.

Schaake, J.C., and Peck, E.L., "Analysis of Water Supply Forecast Accuracy", *Proceedings, 53th Western Snow Conference,* Boulder, Colorado, Apr. 1985, pp. 44-53.

Shafer, B.A. and Huddleston, J.M., "Analysis of Seasonal Volume Streamflow Forecast Errors in the Western United States", *Symposium Proceedings, A Critical Assessment of Forecasting In Western Water Resources Management,* American Water Resources Association, Seattle, Washington, 1984, pp. 117-126.

Shafer, B.A. and Huddleston, J.M., "A Generalized Forecasting System for the Western United States", *Proceedings, 54th Western Snow Conference,* Phoenix, Arizona, 1986, pp. 61-70.

Sorooshian, S., "Surface Water Hydrology: on-line Estimation", Rev. Geophys. Space Phys., Vol. 21, No. 3, 1983, pp. 706-721.

Sorooshian, S., Davis, D.R., and Nevulis, R.H., "Analysis of National Groundwater Level Variations for Hydrogeologic Conceptualization, Hanford Site, Washington", Water Resources Research, Vol. 25, No. 7, pp. 1519-1529.

Stedinger, J.R., Grygier, J., and Yin, H., "Seasonal Streamflow Forecasts Based upon Regression", *Computerized Decision Support Systems for Water Managers,* Labadie, J.W., Brazil, L.E., Corbu, I, and Johnson, L.E., eds., *Proceedings of the 3rd Water Resources Operations Management Workshop,* American Society of Civil Engineers, 1989.

Tangborn, W.T., and Rasmussen, L.A., "Hydrology of the North Cascades Region, Washington 2. A Proposed Hydrometeorological Streamflow Prediction Method", *Water Resources Research,* Vol. 12, No. 2, April 1976, pp. 203-216.

Tangborn, W.V., "Application of a New Hydrometeorological Streamflow Prediction Model", *Proceedings, 45th Western Snow Conference,* Albuquerque, NM, April 1977, pp. 35-42.

Tangborn, W.T., and Brookshier N., "Forecasting Seasonal Runoff for Hydroelectric Operations using Simulated Water Storage", *Symposium Proceedings, A Critical Assessment of Forecasting In Western Water Resources Management,* American Water Resources Association, Seattle, Washington, 1984, pp. 127-132.

Twedt, T.M., Schaake, J.C., Jr., and Peck, E.L., "National Weather Service Extended Streamflow Prediction", *Proceedings, 45th Western Snow Conference,* Albuquerque, N.M., Apr. 1977, pp. 52-57.

Twedt, T.M., Burnash, R.J.C., and Ferral, R.L., "Extended Streamflow Prediction during California Drought," *Proceedings, 46th Western Snow Conference,* Otter Rock, Oregon, Apr. 1978, pp. 92-96.

U.S. Army Corps of Engineers, *Snow Hydrology, 1956.*

Wood, E.F., Lettenmaier, D.P., and Zartarian, V.G., "A Land Surface Hydrology Parameterization with Sub-grid Variability for General Circulation Models", in review, *Journal of Geophysical Research (Atmosphere),* Dec. 1990.

World Meteorological Organization, "Inter-comparison of Conceptual Models Used in Operational Hydrology Forecasting", *Oper. Hydrol. Rep. 6,* Geneva, Swizerland, 1975.

World Meteorological Organization, "Inter-comparison of Models of Snowmelt Runoff", *Oper. Hydrol. Rep. 23,* Geneva, Swizerland, 1986.

Zuzel, J.F., Robertson, D.L., and Rawls, W.J., "Optimizing Long-term Streamflow Forecasts", *Journal of Soil and Water Conservation,* Vol. 30, No. 2, 1975, pp. 76-78.

Appendix A

SNOWMELT MODEL PARAMETERS

Parameter	Definition	Value
DAYGM	Average daily ground melt at the snow-soil interface (mm)	0.4
EFC	Fraction of Area over which evapotranspiration occurs when there is complete snow cover	0.9
MBASE	Base temperature for melt computation during non-rain period (°C)	0.0
MFMAX/MFMIN	Maximum/minimum non-rain melt factors which occur on Jun.21 and Dec.21 respectively [inches/(6 hr.·°F)]	0.9/0.4
NMF	Maximum negative melt factor [inches/(6 hr.·°F)]	0.12
PLWHC	Percent Liquid-water holding capacity	0.07
PXTEMP	Critical temperature to divide rain from snow(°C)	0.5
SCF	Multiple factor to correct for precipitation gage catch deficiency during periods of snow-fall	1.03
SI	Mean areal water-equivalent above which there is always complete areal snow cover (mm)	200
TALR	Lapse rate (°C/100m)	0.5
TIPM	Antecedent temperature index parameter ($0.0 < TIPM \leq 1.0$)	0.3
UDAJ	Average six-hour wind function during rain on snow periods [inches/(in. H_g·6hr.)]	0.1

Appendix B

NANJING MODEL SIMULATIONS FOR THE 1969-80 WATER YEARS

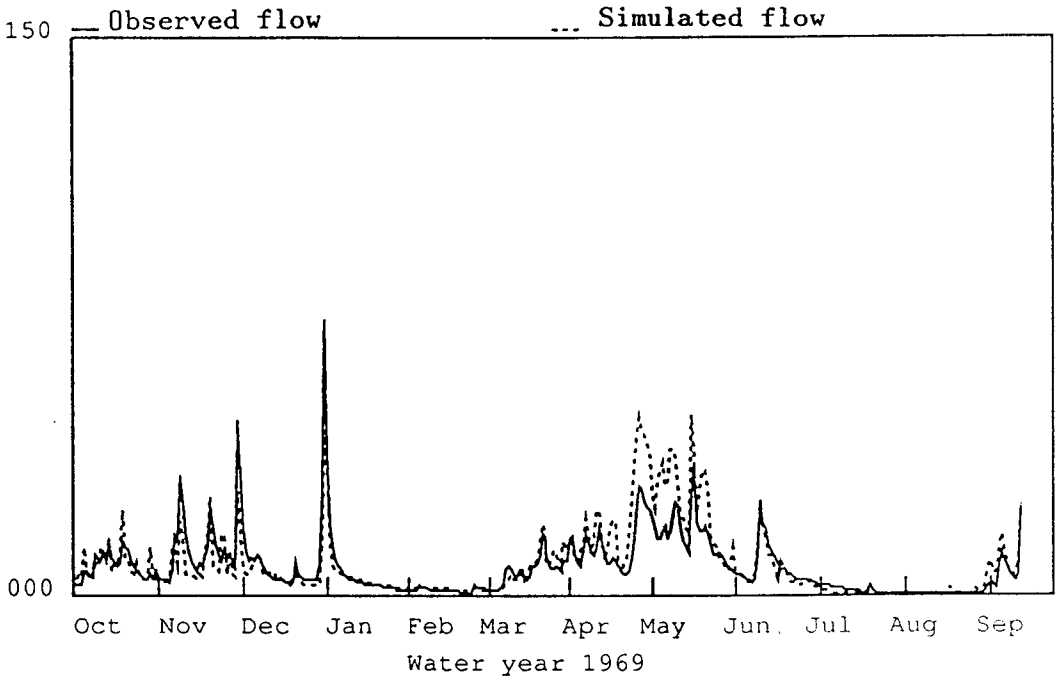
150
000
Observed flow
Simulated flow
Oct Nov Dec Jan Feb Mar Apr May Jun Jul Aug Sep
Water year 1969

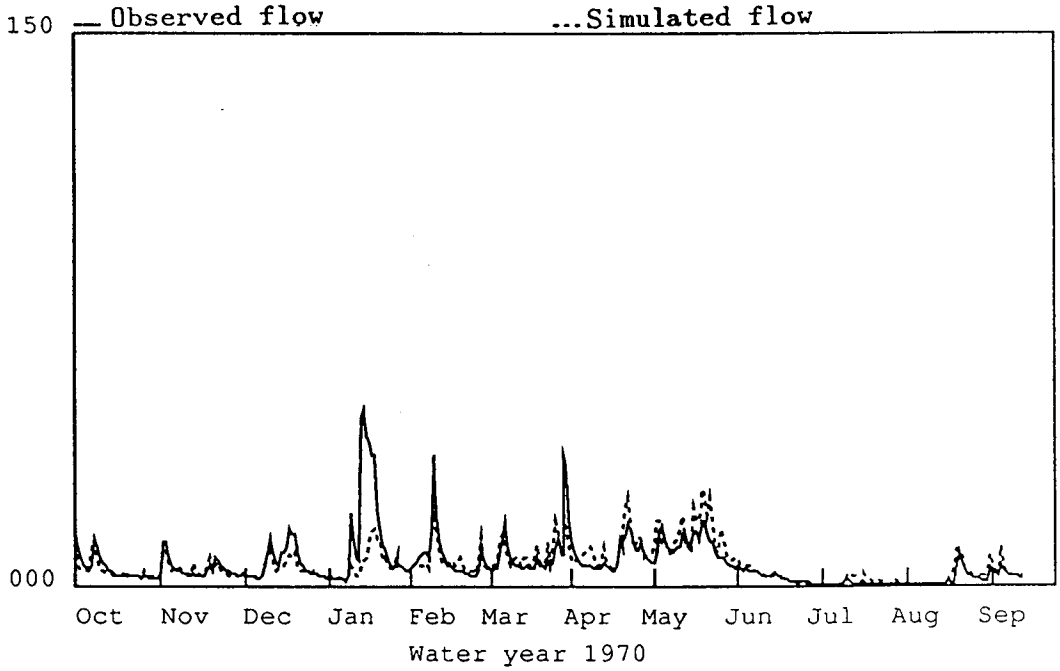
150
000
Observed flow
Simulated flow
Oct Nov Dec Jan Feb Mar Apr May Jun Jul Aug Sep
Water year 1970

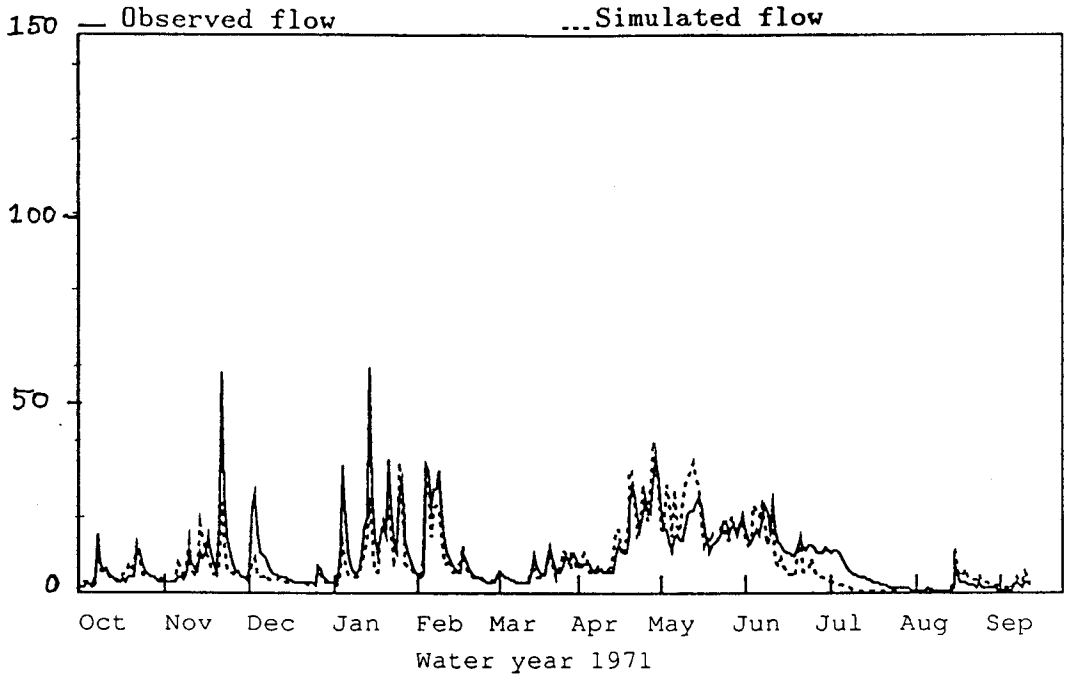
150
100
50
0
— Observed flow
...Simulated flow
Oct Nov Dec Jan Feb Mar Apr May Jun Jul Aug Sep
Water year 1971

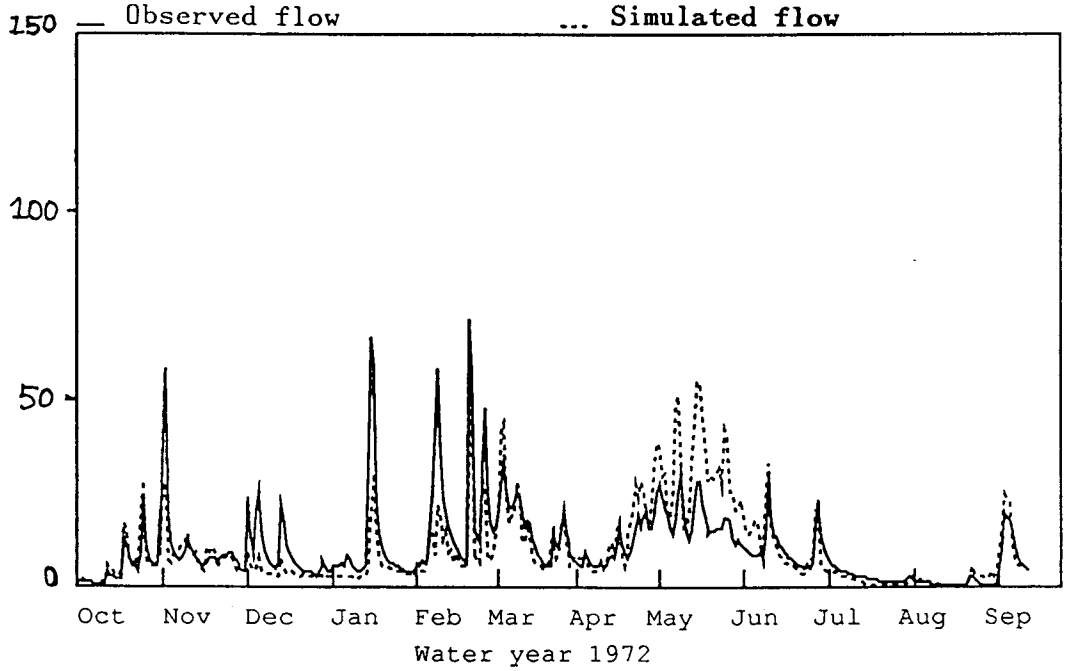
150
100
50
0
— Observed flow
... Simulated flow
Oct Nov Dec Jan Feb Mar Apr May Jun Jul Aug Sep
Water year 1972

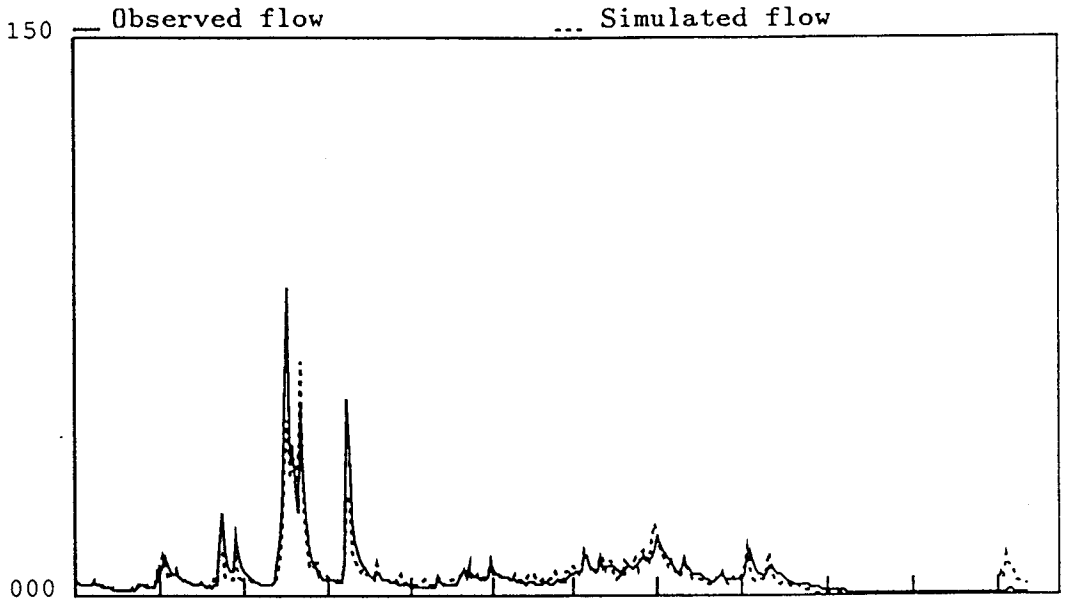
150
000
Observed flow
Simulated flow
Oct Nov Dec Jan Feb Mar Apr May Jun Jul Aug Sep
Water year 1973

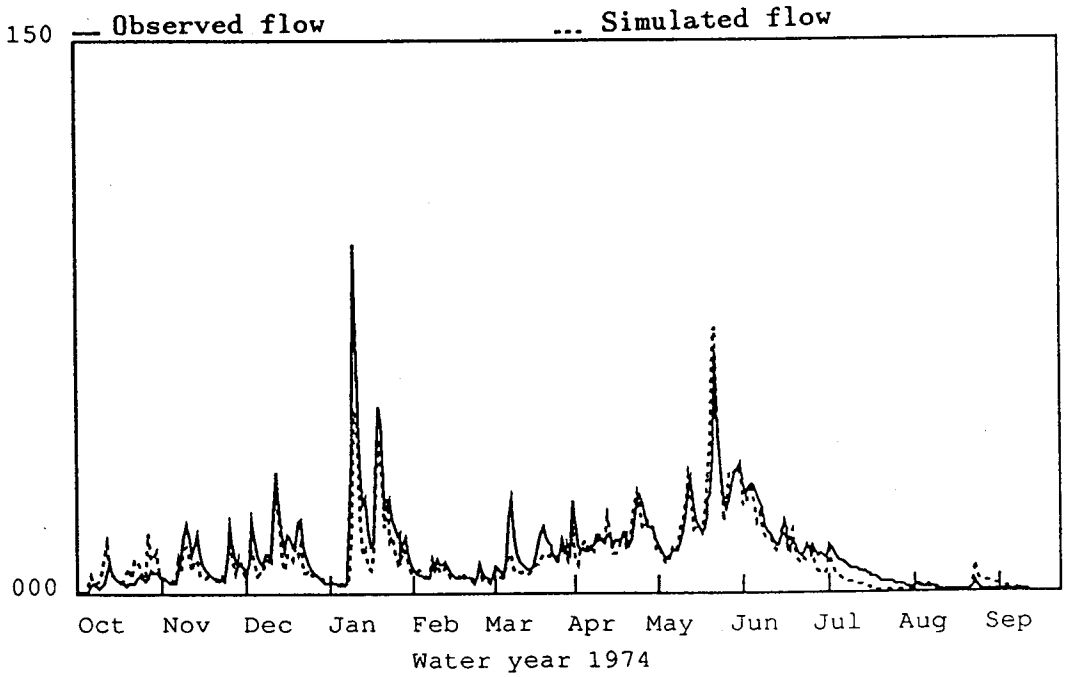
150
000
Observed flow
Simulated flow
Oct Nov Dec Jan Feb Mar Apr May Jun Jul Aug Sep
Water year 1974

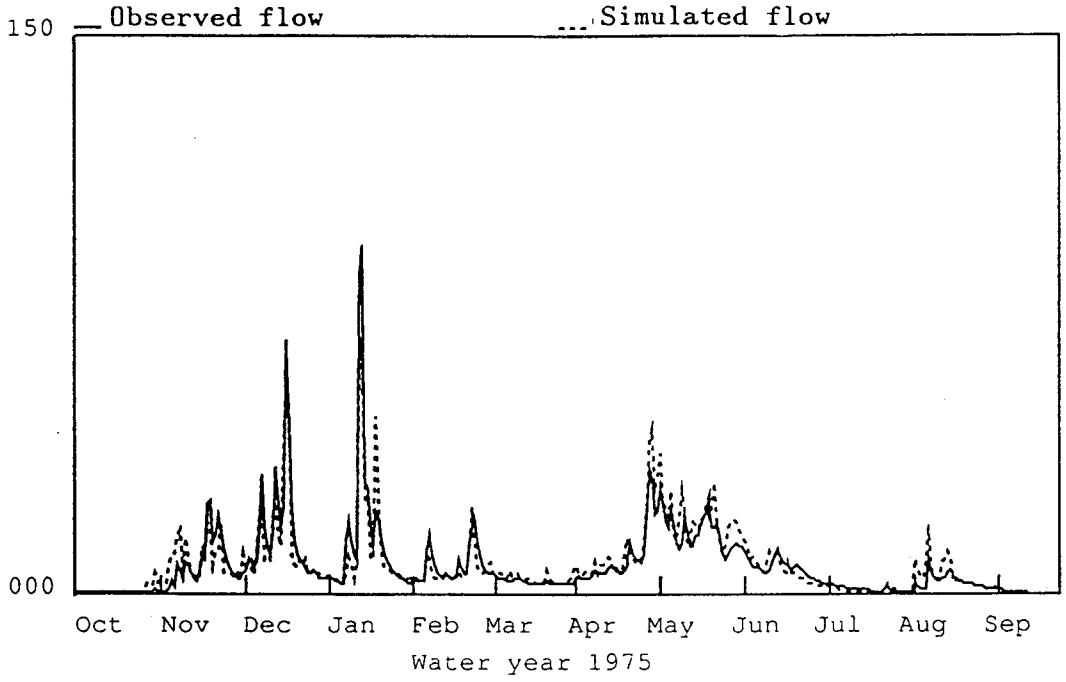
150
000
Observed flow
Simulated flow
Oct Nov Dec Jan Feb Mar Apr May Jun Jul Aug Sep
Water year 1975

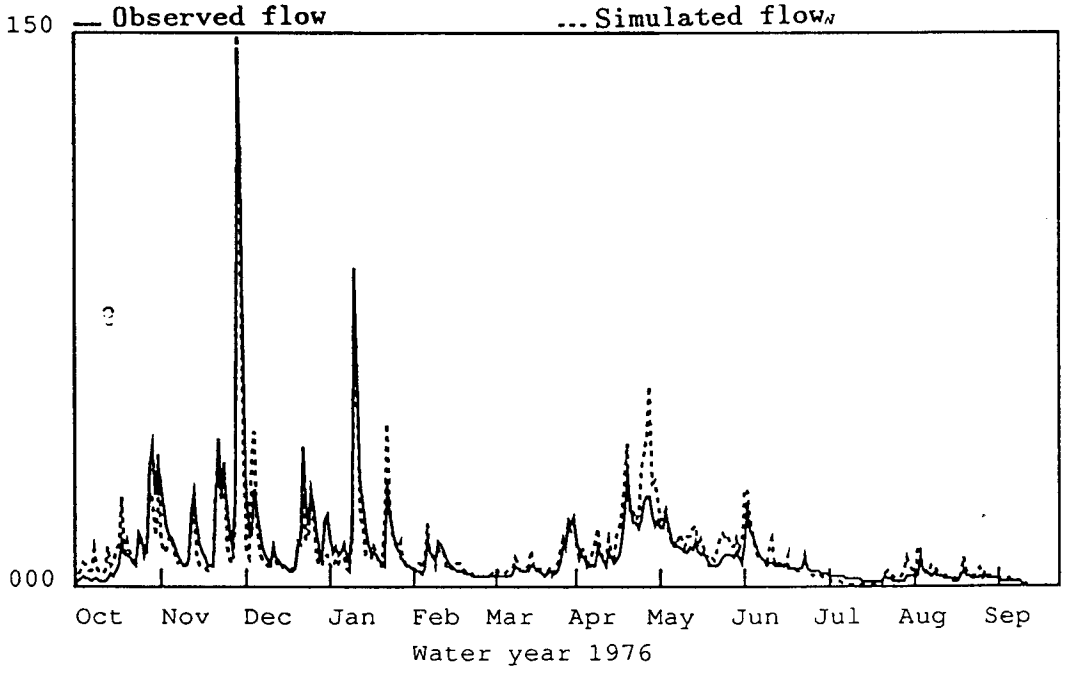
150
000
Observed flow
Simulated flow
Oct Nov Dec Jan Feb Mar Apr May Jun Jul Aug Sep
Water year 1976

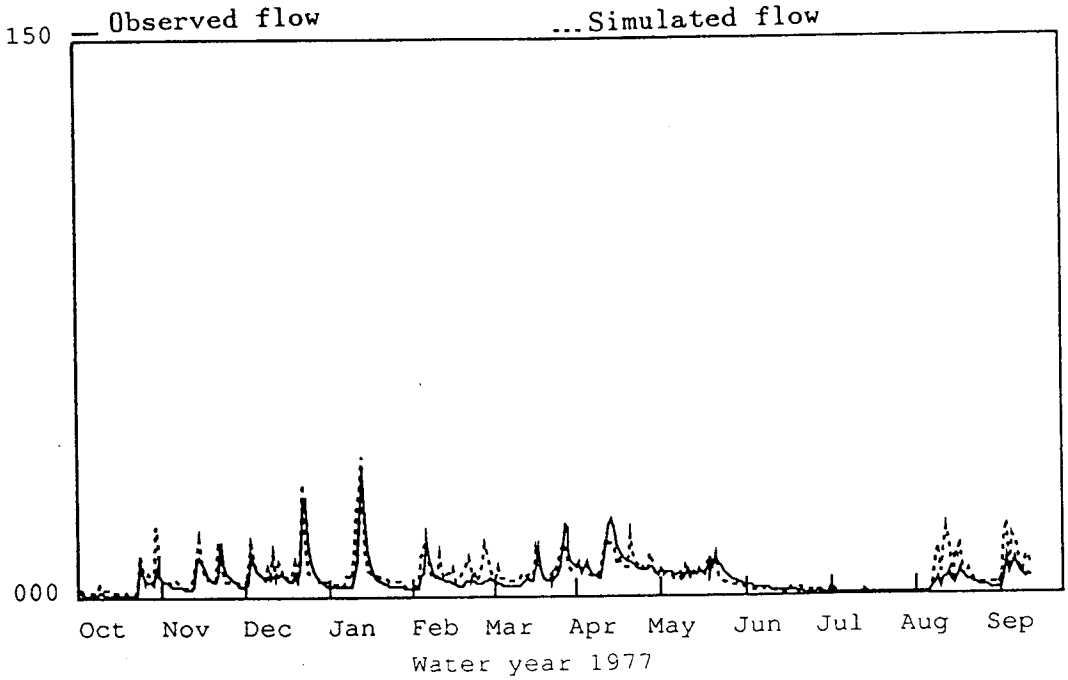
150
000
Observed flow
Simulated flow
Oct Nov Dec Jan Feb Mar Apr May Jun Jul Aug Sep
Water year 1977

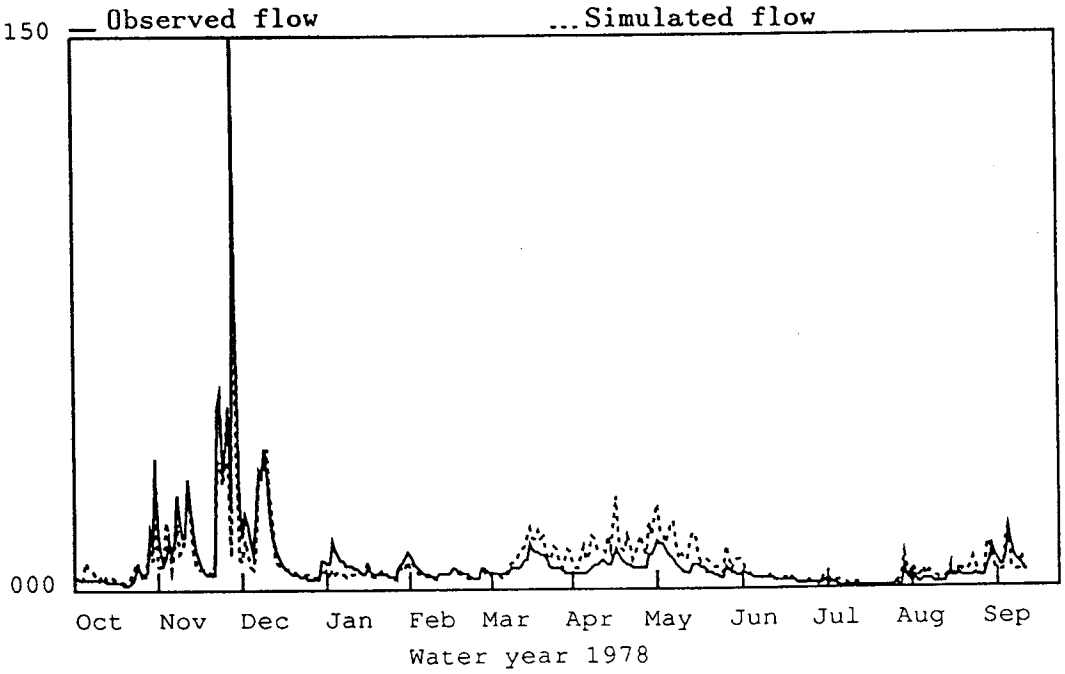
150
000
Observed flow
Simulated flow
Oct Nov Dec Jan Feb Mar Apr May Jun Jul Aug Sep
Water year 1978

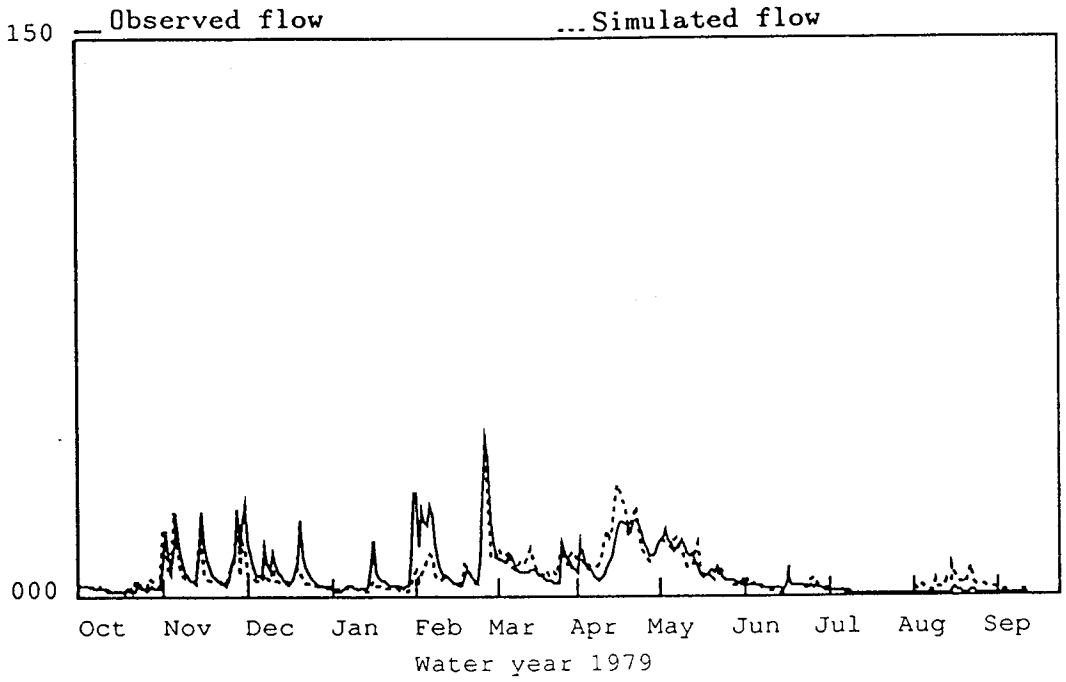
150
000
Observed flow
Simulated flow
Oct Nov Dec Jan Feb Mar Apr May Jun Jul Aug Sep
Water year 1979

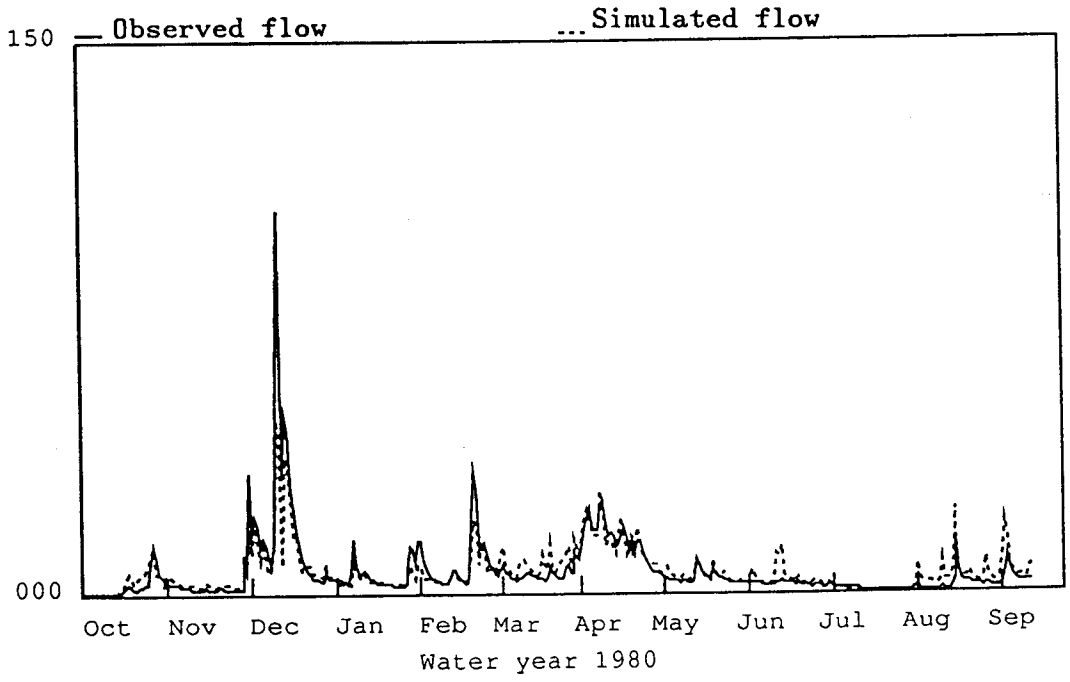
150
000
Observed flow
Simulated flow
Oct Nov Dec Jan Feb Mar Apr May Jun Jul Aug Sep
Water year 1980

Appendix C

ESP FORECAST ERROR DISTRIBUTION RESULTS

ESP FORECAST ERROR DISTRIBUTION, WITHOUT UPDATING

BEGIN DATE= OCT 1

FORECAST %	Exp.No.	1 WK Obs.	2 WKS Obs.	3 WKS Obs.	4 WKS Obs.	1 MO Obs.	2 MOS Obs.	3 MOS Obs.	4 MOS Obs.
98	1	1	0	1	0	0	3	2	2
95	2	5	3	1	1	0	3	5	2
90	4	5	6	3	4	4	4	7	10
80	8	10	8	8	7	7	7	10	16
70	12	13	13	8	11	12	11	14	22
60	16	14	13	16	15	15	20	22	24
50	20	18	16	18	19	21	25	26	29
40	24	19	17	20	23	21	27	31	33
30	28	20	19	23	25	27	30	34	33
20	32	24	30	29	28	29	32	37	35
10	36	28	34	35	36	37	37	38	40
5	38	28	34	36	36	37	38	39	40
2	39	28	35	36	38	38	39	39	40

BEGIN DATE= JAN 1

FORECAST %	Exp.No.	1 WK Obs.	2 WKS Obs.	3 WKS Obs.	4 WKS Obs.	1 MO Obs.	2 MOS Obs.	3 MOS Obs.	4 MOS Obs.
98	1	2	2	2	2	1	1	4	4
95	2	3	3	6	3	3	10	8	6
90	4	4	7	12	12	13	10	9	7
80	8	14	14	15	15	15	17	14	14
70	12	21	22	17	19	18	18	18	15
60	16	22	24	26	24	23	19	20	20
50	20	24	27	26	27	25	22	22	23
40	24	24	28	28	28	28	35	29	27
30	28	24	29	32	31	32	37	33	31
20	32	27	32	35	36	38	37	36	35
10	36	27	33	35	36	38	38	39	37
5	38	27	33	36	36	38	39	40	39
2	39	27	33	36	36	38	40	40	39

BEGIN DATE= FEB 1

FORECAST %	Exp.No.	1 WK Obs.	2 WKS Obs.	3 WKS Obs.	4 WKS Obs.	1 MO Obs.	2 MOS Obs.	3 MOS Obs.	4 MOS Obs.
98	1	3	1	4	6	6	3	2	1
95	2	9	6	4	7	7	4	3	2
90	4	11	15	4	7	7	5	4	3
80	8	14	16	17	10	10	11	9	10
70	12	18	18	21	22	21	14	10	12
60	16	18	19	21	24	24	21	17	15
50	20	22	23	23	25	25	25	21	17
40	24	26	25	26	27	29	28	25	19
30	28	28	29	29	30	30	32	26	22
20	32	28	32	32	34	33	34	30	23
10	36	31	33	34	36	35	35	37	25
5	38	31	35	34	37	38	38	37	34
2	39	31	36	37	38	38	39	39	38

BEGIN DATE= MAR 1

FORECAST %	Exp.No.	1 WK Obs.	2 WKS Obs.	3 WKS Obs.	4 WKS Obs.	1 MO Obs.	2 MOS Obs.	3 MOS Obs.	4 MOS Obs.
98	1	4	2	2	1	1	1	0	2
95	2	4	3	2	2	2	1	0	3
90	4	6	5	3	4	3	3	1	3
80	8	11	8	10	8	8	5	5	5
70	12	14	14	14	13	14	9	5	9
60	16	16	15	18	17	17	15	6	10
50	20	17	17	20	18	19	15	12	12
40	24	20	20	21	18	20	15	15	13
30	28	22	24	22	26	23	23	16	16
20	32	27	25	24	26	27	26	19	24
10	36	28	27	28	30	31	36	25	26
5	38	28	30	30	35	36	37	26	29
2	39	28	31	34	38	38	37	35	34

BEGIN DATE= APR 1

FORECAST %	Exp.No.	1 WK Obs.	2 WKS Obs.	3 WKS Obs.	4 WKS Obs.	1 MO Obs.	2 MOS Obs.	3 MOS Obs.	4 MOS Obs.
98	1	1	2	0	1	1	1	2	2
95	2	6	2	3	3	1	3	5	6
90	4	7	7	4	4	3	3	5	6
80	8	10	11	10	7	7	5	7	7
70	12	12	13	13	8	8	6	8	9
60	16	14	16	14	9	11	6	8	10
50	20	15	17	17	12	13	9	12	13
40	24	17	19	20	18	16	10	14	17
30	28	18	21	24	23	24	12	15	20
20	32	23	24	27	28	28	20	16	20
10	36	26	29	32	31	33	23	21	27
5	38	29	32	35	36	37	27	24	30
2	39	35	35	36	38	38	32	25	32

BEGIN DATE= MAY 1

FORECAST %	Exp.No.	1 WK Obs.	2 WKS Obs.	3 WKS Obs.	4 WKS Obs.	1 MO Obs.	2 MOS Obs.	3 MOS Obs.	4 MOS Obs.
98	1	0	0	1	2	1	3	5	3
95	2	1	1	2	2	3	3	5	5
90	4	2	2	3	3	4	3	5	7
80	8	4	4	4	5	6	10	11	10
70	12	7	6	4	5	7	10	13	12
60	16	11	7	8	9	8	10	14	13
50	20	17	12	9	11	11	11	17	15
40	24	18	14	11	12	12	13	18	17
30	28	22	20	14	13	12	15	18	21
20	32	25	25	21	19	14	19	24	25
10	36	30	30	30	28	25	24	28	27
5	38	34	31	33	30	30	26	28	29
2	39	35	38	34	34	34	27	28	32

BEGIN DATE= JUN 1

FORECAST %	Exp.No.	1 WK Obs.	2 WKS Obs.	3 WKS Obs.	4 WKS Obs.	1 MO Obs.	2 MOS Obs.	3 MOS Obs.	4 MOS Obs.
98	1	0	1	3	5	5	8	9	9
95	2	2	4	6	6	6	9	10	10
90	4	7	7	8	8	9	10	10	10
80	8	7	12	13	12	11	14	10	11
70	12	9	12	14	12	12	17	14	16
60	16	14	13	16	17	17	18	17	18
50	20	17	15	17	19	19	18	18	19
40	24	21	18	17	19	21	20	22	24
30	28	22	19	21	22	22	24	24	27
20	32	25	20	22	24	24	28	31	32
10	36	28	24	24	25	25	33	33	34
5	38	31	26	25	26	26	36	37	37
2	39	33	30	26	29	30	37	37	38

ESP FORECAST ERROR DISTRIBUTION, WITH UPDATING

BEGIN DATE= JAN 1

FORECAST %	Exp.No.	1 WK Obs.	2 WKS Obs.	3 WKS Obs.	4 WKS Obs.	1 MO Obs.	2 MOS Obs.	3 MOS Obs.	4 MOS Obs.
98	1	2	3	2	2	1	1	2	3
95	2	3	3	5	3	4	9	8	6
90	4	5	5	10	9	11	11	9	8
80	8	15	15	12	15	14	17	13	12
70	12	25	22	19	17	18	19	18	15
60	16	27	24	27	26	25	19	19	20
50	20	27	29	27	28	26	23	24	22
40	24	28	31	29	30	31	36	31	28
30	28	28	32	32	34	37	36	33	32
20	32	29	32	36	36	38	37	38	37
10	36	29	33	38	39	39	40	40	38
5	38	29	34	38	39	39	40	40	39
2	39	29	34	38	39	39	40	40	39

BEGIN DATE= FEB 1

FORECAST %	Exp.No.	1 WK Obs.	2 WKS Obs.	3 WKS Obs.	4 WKS Obs.	1 MO Obs.	2 MOS Obs.	3 MOS Obs.	4 MOS Obs.
98	1	7	1	5	6	6	3	2	1
95	2	8	6	5	6	6	5	2	2
90	4	16	18	5	6	6	5	4	3
80	8	24	23	20	13	12	11	9	11
70	12	30	28	27	21	21	18	11	13
60	16	31	29	29	30	31	25	21	16
50	20	31	32	30	33	34	29	26	19
40	24	31	33	30	35	36	31	30	21
30	28	34	33	34	36	36	32	30	23
20	32	35	35	35	38	37	36	30	24
10	36	35	37	37	38	38	39	37	25
5	38	35	37	38	38	38	39	39	35
2	39	35	37	39	40	40	40	39	38

BEGIN DATE= APR 1

FORECAST % Exp.No.	1 WK Obs.	2 WKS Obs.	3 WKS Obs.	4 WKS Obs.	1 MO Obs.	2 MOS Obs.	3 MOS Obs.	4 MOS Obs.
98	1	1	1	1	1	1	2	2
95	2	5	4	3	4	1	2	3	5
90	4	7	9	5	5	5	3	4	5
80	8	12	11	9	7	7	3	6	5
70	12	13	14	14	9	7	5	8	8
60	16	15	16	16	12	12	6	8	9
50	20	17	17	18	13	12	7	10	10
40	24	20	20	22	18	21	9	12	11
30	28	21	22	23	22	24	13	13	15
20	32	22	26	27	25	26	19	14	15
10	36	27	29	30	30	29	25	20	26
5	38	29	34	33	34	35	29	23	30
2	39	33	34	36	36	35	34	24	32

BEGIN DATE= MAY 1

FORECAST % Exp.No.	1 WK Obs.	2 WKS Obs.	3 WKS Obs.	4 WKS Obs.	1 MO Obs.	2 MOS Obs.	3 MOS Obs.	4 MOS Obs.
98	1	2	0	1	2	3	3	3	3
95	2	2	2	3	3	3	3	6	4
90	4	4	3	3	5	4	3	6	6
80	8	6	4	4	5	5	6	7	8
70	12	8	6	4	5	6	8	8	9
60	16	9	8	5	6	6	10	11	10
50	20	11	13	8	9	10	12	13	13
40	24	14	17	12	11	11	13	15	14
30	28	16	20	16	14	12	15	17	17
20	32	24	21	22	19	17	16	18	20
10	36	29	25	26	26	24	19	26	24
5	38	30	29	30	28	26	22	27	27
2	39	34	34	30	29	28	25	27	30

BEGIN DATE= JUN 1

FORECAST % Exp.No.	1 WK Obs.	2 WKS Obs.	3 WKS Obs.	4 WKS Obs.	1 MO Obs.	2 MOS Obs.	3 MOS Obs.	4 MOS Obs.
98	1	1	0	2	3	3	8	7	8
95	2	3	3	3	3	4	8	10	10
90	4	7	8	6	7	8	9	10	12
80	8	9	13	10	10	11	12	12	12
70	12	13	13	13	11	13	16	13	13
60	16	15	14	16	17	16	17	14	16
50	20	17	15	19	18	18	19	18	19
40	24	18	18	20	21	20	20	19	19
30	28	21	20	20	21	21	21	20	21
20	32	27	24	25	23	25	25	29	29
10	36	32	28	26	26	26	30	32	32
5	38	34	29	28	29	29	35	37	37
2	39	35	32	30	30	31	37	37	37

Appendix D

ESP MODEL UPDATING RESULTS

Estimated soil water storage W_0 on forecast date after updating (mm)

	Jan.1	Feb.1	Mar.1	Apr.1	May 1	Jun.1
1948	85.29	10.31	92.91	87.23	93.36	149.93
1949	22.99	102.90	73.19	64.71	18.38	133.92
1950	126.63	99.56	93.02	84.26	96.97	94.06
1951	114.62	47.19	69.95	149.99	132.27	103.32
1952	17.87	98.54	56.66	82.88	22.15	117.64
1953	12.53	105.31	70.71	89.84	121.15	97.53
1954	102.39	99.31	105.06	41.77	17.27	115.41
1955	132.85	108.69	51.75	60.93	69.71	149.27
1956	34.39	44.75	35.56	6.54	131.54	148.47
1957	53.16	27.85	89.04	95.22	135.35	102.19
1958	129.14	71.70	116.36	53.61	96.97	60.73
1959	124.54	56.17	90.86	143.76	167.86	79.48
1960	20.73	79.94	62.51	116.43	134.66	112.62
1961	128.32	71.33	117.15	116.53	118.95	94.06
1962	122.51	0.38	64.05	94.89	128.95	86.21
1963	93.82	95.42	127.12	93.99	109.74	47.00
1964	100.85	49.41	67.91	150.00	147.08	0.00
1965	115.87	74.81	112.28	130.26	118.11	105.62
1966	129.66	25.31	53.34	8.52	98.25	146.32
1967	120.57	74.60	86.89	51.87	68.24	97.56
1968	81.04	17.21	121.38	103.99	150.26	90.31
1969	54.02	32.47	27.81	113.11	20.27	161.88
1970	129.56	19.64	89.29	63.96	123.74	105.52
1971	127.73	92.07	92.90	115.73	108.75	118.36
1972	121.72	85.51	135.31	111.07	11.73	0.00
1973	125.67	3.90	74.97	64.04	100.34	83.84
1974	124.80	85.68	73.13	106.60	159.89	93.05
1975	66.11	35.28	91.24	60.97	80.74	136.55
1976	126.69	56.14	72.75	80.91	155.15	96.60
1977	71.12	10.38	98.80	117.81	144.94	81.33
1978	16.30	5.46	61.93	116.55	112.29	76.40
1979	25.21	100.75	81.62	58.85	161.22	86.58
1980	40.21	9.25	114.23	58.59	161.40	69.99
1981	133.31	113.74	108.14	83.57	164.18	41.07
1982	126.56	88.54	100.25	31.86	99.24	128.83
1983	15.38	10.67	88.29	140.70	106.42	49.00
1984	54.80	57.33	67.72	103.45	94.05	114.40
1985	34.88	35.90	66.40	129.56	136.00	146.59
1986	16.42	103.10	135.26	150.00	119.20	72.90
1987	84.46	106.00	58.67	53.58	130.40	101.88

Estimated soil water storage W_0 on forecast date before updating (mm)

	Jan.1	Feb.1	Mar.1	Apr.1	May 1	Jun.1
1948	112.66	54.63	92.91	71.02	95.39	125.99
1949	35.39	18.40	73.19	86.91	137.44	117.97
1950	108.53	48.20	93.02	83.43	112.56	136.76
1951	124.93	62.48	69.95	73.84	124.67	95.91
1952	49.55	71.07	56.66	92.74	129.77	106.70
1953	46.09	142.58	70.71	86.23	130.33	103.83
1954	116.18	45.85	105.06	66.32	81.97	138.49
1955	111.14	70.14	51.75	52.95	82.86	134.52
1956	88.23	56.77	35.56	85.49	127.43	133.45
1957	104.57	30.39	89.04	84.51	140.13	87.04
1958	94.18	107.12	116.36	88.86	114.08	83.17
1959	142.52	117.41	90.86	124.76	138.40	112.78
1960	74.26	65.67	62.51	115.80	126.16	128.52
1961	56.57	111.17	117.15	98.01	126.06	124.83
1962	130.18	131.78	64.05	95.44	114.76	98.44
1963	117.76	40.07	127.12	91.20	101.86	57.30
1964	96.32	76.32	67.91	94.46	92.13	139.14
1965	61.87	140.80	112.28	68.40	136.96	125.74
1966	43.46	62.68	53.34	120.46	114.33	74.64
1967	112.26	124.45	86.89	76.75	79.09	119.56
1968	118.70	99.28	121.38	115.68	118.70	125.31
1969	54.97	43.93	27.81	104.61	132.38	139.09
1970	66.61	96.20	89.29	92.71	93.78	127.13
1971	57.87	142.28	92.90	88.55	117.75	125.60
1972	48.03	81.67	135.31	110.71	104.48	137.85
1973	119.30	73.44	74.97	66.30	83.60	70.29
1974	92.47	127.53	73.13	104.33	122.46	130.84
1975	93.37	101.42	91.24	68.02	95.39	134.36
1976	128.83	129.29	72.75	69.08	140.47	105.83
1977	106.51	76.36	98.80	86.69	106.86	74.95
1978	67.18	58.27	61.93	122.20	123.74	101.10
1979	59.40	33.49	81.62	89.69	138.84	93.56
1980	88.88	44.37	114.23	95.84	123.90	78.04
1981	132.45	56.49	108.14	90.82	137.94	72.29
1982	61.61	118.19	100.25	75.66	116.81	121.02
1983	54.18	83.06	88.29	117.79	99.83	45.06
1984	44.59	119.85	67.72	101.62	87.16	114.48
1985	44.39	29.20	66.40	78.73	124.73	123.12
1986	24.08	82.51	135.26	113.42	101.78	92.52
1987	74.81	61.01	58.67	94.82	133.16	90.07